Journal of Power Sources 413 (2019) 259–283

Contents lists available at ScienceDirect

Journal of Power Sources

journal homepage: www.elsevier.com/locate/jpowsour

Review article

A review on modeling of electro-chemo-mechanics in lithium-ion batteries

Ying Zhao[a,b,*], Peter Stein[a], Yang Bai[a], Mamun Al-Siraj[a], Yangyiwei Yang[a], Bai-Xiang Xu[a,**]

[a] Mechanics of Functional Materials Division, Department of Materials and Earth Sciences, Technische Universität Darmstadt, Otto-Berndt-Straße 3, 64287, Darmstadt, Germany

[b] Department of Engineering, University of Cambridge, Trumpington Street, CB2 1PZ, Cambridge, UK

HIGHLIGHTS

- Comprehensive review of electro-chemo-mechanical modeling of lithium-ion batteries.
- Step-by-step instruction of the model for interested newcomers to the field.
- Modeling on three length scales: particle, composite electrode and battery cell.
- Review and perspective on the mechanically coupled modeling of solid-state batteries.

ARTICLE INFO

Keywords:
Lithium-ion battery
Electro-chemo-mechanical coupling
Electrode active particle model
Composite electrode model
Battery cell model
Solid-state battery

ABSTRACT

Investigations on the fast capacity loss of Lithium-ion batteries (LIBs) have highlighted a rich field of mechanical phenomena occurring during charging/discharging cycles, to name only a few, large deformations coupled with nonlinear elasticity, plastification, fracture, anisotropy, structural instability, and phase separation phenomena. In the last decade, numerous experimental and theoretical studies have been conducted to investigate and model these phenomena. This review aims, on one hand, at a comprehensive overview of the approaches for modeling the coupled chemo-mechanical behavior of LIBs at three different scales, namely the particle, the electrode, and the battery cell levels. Focus is thereby the impact of mechanics on the cell performance and the degradation mechanisms. We point out the critical points in these models, as well as the challenges towards resolving them. Particularly, by outlining the milestones of theoretical and numerical models, we give a step-by-step instruction to the interested readers in both electrochemical and mechanical communities. On the other hand, this review aims to facilitate the knowledge transfer of mechanically coupled modeling to the study of all-solid-state batteries, where the mechanical issues are expected to play even more diverse and essential roles due to the additional mechanical constraintimposed by the solid electrolytes.

1. Introduction

Rechargeable lithium-ion batteries (LIBs) are widely used in portable electronic devices and electric vehicles, and are prominent solutions for the storage of intermittent renewable energies [1,2]. The working principle of LIBs lies essentially in the electrochemical-potential-driven redox reaction in the electrode active materials, involving lithium ions and electrons. Electrons flow through conductive agents and current collectors to the external circuit, while lithium cations shuttle between the anode and cathode through the electrolyte.

Mechanics can have a critical influence on the performance and the lifetime of LIBs. It is well known that LIBs suffer from considerable chemo-mechanical degradation, which is one of the bottleneck issues for current commercial batteries failing to meet the increasing demand in wide application [3]. In pursuit of larger capacity and longer cycle/calendar life, numerous efforts have been made in the community of electrochemistry and related fields, to develop next-generation battery systems with novel electrode materials. Nevertheless, most material candidates with promising electrochemical properties have insufficient chemo-mechanical stability. That is, electrode materials with a high theoretical capacity suffer from irreversible mechanical degradation already after few cycles due to high internal stress [4]. This is the long recognized dilemma between capacity and cyclability of LIBs.

There are various types of mechanical degradation in LIBs which

* Corresponding author. Department of Engineering, University of Cambridge, Trumpington Street, CB2 1PZ, Cambridge, UK.
** Corresponding author. Mechanics of Functional Materials Division, Department of Materials and Earth Sciences, Technische Universität Darmstadt, Otto-Berndt-Straße 3, 64287, Darmstadt, Germany.
E-mail addresses: yz575@cam.ac.uk (Y. Zhao), xu@mfm.tu-darmstadt.de (B.-X. Xu).

https://doi.org/10.1016/j.jpowsour.2018.12.011
Received 20 October 2018; Received in revised form 4 December 2018; Accepted 5 December 2018
0378-7753/ © 2018 Published by Elsevier B.V.

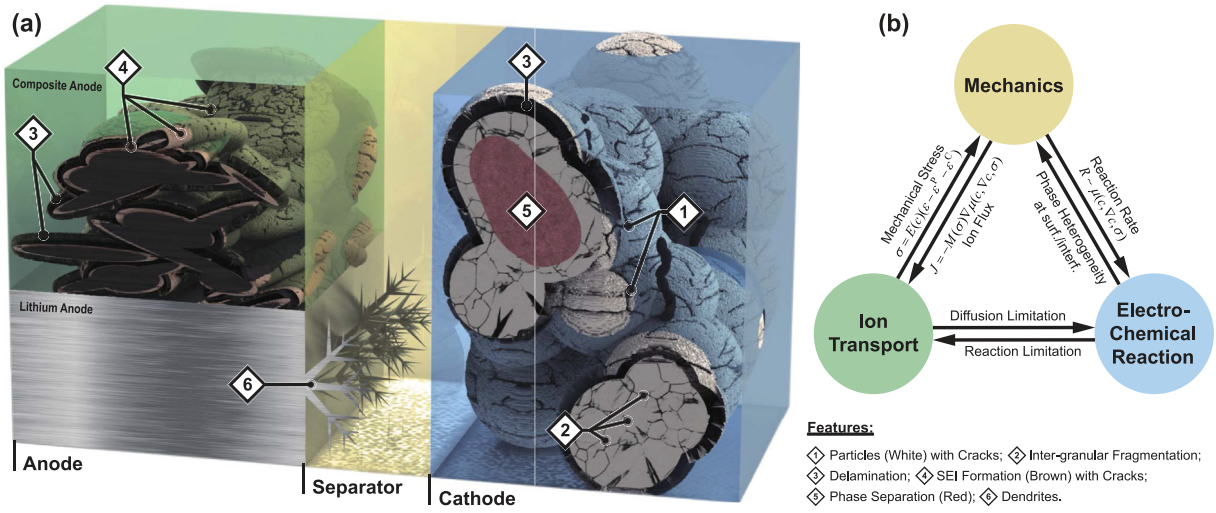

Fig. 1. Schematics of (a) mechanistic and (b) mechanical degradation mechanisms of a lithium-ion battery cell with a composite anode and a lithium metal anode, respectively.

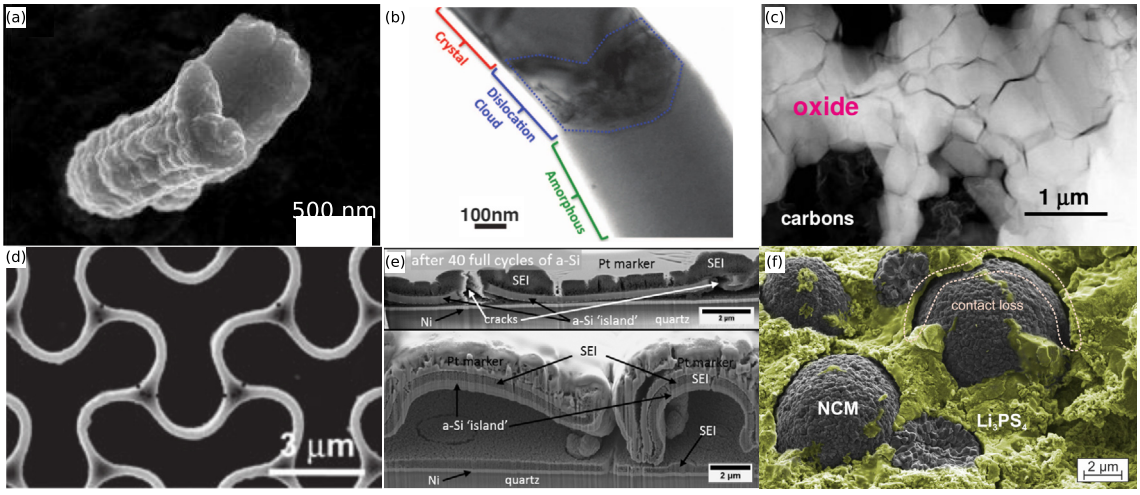

Fig. 2. (a) Fracture in a Si nanopillar [10]. (b) Formation and propagation of a dislocation cloud at the reaction front in a SnO nanowire during lithiation [11]. (c) Fragmentation of $LiNi_{0.8}Co_{0.15}Al_{0.05}O_2$ secondary particles [3]. (d) Buckling of a planar silicon honeycomb anode [12]. (e) Fracture in the SEI [13]. (f) Delamination of a particle from solid electrolyte [14]. (For interpretation of the references to colour in this figure legend, the reader is referred to the Web version of this article.)

contribute significantly to capacity fade and impedance increase of a battery over charge/discharge cycles. A selection of mechanical phenomena and degradation mechanisms are illustrated in Fig. 1 (a). In electrode active materials, Li insertion/extraction is, in general, accompanied by local deformation and volume change of the materials. Nowadays, commercial batteries usually employ graphite as active material for the battery anode (with a theoretical capacity of 372 mA h g^{-1} [5]), which exhibits volume changes of 10% under intercalation [6]. Si and Sn, on the other hand, two promising candidate materials with higher theoretical capacities of 4200 mA h g^{-1} [7] and 873 mA h g^{-1} [8], respectively, show corresponding volume changes of 310% and 260% [9]. Due to the intrinsic non-equilibrium working condition of LIBs, this deformation is inhomogeneous in the materials, giving rise to high internal stress that eventually lead to fracture, fragmentation, or pulverization. A selection of the observed damage phenomena is given in Fig. 2(a–d).

Due to a loss of contact to conductive agents or electrolyte, the active materials may become partially inactive, thus contributing to the overall capacity and power loss. Besides the aforementioned fracture within the active materials, the mismatch between active and inactive materials also tends to promote fracture or delamination at the interface. The solid-electrolyte-interphase (SEI), which is formed on the surface of active materials due to irreversible side reactions of active materials with the electrolyte, further contributes to capacity fade. These side reactions are widely believed to be able to chemically stabilize themselves as the formed SEI layer prevents further side reactions. However, the mechanical mismatch between the active particles and the SEI layer promotes cracking at the particle surface. Consequently, more active material is exposed to the electrochemical reactions at the fresh crack surface, which leads to formation of new SEI and hence to a loss in capacity fade and increase in resistivity. This positive feedback between SEI formation and cracking brings on a progressive failure [15,16] (Fig. 2(f)). In the case of solid electrolyte, delamination between the particle and the electrolyte can become more prominent than in the case of liquid electrolyte (Fig. 2(e)). The formation of micro-cracks within the solid electrolyte is expected to reduce its effective ionic conductivity, and micro-cracks may provide a pathway for Li dendrite growth, eventually causing the cell to short-circuit [17]. On the cell level, fracture and delamination can further take place between electrode and current collector [18], which can be alleviated to some degree by introducing additional buffer layers in the material [13].

In addition to degradation, mechanics can have a significant influence on both Li transport and electrochemical reactions, which are two

essential mechanisms of the working principle of LIBs, as shown in Fig. 1(b). The mechanical energy makes a contribution to the system's free energy and thus to the chemical potential, which, in turn, regulates both the Li transport in the solid phases and the electrochemical reactions at the interfaces. The driving force for the Li transport in solid phases does not only comprise a diffusion contribution but also a drifting force due to stress inhomogeneity. In the simple isotropic case, Li transport is sensitive to the gradient of the hydrostatic pressure, since guest atoms tend to move to regions with sufficient space to accommodate them. Assuming purely elastic mechanical behavior, the outer layers of an electrode particle are compressed during intercalation, while its interior is stretched. Thus, the stresses can enhance lithium diffusion towards the interior of the particle, facilitating fast intercalation [19]. This results in a change in surface concentration and hence in the chemical potential at the surface, which can further impact the surface reactions. Mechanical stresses can also regulate the cell potential so that it evolves more stably during charge and discharge, which is beneficial to the functionality of a battery. In phase-separating materials, the elastic energy contributions due to mismatch strains at the interface can outweigh the chemical energy contributions, resulting in a suppression of phase separation in the material. It has further been reported that stresses can help to suppress lithium dendrite formation in a lithium-metal battery [20,21]. In nanostructured materials, surface stresses become more prominent and can change the capacity and diffusivity of the particle through the induced internal stresses. The mechanical stresses are thereby strongly correlated with the extrinsic features of the particles, such as size and shape. Understanding and controlling the effects of stress and strain on ion transport, phase transformations, and catalytic pathways in energy materials can be a key for improving the performance and the durability of battery devices.

In the last two decades, a vast amount of studies has been undertaken concerning the role and the impact of mechanics in the performance and degradation of LIBs. Advanced experiments characterized and provided evidence for the chemo-mechanical behavior and fracture of electrodes, as summarized in the review article by Cheng and Pecht [22]. The understanding and the prediction of the lithiation behavior has concurrently been expanded by a number of theoretical works, both with regard to modeling and numerical simulations. These form the bases for an optimization of batteries at the level of individual particles, the electrode, and a whole battery cell.

The subset of studies regarding modeling of LIBs has been reviewed in several papers. These reviews focus on multiscale modeling and homogenization techniques [23,24], particle-level modeling [4,25,26], and combined experimental-theoretical approaches [27–30]. However, there is no review article in the literature which summarizes the extensive mechanically coupled modeling of LIBs and the knowledge acquired thereby. In the review by Grazioli et al. [24], modeling of micromechanical effects in active materials was addressed at the particle level. However, the influence of mechanics extends over different regions and length scalesand is not limited to the active particles. Xu and Zhao [26] also provided a brief yet in-depth overview on different theories and observations of electro-chemo-mechanics of electrode particles in LIBs. They focused, however, only on a phenomenological and conceptual description with schematic illustrations. A detailed survey of the extensive literature is missing. Herein lies the motivation for this review article. The present paper reviews the modeling and simulation work on the impact of mechanics, particularly in terms of mechanisms and degradation on particle, electrode and cell scales. On one hand, we outline the theoretical and numerical development of mechanically coupled investigation of LIBs. On the other hand, we highlight the results on mechanical impact obtained in the reviewed papers, to make the knowledge accessible to the readers with different background.

With the present paper we aim to fulfill two goals. Firstly, we want to give a comprehensive overview of the approaches to modeling the coupled electro-chemo-mechanical behavior of LIBs at three different scales: the particle, the electrode, and the battery cell levels. Focus is thereby the impact of mechanics on the mechanisms for operation and degradation at these length scales. Secondly, we outline the evolution of theoretical and numerical models for the mechanically coupled investigation of LIBs in the hope of aiding newcomers to the field and experts alike. We highlight noteworthy results and critical points in these models, as well as the challenges towards resolving them. This should provide pointers towards the future development of the field. Furthermore, a special section is devoted to all-solid-state lithium batteries, which have emerged as promising alternatives to current liquid-electrolyte LIBs. These raise more profound mechanical issues during operation and thus deserve more attention from mechanics community.

In order to facilitate this ambitious endeavor, we need to limit the scope of our considerations. In this paper we will therefore exclude thermal runaway related to dendrite penetration in metal-air and metal-sulfur rechargeable batteries. Moreover, we will not regard safety issues stemming from mechanical abuse of battery cells. Such effects have however found attention in the recent review by Kermani and Sahraei [18]. We also restrict our study to a continuum view, which ranges from the particle level (microns and sub-microns) to the battery scale. The models based on first principles are out of scope for this review paper but have been reviewed in the article by Islam and Fisher [364].

Even though this review focuses on the mechanically coupled issues in LIBs, the essential knowledge and methodology on mechanical degradation and the contribution of mechanics to ion transport and electrochemical reactions are well applicable to other battery chemistries such as Na-ion or Mg-ion batteries. In a more general sense, they are also helpful to understand the role of mechanics in other energy conversion and storage processes in materials, for instance photovoltaics and catalysis.

We begin the review at the electrode particle level in Section 2 with an introduction to a basic model accounting for the electro-chemo-mechanics of a single stand-alone particle of active material in order to provide the reader with a general understanding of the multi-physics phenomena taking place within an active particle during charge and discharge. Based on the limitations of this basic model, we discuss its extensions for different mechanical behavior and degradation mechanisms. Section 3 and Section 4 are then dedicated to the modeling of mechanical influence at two larger scales: the electrode level and the cell level. Due to the complexity of the battery structure, a full modeling with all particles is possible on neither of the two scales. Therefore, simplified models are proposed. At the electrode level, there are two different approaches: micro-structurally resolved models and homogenized models. The former resolves all the details but is limited to countable particles with the surroundings, whereas the latter employs micromechanics-based homogenization techniques to obtain effective quantities for the composite electrodes with different microstructures. At the cell level, model variations that are adapted from battery cell theory from the electrochemistry community [31] are extended in order to incorporate mechanical effects. However, due to the compliant nature of liquid electrolyte, mechanical issues are at this level not as significant as others, for instance electrical, chemical and thermal effects. The mechanically coupled modeling research is thus also lacking. However, a recent trend is towards replacing the liquid electrolyte with solid electrolyte, where mechanical effects play a more pronounced role in batteries. This poses a big challenge not only to the electrochemistry, but also to the mechanics community. Consequently, we address this enhanced importance of mechanical effects separately in Section 5.

2. Particle level

Electrode active materials are crucial to batteries because they directly influence battery capacity. Lithium ion intercalation and de-intercalation in an electrode particle will give rise to, among other

phenomena, stress generation, phase separation, volumetric expansion, and particle fragmentation. In this section, mechanistic models are firstly introduced for a better understanding of the functioning of active particles during lithiation and delithiation. On this basis, various degradation models are given to discuss the failure of electrode particles.

2.1. Modeling of diffusion-induced stresses and stress-assisted diffusion: the basic model

Modeling of chemically induced stresses can be dated back to the 1960s, beginning with the work of Prussin [32] who described the stresses developing in Si wafers using an analogy to thermal stresses, an ansatz which finds application to the present day. The thermodynamics of diffusion interacting with stresses has later been formulated by Li [33] and, in a series of papers, by Larché and Cahn [34–36], which have later been extended to account for concentration-dependent material parameters [37]. A general theory for diffusion in stressed solids has been described by Aifantis [38]. Analytical solutions for this model have been derived in Refs. [39,40]. Extension towards diffusion in viscoelastic media and within solids undergoing large elastic deformations are described by Taylor and Aifantis [41] and by Stephenson [42], respectively. Early applications of these stress-diffusion models can be found, for instance to modeling hydrogen embrittlement, by Girrens and Smith [43]. Modeling of lithium intercalation induced stresses in lithium batteries has, however, not found attention until 2005, when García et al. [44] developed a mechanically coupled 2D battery cell model with spatially varied porous electrode microstructures beyond the mean-field methods. In their work, they split the total strain (ε) into elastic strain (ε^{el}) and inelastic strain (ε^{ch}) due to lithium insertion. Following Vegard's law, the chemical strain is proportional to lithium concentration inside the particle,

$$\varepsilon^{ch} = (c - c_{ref})\boldsymbol{\beta}, \tag{1}$$

where $\boldsymbol{\beta}$ denotes the Vegard coefficient, c the lithium concentration, and c_{ref} a reference strain-free concentration. With that model, they captured the overall stress distribution across a group of representative particles during discharge.

Meanwhile, Christensen and Newman [19] derived a stand-alone electrode particle model in which they considered mechanical stresses and fracture in lithium insertion materials. In their model, instead of strain decomposition, the total stress is split into an elastic stress and a thermodynamic pressure, that is, an equivalent elastic pressure to deform the particle by a chemically induced volumetric strain. In this model, the thermodynamic pressure also contributes to the diffusion of lithium inside the particle, thus establishing a two-way coupling between chemical and mechanical behavior. This means that, at any instance of time, the transport of lithium will give rise to distributed stresses, which, in turn, affect the diffusion of lithium in the electrode active material. The chemical and mechanical fields are thus dependent on each other.

For simplicity, this effect of the stresses on the chemical behavior is ignored in many of the early models. By introducing an eigenstrain (or stress-free transformation strain) expressed as Eq. (1) in an analogue to the thermal strain, the problem is thus reduced to a purely mechanical problem. The lithium concentration distribution is thereby either prescribed through a steady-state function or it is computed independently by solving Fick's diffusion equation, with the stresses generated here being known as *diffusion-induced stresses* (DIS). Since a constant homogeneous concentration field in a free-standing solid will only give rise to homogeneous and stress-free swelling, gradients or discontinuities in the lithium concentration are necessary to generate a stress field.

However, mechanical stresses also play an important role in assisting the diffusion process. An alternative approach to that of Christensen and Newman, that is, considering the stress-assisted diffusion, is to modify the diffusivity in Fick's diffusion law in the light of thermodynamics. As an example, consider the mechanical confinement of the active electrode material which has been identified as a strategy to mitigate the large volumetric expansion of materials such as Si [45–47]. This necessarily causes compressive stresses within the active material and hence an overpotential which can limit the accessible capacity of the material [48–50] and the rate of lithiation [51]. Mechanical stress can thus be used to enhance the diffusivity of the active material [365], for instance in $LiCoO_2$ [52,53], $Li_xV_2O_5$ [54], and $LiFePO_4$ [366]. A full consideration of the interaction between electrochemistry and mechanics (two-way coupling) is thus very important for a better understanding of the coupled behavior in an electrode active particle and for the correct prediction of stress levels in the active material [55] and for surface reaction rates. In particular the latter are increasingly affected by surface stresses upon progression towards nanoscale electrodes, a fact that sof ar has only found scarce attention in the scientifc community [367–369].

In this section, a simple yet practical two-way coupled model is summarized that considers mechanical stresses and lithium diffusion inside the particle. It is mostly based on the work of Zhang et al. [56] and is built based on the following assumptions:

• Electron transfer is fast enough compared with lithium transport so that electrons can always equilibrate at any time instant. This is valid during normal operation of a battery since the diffusion under direct current pulse (or slow alternating current pulse) is the dominant mechanism. The electronic conductivity is several orders of magnitude larger than lithium diffusivity in active materials such as $LiMnO_2$ [57]. This assumption helps to eliminate the governing equations for the electron transport. Moreover, since we assume the electrode material to be electronically conductive, the whole electrode particle is in isopotential state, which again helps to cut down the efforts for solving the governing equation for electro-static potential throughout the electrode particle. Electrons are thus disregarded.

- The diffusion model is adapted from a dilute solution model, which can be valid only if lithium migrates among interstitial sites. Li vacancy sites are thus not conserved.
- Since only interstitial intercalation is assumed in the model, it is natural to also assume that the structure of host materials is only slightly affected and can fully recover. With this assumption, plastic strains and phase transformation of the host material are disregarded. The particles show only small deformations under the coupled diffusion process, and material properties remain constant under lithiation and delithiation.
- It is assumed that the host material is either polycrystalline or amorphous, possessing homogeneous and isotropic chemical and mechanical properties. The particles are considered to be large enough so that surface stresses can be disregarded. The particles are free-standing, that is, there is no interaction with neighbor particles.

Since lithium transport inside the electrode is a complex process, involving not only lithium but also other species such as electrons, host atoms, and vacancies, these assumptions can be violated in some specific systems. We will elaborate this point in more detail in Section 2.2.

In the model, the chemical potential gradient is employed as the driving force for the movement of lithium ions, following the idea of Verbrugge and Koch [58] and Botte and White [59]. The chemical potential of 1 mol lithium inside an active particle body $\mathscr{B}$ is expressed as

$$\mu = \mu_0 + \mathrm{RT}\ln c - \Omega\sigma_h, \tag{2}$$

where μ_0, R, T, and c are reference chemical potential, gas constant, absolute temperature, and lithium molar fraction, respectively. Ω is the lithium partial molar volume, which represents the volume change of an active particle upon adding 1 mol lithium into it. Further, σ_h denotes the hydrostatic stress, expressed as $(\sigma_{11} + \sigma_{22} + \sigma_{33})/3$. Equation (3) can potentially include further terms, describing, for instance the non-

ideality of solution [370]. The lithium transport inside the particle (assuming the particle to be an ideal electronic conductor and being in an isopotential state) is then expressed as

$$\frac{\partial c}{\partial t} = -\nabla\cdot\mathbf{J} = \nabla\cdot\left(\frac{\mathrm{D}c}{\mathrm{RT}}\nabla\mu\right) = \nabla\cdot\mathrm{D}\left(\nabla c - \frac{\Omega c}{\mathrm{RT}}\nabla\sigma_\mathrm{h}\right) \quad \text{in } \mathscr{B}, \tag{3}$$

where D denotes the diffusion coefficient and where $\mathbf{J}$ is the lithium molar flux. Here, Ω can be interpreted as a chemo-mechanical coupling coefficient. Its derivation from nano-indentation experiments has been described recently by Papakyriakou et al. [60]. This non-classical diffusion can be modified further, including, for instance, drift terms due to electrostatic interaction or due to local deformation velocity, which can even outweigh the flux due to a concentration gradient [61,371].

For the mechanical part, a linear elastic material is assumed, whose constitutive relation reads

$$\boldsymbol{\sigma} = \frac{\mathrm{E}\nu}{(1+\nu)(1-2\nu)}\mathrm{tr}\,\boldsymbol{\varepsilon}^\mathrm{el}\mathbf{1} + \frac{\mathrm{E}}{1+\nu}\boldsymbol{\varepsilon}^\mathrm{el} \tag{4}$$

where E and ν are Young's modulus and Poisson's ratio, respectively, and where 1 is the second-order unit tensor. The elastic strain is expressed as $\boldsymbol{\varepsilon}^\mathrm{el} = \boldsymbol{\varepsilon} - \boldsymbol{\varepsilon}^\mathrm{ch}$, where $\boldsymbol{\varepsilon} = (\nabla\mathbf{u} + (\nabla\mathbf{u})^T)/2$. Starting from Eq. (1), we can derive a simplified expression for $\boldsymbol{\varepsilon}^\mathrm{ch}$ upon assuming isotropic lithiation-induced deformations:

$$\boldsymbol{\varepsilon}^\mathrm{ch} = \frac{\Omega}{3}(c - c_\mathrm{ref})\mathbf{1}. \tag{5}$$

The local force balance is then

$$\nabla\cdot\boldsymbol{\sigma} = 0 \quad \text{in } \mathscr{B}. \tag{6}$$

The virtue of this model lies in the fact that, for stand-alone particles with simple geometries and sufficient symmetry (such as spheres and cylinders), a closed-form expression of hydrostatic stress σ_h with respect to the concentration c can be derived [56,62,372,397]. One can thus recast Eq. (3) into

$$\frac{\partial c}{\partial t} = \nabla\cdot[\mathrm{D}(1+\gamma c)\nabla c] \quad \text{in } \mathscr{B}, \tag{7}$$

where $\gamma = (2\Omega^2\mathrm{E})/[9\mathrm{RT}(1-\nu)]$ is a parameter representing the coupling between mechanical stresses and concentration. In other words, for such simple geometries, the chemical and the mechanical problems can be decoupled. It can further be observed from this model that the effective lithium diffusivity is actually enhanced by mechanical stresses from D to $D(1+\gamma c)$, and that the effective diffusivity increases with increasing concentration.

Based on this model, the lithium diffusion and the mechanical stresses in spherical and cylindrical particles can be determined by the finite difference method. However, this simple approach falls short in simulating complex geometries and boundary conditions, which warrants use of the finite element method. Considering the aforementioned isotropic material and the strain decomposition shown in Eq. (5), the gradient of hydrostatic stress can expressed by primal variables (displacement $\mathbf{u}$ and molar fraction c) as

$$\nabla\sigma_\mathrm{h} = \frac{\mathrm{E}}{1-2\nu}[\nabla(\nabla\cdot\mathbf{u}) - \Omega\nabla c], \tag{8}$$

which renders Eq. (3) a third-order partial differential equation. A direct treatment using C^1 -continuous shape functions is described by Stein and Xu [63], where the force balance and the diffusion equations are solved monolithically for the primal unknowns. Alternatively, one can also solve this problem using a mixed formulation or a staggered scheme [64–66]. For the former approach, a proper combination of discretization of the concentration field and the extra field (usually σ_h or μ) is crucial for the convergence of the solution. For the staggered method, care should be taken of the choice of the time step size for a more accurate solution.

For the electrode surface, proper boundary conditions need to be given. Mechanically, traction-free boundary conditions are commonly applied on the outer surface and a fixed central point is imposed to prevent rigid-body movements. For a finite element treatment, an octant of a 3D sphere or a quarter of a 2D disc is generally constrained by symmetry boundary conditions [63].

The chemical boundary conditions are highly dependent on the experimental electrochemical setups to be simulated. To characterize different electrochemical properties of insertion materials, experiments are conducted with different electrochemical methods [30,67,68]. These conditions need to be carefully treated in the simulation in order to reproduce the experimental results. To simulate galvanostatic charge/discharge, the Neumann boundary condition

$$-\mathbf{J}\cdot\mathbf{n} = \frac{\hat{\imath}}{z\mathrm{F}} \quad \text{on } \partial\mathscr{B}_\mathrm{galvano} \tag{9}$$

is applied on the electrode-electrolyte interface with the normal vector $\mathbf{n}$ pointing towards the electrolyte. $\hat{\imath}$ is the applied current density flowing into the electrode particle, z is the charge number of an inserted/extracted ion and F is Faraday's constant. On the electrode-substrate interface, which is impermeable to the ions of active species, $\hat{\imath}$ is set to be zero. For a potentiostatic charge/discharge process the Dirichlet boundary condition

$$c = \hat{c} \quad \text{on } \partial\mathscr{B}_\mathrm{potentio} \tag{10}$$

is often employed in simulations under the assumption that the surface reactions are kinetically sufficiently fast such that the equilibrium concentration $\hat{c}$ of the active species is instantly reached on the surface. Consequently, the overall insertion/extraction rate is governed by bulk lithium diffusion (diffusion-limited dynamics) [69]. Alternatively, the surface flux can also be computed by considering the simple reaction

$$\mathrm{Li}^+ + \mathrm{e}^- + \mathscr{H} \underset{\text{de}-\text{intercalation}}{\overset{\text{intercalation}}{\rightleftharpoons}} \mathrm{Li}\mathscr{H} \tag{11}$$

where $\mathscr{H}$ is the host active material. A phenomenological Butler–-Volmer expression can thus be given as the boundary condition [31].

$$-\mathbf{J}\cdot\mathbf{n} = \frac{i_0}{\mathrm{F}}\left\{\exp\left(\frac{(1-\beta)\mathrm{F}\eta}{\mathrm{RT}}\right) - \exp\left(-\frac{\beta\mathrm{F}\eta}{\mathrm{RT}}\right)\right\}, \tag{12}$$

with i_0 being the exchange current density, β a symmetry factor representing the fraction of the applied potential that promotes forward reaction in Eq. (11), and η the electro-chemical over-potential, expressed as [70–73].

$$\eta = V(\mathbf{x}, t) - U(c_\mathrm{s}), \tag{13}$$

where V is the space- and time-dependent applied potential and U is the equilibrium potential, a function of the surface concentration c_s. In this approach, no assumptions of fast reaction kinetics is required and numerical experiments can be carried out with different reaction-diffusion relations. This boundary condition is particularly suitable for describing potentiostatic and -dynamic loading. It is also widely used in different cell models as shown in the following sections, where electrolyte potentials can be calculated at the battery level.

2.2. Model variations based on deformation/lithiation mechanism

The model described in the preceding section is a good starting point to understand the coupling between chemical intercalation and mechanical stresses and it can offer a reasonable explanation of the electro-chemo-mechanical behaviors of electrode particles. However, due to over-simplified assumptions as described in the last section, it needs to be extended for different material systems which are influenced by additional mechanisms.

Remark: It is well accepted that electrode materials can be classified into two main categories based on lithiation/delithiation reaction: intercalation and conversion (including alloying) materials. The former includes graphite, TiO_2, $LiCoO_2$, $LiFeO_4$, whose crystal structures remain unchanged or which experience only slight distortion. The latter

includes alloy anodes such as Si and Sn as well as metal halides, which undergo structural change, accompanied by chemical bond breaking and recombination. In this review, however, we do not follow this classification for the mechanical models. The reason is twofold: firstly, different mechanical mechanisms can be present within one material category. Secondly, materials from different categories can also exhibit the same mechanical mechanisms. For instance, phase transformation is much less obvious in materials such as graphite, $LiCoO_2$ and a-Si than in materials like $LiFeO_4$ and c-Si. Therefore, the focus of the classification in this review is the mechanical significance during lithiation/delithiation.

2.2.1. Host material lattice distortion and plastic strain

It is very desirable for an intercalation material to maintain minimal volume changes during charge and discharge in order to ensure stable cyclability. Cathode materials usually exhibit relatively small volumetric deformation (≈5 %). Graphite—which is by far the most successful commercial anode material—shows a volume expansion up to 10%. The observed strains are already beyond the linear kinematic assumption (small deformation). It is thus inappropriate to use linear elasticity theory for such materials. Moreover, many high-capacity anode materials can expand to several times their original size when fully lithiated. For instance, the particle volume of Si can increase up to 310% with an uptake of 4.4 Li atoms per Si atom. Furthermore, accumulated evidence has shown that part of the incurred strain is inelastic and irreversible even for amorphous Si (a-Si) [74–78], indicating a possible plastic strain. Yield stresses of ca. −1.75 GPa (compression) and 1 GPa (tension) have been estimated for a silicon thin film electrode by Sethuraman et al. [76].

In order to account for this phenomenon, Bower et al. [79,80,373] employed a multi-component Larche–Cahn model [81] which permits unoccupied Si lattice sites to be created or destroyed. They found that there is a large irreversible deformation change when initially unoccupied Si sites are introduced. Similar models considering the interdiffusion between the host and guest atoms have been proposed by Gao et al. [82] and Baker et al. [83]. They formulated a mechanically coupled three-field problem of the elastic deformation, the concentration of lithium, and the concentration of host atoms (in this case, silicon) and described its mixed-variational Finite Element implementation. Their results show that interdiffusion can reduce the intercalation-induced stresses even below yielding threshold for plasticity.

Recently, Salvadori et al. [84] proposed a coupled model for heat and mass transfer, mechanics, chemical reactions, and trapping of the mobile species. Their model considers trapping of mobile species in the host material, inducing inelastic straining of the host material, and it is applied to the analysis of vacancy redistribution in metals, hydrogen embrittlement, and the insertion/extraction into a spherical $LiCoO_2$ electrode particle. Singh and Bhandakkar [85] studied the stresses developing in a free-standing elastic-perfectly plastic spherical electrode particle covered by viscoelastic binder. They found that high binder stiffness and viscosity may lead to yielding of the encapsulated particle.

In continuum models, the plastic strain (ε^{pl}) is an additional contribution to the total strain. In the large deformation regime, a multiplicative decomposition of total deformation gradient $\mathbf{F} = \mathbf{F}^{el}\mathbf{F}^{pl}\mathbf{F}^{ch}$ is introduced, where $\mathbf{F}^{el}$, $\mathbf{F}^{pl}$, and $\mathbf{F}^{ch}$ are the elastic, plastic, and the lithium-intercalation-induced contributions to the deformation gradient, respectively [86,374]. To determine the plastic strain, a standard rate-dependent or rate-independent plastic rule can be employed, which is based on a von Mises yield criteria and an associated flow rule stemming from the 2nd invariant J_2 of the stress deviator σ_{dev} [65,79,86–90,375,376]. However, it can also be argued that in some materials such as silicon, the yield surface depends on both the mechanical and chemical history. Consequently, the chemical reactions taking place in the material would change the yield resistance and hence promote plastic flow. This approach denoted as “reactive flow” was put forward by Zhao et al. [78] and found consideration in a series of papers [91–95].

A related factor is the formation of dense dislocation clouds under lithiation of SnO nanowire anodes [96,97] and $LiCoO_2$ cathodes after high-rate charging [96,97], see Fig. 2(b). The high density of dislocations results in the loss of crystal structure of the host material. Although the dislocations themselves do not seem to cause any performance decay, they can at least be seen as a symptom for the structural degradation of the electrode material [11,98]. On the other hand, dislocations have been known for a long time to constitute paths of enhanced diffusion, particularly in metals [99], and it has been hypothesized that a similar beneficial effect will arise in the electrodes of Li-ion batteries [100–102].

One of the earliest works to incorporate dislocations and their effects into models for electrode particles was described by Wei et al. [103]. In their model, as in the later approaches that followed, dislocations are regarded merely as an additional source of stresses that have no influence on diffusion. Following Prussin [32], the dislocation density is assumed to evolve proportional to the concentration gradients. Using a result of Estrin [104], they describe a *scalar stress* that develops due to the dislocation density and which is subsequently superimposed onto the radial and tangential diffusion-induced stresses in a spherical particle. The additional stresses due to the dislocations lead to a reduction of tensile stresses that develop during intercalation. Furthermore, these dislocation-induced stresses can convert tensile stresses to compressive stresses and hence reduce the tendency for crack initiation.

However, this approach has been disputed by Yang [105] on the grounds that the resulting stress fields violated the stress-free boundary conditions described by Wei et al. [103]. As an alternative, he proposed an elastic-plastic approach wherein the dislocation density affects the deviatoric stress components via the plastic strain. In his approach, the dislocation density would evolve with the curl of the concentration field instead of its gradient. Unfortunately, he only outlined his approach and did not give any results. In a separate paper, however, Yang [106] describes a simple model for the evolution of dislocation density in lithiated particles. By this, he demonstrated a size effect in the incurred dislocation density: he predicts a growing dislocation density due to lithiation with decreasing particle size. The eigenstrains caused by the formation of dislocations are further shown to reduce the intercalation-induced stresses.

Nevertheless, models using the approach by Wei et al. [103] have been applied for the computation of stresses in thin films [107], hollow spherical particles [108], or cylinders [109]. Chen et al. [110] applied this approach for the description of a phase transformations in a spherical particle and compared the resulting stress profiles with that of a simple phase-transforming particle and a single-phase material. Thereby, they expressed the dislocation density in terms of the lattice mismatch at the moving sharp phase boundary. They later used this model to derive stress intensity factors for a phase-transforming material [111]. The model proposed by Wei et al. [103] was further modified to include strains from forward and backward intercalation reactions [112] or, following the approach described in Refs. [113,114], to analyze the effects of surface stress in nanospheres [115] and nanowires [116], both of which affect the stress profiles within the considered electrode particles. The model has found further application by Ma et al. [117] for the analysis of irradiation-induced changes in the elastic constants and the plastic behavior of active electrode materials. The shown results agree well with the described experimental data, despite the aforementioned shortcomings of the underlying model.

Wang et al. [118] established a theoretical framework for relating the indentation hardness of a material sample to its state of charge. They make use of Prussin's relation between concentration gradients and dislocation density, from which they directly compute the material hardness by virtue of the Taylor orientation factor. An extension of their work considering elastic softening has been done by Ma et al. [119].

Huang and Wang [120] analyzed the stress fields due to several

dislocations in $LiFePO_4$ and discussed the onset of fracture in this material in terms of dislocation interaction. An analytical model for the generation of misfit dislocations has been proposed by Li et al. [121], where the generation rate is proportional to the strain energy within the layers of a thin film.

2.2.2. Phase separation

Phase transformation occurs in both anode and cathode materials. At the anode side, during the first cycle, crystalline silicon (c-Si) undergoes phase transformation to a-Si [122–127]. Even in a-Si, a two-step lithiation mechanism is observed, where two phases of a-Si coexist during the first lithiation, with single-phase lithiation in subsequent cycles [128,129]. Cathode materials such as $LiFePO_4$ and $LiMnO_2$ are also phase-separating materials, where two phases can coexist in a single crystal during (de-)lithiation [130,131]. Differential strains at phase interfaces lead to large mechanical stresses, which will not necessarily disappear even with open circuit condition. Moreover, Huang et al. [132] and Yang et al. [133] found that phase separation can change the sign of the stresses at the shell of a spherical Si particle. A particle under lithiation can hence experience tensile shell stresses, which runs against the common belief of compressed outer layers during ion insertion (e.g. Ref. [19]). They argued that the large compressive stresses in the shell at the onset of lithiation cause an immediate plastification of the shell and hence the release of compressive stresses.

In order to account for phase-separating behavior, two different models are employed: sharp-interface and phase-field (diffuse-interface) models. In the former, a discontinuity is imposed at the interface, and a subsequent strain mismatch will give rise to stress concentration at the interface [134]. This discontinuity can be described explicitly by a jump condition on an interface layer between two different domains (e.g. Ref. [135]); it can also be achieved by assuming a non-linear diffusivity that is infinitely large when $c = 1$, which effectively promotes a sharp reaction front [136]. These models have been employed in order to compute the stress build-up both in the bulk and at the interface in spherical and in hollow spherical particles [135,137,138] as well as in thin films [139]. They can also capture the velocity of a migrating interface in combination with reaction models such as the Butler–Volmer equation and bond-breaking kinetics at the interface [140,141]. It has further been found that lithiation-induced elastic softening of a-Si at the first cycle mitigate stresses in the following cycles [142]. Further, it has been found that external mechanical loading regulates lithiation and can lead to isotropic deformation even with anisotropic reaction kinetics in Si nano pillars, as shown in Fig. 3(a).

However, these sharp-interface models in general require sophisticated interface-tracking techniques when a solution with a moving interface is sought numerically. Phase-field models are thus employed as an alternative to sharp-interface models. Here, the interface is captured by a field variable, a so-called “order parameter”, and the tracking of the interface by an adaptive mesh can be avoided [72,86,145]. In phase-field methods, the expression of chemical potential Eq. (2) is modified so that it allows for two-phase coexistence. A simplest expression considering linear elasticity and a regular-solution model is given by Refs. [145,146].

$$\mu = \mu_0 + \mathrm{RT}[\ln c - \ln(1-c)] + \mathrm{RT}\chi(1-2c) - \kappa\Delta c - \Omega\sigma_\mathrm{h}, \tag{14}$$

where spinodal decomposition of two phases can occur for $\chi > 2$. The term containing the Laplacian of concentration (Δc) is an energetic penalty of forming a phase interface, with κ being a parameter related to this interfacial thickness. A Cahn–Hilliard-type equation is thus in place to govern lithium concentration evolution

$$\frac{\partial c}{\partial t} = \nabla\cdot\frac{\mathrm{D}c(1-c)}{\mathrm{RT}}\nabla\mu = \nabla\cdot\mathrm{D}\left\{[1-2\chi c(1-c)]\nabla c - \nabla(\kappa\Delta c) - \frac{\Omega c(1-c)}{\mathrm{RT}}\nabla\sigma_\mathrm{h}\right\} \quad \text{on } \mathscr{B}. \tag{15}$$

Since Eq. (15) is a fourth-order non-linear partial differential equation, numerical treatment is challenging in solving this, in particular for finite element method. One can use a mixed formulation [147], isogeometric analysis [144], or a staggered scheme for the numerical solution.

In specific applications, Eq. (14) needs to be modified for different materials. For instance for silicon, Eq. (14) needs to be formulated in a large deformation regime, potentially with consideration of plastic deformations [144,147,148,377–379]. Zhao et al. [149] extended this model to consider large deformation and Butler–Volmer-type surface reaction. They found through a simulation with a spherical particle that phase separation can be very different in a diffusion-limit regime and a reaction-limit one. Zhang and Kamlah [398] studied the impact of particle size and elastic parameters on the miscibility gap in $Li_xMn_2O_4$ and Li_xFePO_4 nanoparticles and discussed thehibiting conditions for inphase separation. Cogswell and Bazant [150] modified Eq. (14) with an orientation-informed elastic energy for the coherency strain between two phases in order to capture a striped pattern during lithium intercalation, known as a “domino-cascade” phenomenon [130]. A recent contriution by Nadkarni et al. [151] considered an anisotropic interface thickness tensor $\boldsymbol{\kappa}$ and studied its impact on phase stability in Li_xFePO_4 nanoparticles under lithiation and delithiation. Apart from strains, the diffusion mobility tensor can also be modified to capture the anisotropy of the interface [152].

Experimental observations indicate that nanosized olivine electrode particles exhibit amorphization in addition to phase separation. In order to study the conditions for amorphization, Chiang et al. formulated a phase-field model with the three state variables local concentration, crystallinity, and displacement [153–155]. Their model considers the interaction between diffusion and mechanical stresses, and its results indicate a critical particle size below which a particle will undergo amorphization in order to relieve stresses. As they show further, this behavior is driven by the applied overpotential and the lattice misfit between lithium-rich and lithium-poor phases. Their model finally contains an asymmetry in the energy barriers for the transition from a crystalline to an amorphous phase, which leads, over several charge-discharge cycles, to a gradual loss of crystalline structure of the active material.

2.2.3. Host material elastic stiffening/softening

The elastic properties of both cathode and anode materials vary with lithium concentration [156–159]. Deshpande et al. [160] used a concentration-dependent Young's modulus in the simulation of a cylindrical electrode particle and found that lithium stiffening is beneficial to avoid surface cracking during delithiation, and that a moderate lithium softening can alleviate particle cracking from the center under lithiation. Yang et al. [161] concluded that the composition-dependent modulus plays a significant role in determining the diffusion process as well as the stress field. First principal studies also suggest the consideration of change of Young's modulus in continuum level models. For graphite negative electrode, Qi et al. [6] have shown a softening in carbon-carbon bonds within the basal plane and a stiffening of interlayer bonds during lithiation. This results in three-fold increase in the elastic moduli. On the other hand, lithiation can also cause monotonic decrease/softening of elastic modulus for LiSn alloy negative electrodes material along with increase of Li concentration, as shown by Stournara et al. [5]. Guo et al. [162] presented a continuum model for a cylindrical Li-ion battery. In their contribution, the hydrostatic stress and concentration-dependent elastic moduli were taken into account. They found that the hydrostatic stress, other than the variable elastic

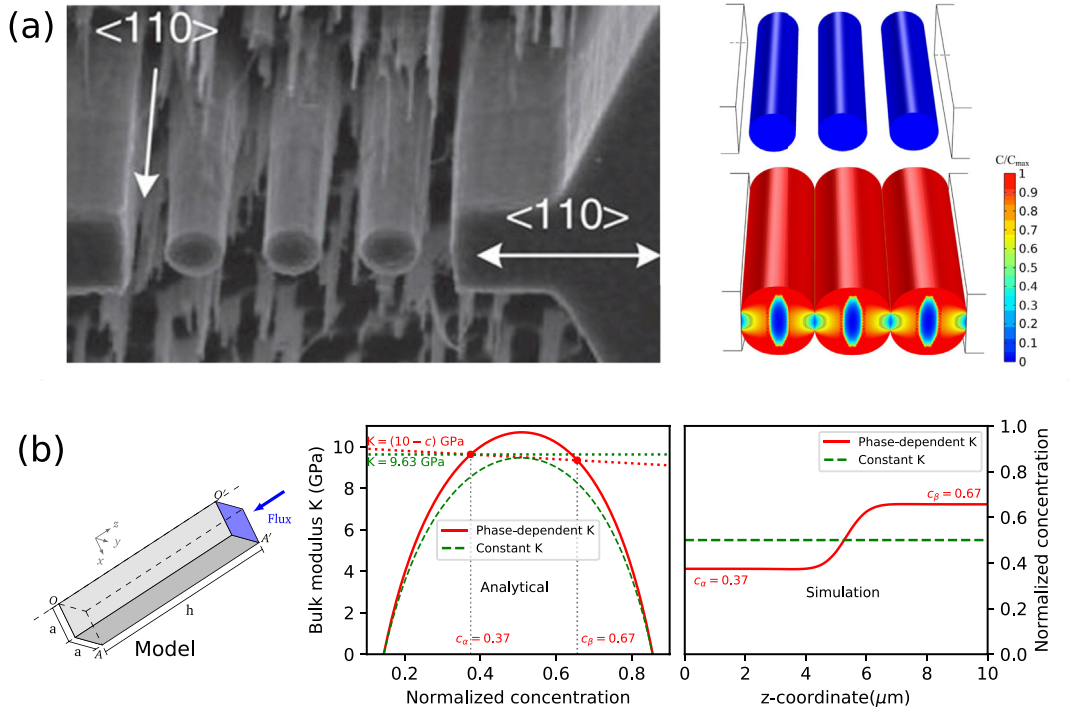

Fig. 3. (a) Experimental and modeling study of multiple Si nanowires lithiation and mechanical interaction. The geometrical confinement transform typical anisotropic lithiation behavior in Si to an isotropic one in the first cycle. Such modification should lead to lesser stress inhomogeneity and degradation of the Si anode. The results were then captured by finite element simulation [143]. (b) The influence of the mechanical constraint on a bar-shaped particle under fixed displacement boundaries. Analytical calculations and numerical simulations show that the phase separation behavior in equilibrium can be different with or without consideration of phase-dependent elastic moduli [144].

modulus, has little effect on the distribution of hoop stresses and radial stresses. Zhao et al. [144] used concentration-dependent elastic moduli in a phase-separating material, and found that variable elastic moduli admit a phase-separation where concentration-independent parameters would allow only for a homogeneous phase, as shown in Fig. 3 (b).

2.2.4. Anisotropy

Due to their anisotropic crystalline structure, nano-scale particles in general exhibit anisotropic properties. Lithiation of a c-Si nanoparticle is always associated with an a-Si shell and a polyhedral c-Si core crack initiation [138,163–166].

Levitas and Attariani [167] proposed a model which considered nonhydrostatic (deviatoric) stress contributions to the chemical potential of a-Si during lithiation and delithiation. They concluded that, despite the material isotropy of a-Si, deviatoric stresses cause anisotropic (tensorial) compositional expansion/contraction during Li insertion/extraction. Yang et al. [168,169] developed a model to study the phase and morphology evolution in silicon nanowires during lithiation. In their work, while the elastic modulus and bulk diffusion in two respective phases were treated as isotropic, the diffusivity inside the interface layer was assumed to depend on the local crystallographic orientation of the exposed c-Si surface. Anisotropic lithiation lead to stress inhomogeneities and fracture. In order to mitigate anisotropy-induced mechanical stresses, An et al. [170] engineered anisotropic morphologies of pristine c-Si particles that are deliberately designed to counteract the anisotropy in the crystalline/amorphous interface velocity.

$LiFePO_4$ crystals exhibit strong orthotropic behaviors. They offer exclusive 1D channels for lithium intercalation at interfaces between $LiFePO_4$ and $FePO_4$ phases [130]. Cogswell and Bazant [150], Tang et al. [152] employed phase-field models with orthotropic interfacial energy, diffusion models with orthotropic mobility, and elastic models with orthotropic elastic moduli in order to capture orthotropic phase separation during lithiation and delithiation. Recently, Li et al. [380] extended these models by surface diffusion effects and discussed, how these can circumvent the low ionic diffusivity across phase boundaries in strongly anisotropic phase-separating intercalation compounds.

In polycrystalline particles, due to the different orientations of different grains, the mismatch strains at grain boundaries give rise to large stresses and an increased electrical resistance. Hu et al. [171] presented a phase-field model for a composite with multiple aggregated rutile TiO_2 single crystals. They found that, the anisotropic diffusivity in a randomly distributed aggregates will result in inhomogeneous lithium distribution and smaller capacity. Moreover, the diffusion along the grain boundary is also different from inside bulk. Han et al. [172] studied the effect of grain boundary upon the generated stress inside particles. They have shown that the fast diffusion pathways along the grain boundary network minimize stress evolution inside the grains and result in higher accessible capacities.

2.2.5. Particle morphology and size effects

Within the common active electrode materials for LIBs, Li ions exhibit a rather low diffusivity. This results in high concentration gradients, and by virtue of the misfit strain, in high stresses, which can cause mechanical degradation of the electrodes. Vanimisetti and Ramakrishnan [173] performed a general survey on the impact of particle size and shape on the magnitude of the DIS. To that end, they calculated the stored strain energy as a function of the particle sphericity and found that fibrous or flake-like particles exhibit reduced stress levels. Similar observations have been made by Stein and Xu [63] who performed parameter studies on prolate and oblate ellipsoidal electrode particles under galvanostatic conditions. They could show that a belt-like zone of high mechanical stresses develops around the particles' equator. With increasing distance to this belt region, the stress levels decay rapidly, as can be seen in Fig. 4(a and b).

A reduction of diffusion path lengths can, for instance be realized by

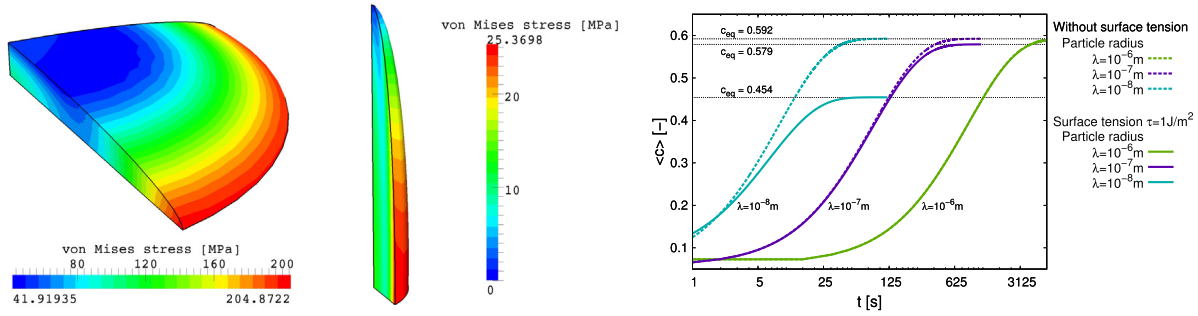

(a) (b) (c)

Fig. 4. Maximum von Mises stress distributions in oblate (a) and prolate (b) ellipsoidal particles for different aspect ratios Stein and Xu [63]. (c) Influence of the surface-stress-induced pressure in spherical electrode particles on the achievable state-of-charge. Through increase of the particles' electrochemical potential, the equilibrium concentration for a given potential will be reduced for a given stress. For smaller particle sizes, the relative impact of surface stresses (and hence the magnitude of the induced pressure) increases, yielding the particle-size-dependence of the capacity as shown above [174].

adopting hollow particles. Corresponding stress analyses have been performed by Harris et al. [175] and, under consideration of phase transitions, by Jia and Li [176]. Purkayastha and McMeeking [177] analyzed the intercalation into cubic electrode particles. The behavior of composite slabs/cylinders/spheres has been investigated by Suthar and Subramanian [178]. A common feature of these approaches is the use of analytical geometries such as spheres or cylinders [179].

It is clear that these idealized geometries are unable to reproduce the stress concentrations that emerge in the rugged, rough surfaces of realistic particles. These enhance the probability of fracture over the charge cycles. Studies on realistic particle shapes, for instance obtained from computer tomography (CT) scans, have been performed by Lim et al. [180], Chung et al. [181], Malavé et al. [182], and Hun et al. [183]. From their works it can be seen that the stresses in actual electrode particles exceed those in analytical geometries by as much as 410% [180]. Furthermore, these works demonstrated that irregular particles can fail locally even when the overall stress level in a particle is low.

However, such a fine-grained investigation of electrode particles requires huge computational efforts. In order to somewhat lessen these computational requirements, and to incorporate the immediate particle surroundings, phase-field methods can be adopted. Such frameworks have been described by Hu et al. [171] and by Lu and Ni [184]. Both groups describe the (agglomerate) particle geometry in terms of a phase-field model, where an order parameter describes the transition from electrolyte to active material. Hu et al. [171] extend this by further order parameters describing individual particle domains and their respective orientation. These models have been applied for the study of plasticity [184] and for charge transport [171] in agglomerate particles.

In recent years, nanostructuring of the battery electrodes has been proposed in the literature as a means to reduce DIS and to overcome the inherent low diffusivity of Li in the bulk material [185–190,381]. This trend is supported by experimental data indicating a high reversible capacity and stable cycling behavior [191] as well as a higher robustness against diffusion-induced mechanical degradation [7]. Accordingly, one can find studies on various nanoparticle morphologies such as nanowires [7], nanoflakes [192], nanowalls [193], inverse opal structures [194,195,382,383], hierarchical porous particles [196], or nanoporous electrodes [197]. This trend is further supported by additive manufacturing techniques which drastically widen the design space for electrode structures [198].

The size-dependent material behavior can be attributed not only to a lower defect density [384] and to reduced diffusion path lengths in the micro-structured material, but also to the effects of surface stresses, which gain an increasing influence with decreasing electrode particles size [199,200].

Classical models of elasticity cannot represent such size-dependent effects. However, they can be extended correspondingly through incorporation of surface elasticity models [201,202]. Said models trace their origins back to the work of Gibbs [203] and the contributions of Shuttleworth [204] and Herring [205]. The fundamental mathematical theory of surface elasticity has been established by Gurtin and Murdoch [206], who assumed the surface to be an infinitesimally thin layer around a solid body. In order to capture its behavior, they formulated elastic relations analogous to solid elasticity. A nonlinear thermo-mechanical diffusion model incorporating viscoelasticity and surface effects has been formulated by McBride et al. [207].

The first group to consider surface effects in modeling the behavior of nanostructured electrode particles have been Cheng and Verbrugge [113]. They set up an analytical model for the diffusion in spherical nanoparticles under surface stress. In their model, the effect of surface stress was considered as a particle-size-dependent pressure boundary condition. For convex particles, this (average) pressure can be determined from the particle's surface-to-volume ratio and the acting surface stresses using the Weissmüller–Cahn equation [208]. This caused a shift of the DIS towards the compressive regime, inducing an asymmetry between the charge and discharge behavior of the particle. However, in their model, they considered the diffusion to be decoupled from the stress field. This model has been later applied to the analysis of stresses in nanowire electrodes by Deshpande et al. [114].

The impact of surface stresses on the stress levels in insertion particles has later on been regarded by Hao et al. [209], DeLuca et al. [210], Gao and Zhou [385], and Zang and Zhao [211] in simulations of (hollow) nanowires and, in the case of the latter two, hollow nanospheres. Gao et al. [386] describe a model framework for the stress-coupled diffusion with surface stresses and applied it to the analysis of nanoporous materials. Liu et al. [135] extended these considerations by phase separation effects and showed that, despite the compressive stresses exerted on the hollow nanosphere by the surface stresses, strong tensile stresses can develop at the moving phase interface within the particle.

These approaches regarded spherical and cylindrical geometries, in which surface stresses will cause a homogeneous pressure. As in the case of DIS, the particle shape has a significant influence on the magnitude and distribution of the pressure field within the particle. Stein et al. [174] studied the interaction of constant surface stresses, stress-assisted diffusion, and electrochemical surface reactions in spherical and ellipsoidal electrode nanoparticles. They have shown that due to surface stresses, a pressure gradient arises in ellipsoidal particles which makes an appreciable contribution to the diffusional driving forces. Moreover, this pressure leads to a shift of the electrochemical potential which further affects the intercalation reactions at the surface (here modeled through a modified Butler-Volmer equation). Their results show that the interior pressure due to surface stress, while providing

mechanical stabilization, actually reduces the accessible capacity of the nanoparticles, as shown in Fig. 4 (c). Similar results have been obtained by Lu et al. [212] for spherical electrode particles under surface stress, considering variable surface stresses.

Stein et al. [213] recently calculated the migration energy barriers for Li vacancies in faceted $LiCoO_2$ nanoparticles which features strongly anisotropic surface stresses. Using finite element simulations and the defect dipole tensor concept, they could show that a heterogeneous pressure field develops in the nanoparticle under surface stress. Although this pressure distribution is expected to have a large impact on the diffusion of ions in the material, its energetic impact in migration barriers was shown to be negligible.

2.2.6. Buckling and wrinkling

Nanostructured electrodes usually exhibit slender features which, in combination with the intercalation-induced stresses, possess an inherent risk of mechanical instability, viz. “buckling”. This can be clearly seen in the work of Bagetto et al. [12], who produced planar silicon honeycomb structures as battery anodes. The morphology changes due to lithiation are illustrated in Fig. 2(d). Upon delithiation, the thin struts return *nearly* to their initial shape, with some struts some showing cracks at the center of the ligaments. This work motivated Bhandakkar and Johnson [214] to analyze the stability of these structures using an elastoplastic model, and to study the impact of a stabilizing, conductive scaffold within the structure. This has shown that buckling can be exploited so as to reduce diffusion-induced stresses in the microstructure. The critical buckling length of constrained nanowires was examined by Chakraborty et al. [215], who describe a large-deformation, elastoplastic model for diffusion-induced swelling and stress-drift. Zhang et al. [216] compared the critical state of charge for buckling with different diffusion paths, and they concluded that both nanowire length and current density play important roles in determining the critical state of charge when the buckling occurs. Zhang et al. [217] have extended this model to regard binary phase separation and could demonstrate that both single-phase and two-phase segregation possess, given identical geometry and loading parameters, an identical critical buckling time. Similarly, the critical buckling length depends only the prescribed constraints and the applied charge rate, not on the lithiation mechanism.

Yu et al. [218] reported that thin-film electrodes on compliant substrates can mitigate mechanical degradation and maintain a good cyclability. They further offer a way to mitigate lithium dendrite growth [219]. Jia and Li [220] attribute the enhanced cycling performance to wrinkling-induced stress relaxation. They also pointed out through modeling and calculation that a risk of necking bands near wrinkling troughs or peaks can occur, which may lead to fragmentation of the anode (e.g. Fig. 2(e)).

2.3. Model variations based on degradation mechanism

The preceding discussions focused on the extensions of the basic model based solely on the mechanism of lithiation and the incurred mechanical stresses. Right from the beginning of the collected modeling efforts, degradation has been a key issue in modeling LIBs. In this section, our discussion now rests on extensions of the basic model regarding specific degradation mechanisms.

2.3.1. Fracture

Fracture and delamination are critical factors that account for the deterioration of LIBs. High-capacity anode materials such as Si tend to fracture already during the initial few cycles whereas anode materials such as graphite in general exhibits stable cyclability. Large volumetric deformation of Si is also likely to give rise to delamination of Si from the current collector [221,222]. Commercial cathodes are usually fabricated as secondary particles, consisting, in turn, of crystallites with different orientations, also known as primary particles. Unless specified otherwise, all the particles to which we refer in this review are secondary particles, sometimes denotes as “meatball electrodes”. In two recent papers, Xu and Zhao investigate the disintegration of such electrode particles by means of cohesive-zone models for the separation of the primary particles and found that it is primarily the charging rate that drives the damage evolution in the aggregate particle [223,224].

Experiments have shown that both inter- and intragranular cracking of cathode particles are major failure mechanisms of cathodes at high voltage [225–227], especially for materials that undergo a phase change [228]. Due to the crystalline heterogeneity and microcracks, the mechanical properties of these particles, for instance the elastic modulus or the fracture toughness, span a wide range in the literature [229–231].

Extensive fracture models have been developed in an effort to find a proper description of the fracture of high-capacity anode materials, in particular for Si. Conventional cohesive zone models have been employed to study the fracture of Si nanowires [232], strip-shaped Si particles [233], Si nanopillars [234], and cylindrical graphite particles [235], as well as to the delamination of plate-like Si particles from the substrate [236–238,387]. This allows the determination of critical particle sizes and comparison with experiments.

Phase-field fracture models have been developed in order to simulate the crack propagation during cyclic charging of the particles [149,239–242], as shown in Fig. 5(a). These models can also predict crack propagation with different lithium content due to initial point defects in nano-sized anode materials, as shown in Fig. 5(c). Using a phase-field crack model, Zhao et al. [149] and Xu et al. [240] prescribed Butler–Volmer-type electrochemical reactions on both the initial particle surface as well as on the fresh crack surfaces. Based on phase-field models, Klinsmann et al. [241,242] concluded that a crack would initiate from a particle's surface and propagate inwards during delithiation (and vice versa). It is however worth noting that while this conclusion does agree with some experimental observations (e.g. Ref. [10]), it contradicts others (e.g. Ref. [138]), where visible cracks initiate from the surface and propagate inwards during lithiation rather than delithiation. There are several possibly reasons for this unexpected behavior. Firstly, the particles in the aforementioned experiments are, other than in the simulations, not free-standing, and inhomogeneous

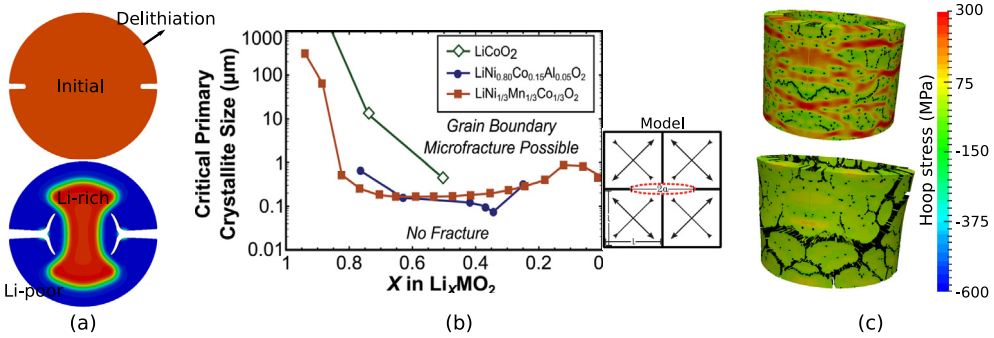

Fig. 5. Particle fracture due to different initial defects. (a) Crack propagation and branching of phase-separating material with initial notches under delithiation [149,240]. (b) Intergranular microcrack critia for secondary particles of selected $LiMO_2$ compounds. M stands for Co, Ni, Al and Mn. For a given SOC, crack can occur when the actual primary crystallite size exceeds the critical value [245]. (c) Crack propagation in a TiO_2 nanotube with randomly distributed initial point defects by an application of 1.26% strain due to lithium insertion.

mechanical/electrochemical boundary conditions can greatly affect the stress distribution inside the particles. Secondly, it can be argued that Si is a phase-separating material which will immediately deform plastically in the Li-rich phase in the shell, thus converting compressive stresses to tension in the shell region [132,136]. Finally, an anisotropic microstructure can increase the tensile stress in the shell so that a crack from the surface can become possible [169].

As an alternative to the two methods mentioned above, Barai and Mukherjee [243,244,388,389] described a stochastic computational methodology to model the crack propagation inside Si nanoparticles, using a lattice spring network to represent the particle.

The basic model in Section 2.1 is based on smeared-out microstructures, which yields a good estimation of stress levels, but which cannot predict stress concentrations across primary particles. Wu and Lu [246] developed a coupled mechanical and electrochemical model to predict intercalation-induced stress in a secondary particle with an agglomerate structure. Woodford et al. [247] derived a fracture criterion for a single $LiMnO_2$ particle with respect to different charge rates (C-rates) and particle sizes based on a continuum model and stress intensity factors. They also derived C-rate-independent criteria for grain boundary microcracks of the particles based on a microstructure-informed model [245], as shown in Fig. 5(b). In a series of papers, Zhao et al. [391–393] investigated the stability and growth of pre-existing cracks in electrode particles under diffusion-induced stresses and derived critival sizes below which the crack growth would be arrested. Similarly, Haftbaradaran et al. [390] investigated the delamination of Si thin films from the current collector using a fracture mechanics model. Gao et al. [394] formulated a J-integral for coupled deformation and diffusion and analyzed driving forces for crack growth in thin-film Si electrodes. Zhang et al. [395] recently employed a combined experimental-numerical approach to analyze the failure of coin-cell electrodes. Sun et al. [248] studied the fragmentation of granular cathode particles and pointed out that intergranular cracking is most severe in the first cycle. They performed sequential diffusion and deformation analysis upon the secondary electrode particles model to understand the mechanical decohesion and fracture between primary particles. Such degradation is clearly related to capacity fade as this would expose fresh electrode surface to electrolyte which will cause mobile Li consumption. To understand the damage between different domains (or particles), the contact area is described with a cohesive zone model. A linear traction-separation law was imposed which is sufficient to locate the crack initiation regions inside the 2D framework of spherical shaped secondary particles.

2.3.2. Solid-electrolyte interphase formation

The solid-electrolyte interphase (SEI) is a passivating layer formed on the electrode/electrolyte interface, which, under ideal conditions, is stable during cycling, permits fast lithium transport and, at the same time, is an electronic insulator. While the SEI is often referred to as the layer formed at the anode side, it can also form on the surface of the cathode particle, where is denoted as cathode-electrolyte interphase (CEI) [249]. In this section, we will consider only battery cells with liquid electrolytes; SEI formation for solid electrolytes will be discussed in Section 5.

Traditionally, SEI formation is more a chemical than a mechanical issue, depending heavily on the choice of the electrolyte. For a review on modeling of SEI formation from a chemical point of view, one can refer to the work of Wang et al. [250]. Nonetheless, mechanical problems arise when active materials with large volumetric change under (de-)lithiation are used. Due to the swelling and shrinkage of the active particles, SEI repeatedly forms and breaks down, resulting in a very thick SEI layer, capacity fade, and an increase in resistance [15]. For the description of the growing SEI and the stresses arising within, Rejovitzky et al. [251] formulated a continuum model, described its finite element implementation, and investigated the stresses on the SEI/anode-particle interface for spherical- and spheroidal-shaped graphite particles. Guan et al. [252] developed a phase-field model to simulate the morphological evolution of the SEI. With a prescribed contact angle between the newly produced SEI species and the graphite anode, they were able to capture the microstructure evolution of the SEI formation.

2.4. Concluding remarks

Lithium (de-)intercalation from and into an active electrode particle is a core mechanism for the functioning of a LIB, involving appreciable mechanical effects. Research into the degradation of battery electrodes has gained significant traction with the proposition of Si as anode material. This material promised to deliver a jump in available battery capacity, but its application highlighted a disappointing cycling performance due to mechanical degradation. Combined experimental and theoretical studies have identified a couple of mechanisms contributing to the behavior of Si particles, including large inelastic deformation, amorphization of the crystal structure, phase separation, anisotropy, fracture, and SEI formation.

Despite the intensive studies and the numerous modeling approaches, there remain several open issues that warrant further attention:

- The intercalation of lithium into a host material potentially leads to large inelastic deformations and the amorphization of the crystal structure. Through this mechanism, intercalation-induced stresses can be mitigated. A host of models has been described in the literature in order to capture this behavior. Based on observations made on metals, it has been hypothesized that the solid-state diffusion of Li ions can be potentially enhanced by a dislocation-rich microstructure. Current modeling approaches consider dislocations only insofar as they generate additional stresses in the bulk material, with the diffusion of ions being decoupled from the (evolving) dislocation density. The challenges that need to be overcome in order to follow this line of work involve the specification of dislocation systems at the microscale and the consistent homogenization towards the larger scales.
- The elastic properties of the active electrode materials have been shown to depend on the concentration of lithium. The resulting softening/stiffening effects can reduce the danger of crack initiation/growth and play a major role in the formation and stability of phases. Under lithiation, Sn exhibits a series of phases with different lattice parameters and elastic properties. The models discussed here have so far assumed a linear relationship between elastic properties and lithium concentration and deserve an extension towards more faithful, nonlinear relations between elastic properties and lithium concentration.
- Anisotropic properties are common in nano-scale particles due to lattice structures. These will influence diffusion directions, elastic stretching, and phase separation. They can also induce mismatch strains in polycrystalline particles among grains. Anisotropic elastic and chemical properties are readily incorporated into continuum models through the corresponding tensors. A factor that so far has found scarce attention is that fact that the chemical eigenstrain due to intercalation may have non-spherical components. The required information can be gained from atomistic simulations and can be integrrated into continuum-level models by means of the defect dipole tensor concept [53,213,253].
- The impact of surface stresses on the chemo-mechanical behavior has predominantly focused on the pressure induced by the surface stress, which provides mechanical stabilization. However, the interaction of the, in general, heterogeneous pressure field with the ion transport has only found scarce attention. The studies so far concentrate on simple, analytic particle geometries and mostly on isotropic, deformation-independent surface stress. Realistic electrode nanostructures with surface stress effects have not been investigated yet. We do not expect the extension of the considered

surface stress models to pose significant problems. Further attention, however, has to be paid to the determination of suitable surface-elastic parameters from atomistic computations and their incorporation into the continuum setting.

- With the trend towards slender nanostructured electrode morphologies arises the risk of mechanical instability and failure through buckling. For elastic materials, this can be beneficial, allowing to relax stresses through a structure's evasion from the stressed initial state. Current studies focus on honeycomb structures and constrained nanowires, and first steps have been made in deriving critical buckling lengths and charge conditions for nanowire electrodes. The growing field of additive manufacturing also opens up new design directions for electrode microstructures, for instance in the form of inverse opal structures or microlattice frameworks. Although their high stiffness at relatively low weight and their high surface-to-volume ratio renders them interesting candidates for application as battery electrodes, these morphologies have not found attention in the mechanical community yet.
- Formation of the solid-electrolyte interphase is a major degradation mechanism in Li-ion batteries, featuring a loss of Li through formation of a passivating layer. Phase-field models again prove to be very efficient means for the description of this phenomenon. Despite the suitability of these model for the description of crack formation and propagation, studies on the formation and cracking of the SEI have not been undertaken yet. The dendritic growth of metallic lithium is a related factor, which can, through penetration of the separator layer, result in short-circuiting of the battery cell. Although it is generally believed that lithium dendrite formation is related to mechanical constraints in solid-state electrolyte, a convincing mechanism is not yet ready.

3. Composite electrode level

Most commercial batteries employ composite electrodes for both anodes and cathodes. These composite electrodes comprise, in general, active particles with a wide variation of sizes and morphology. These particles are supported by binders and conductive agents for improved mechanical integrity and electrical conductivity, respectively. The pores of this structure are filled by liquid electrolyte which wets the surface of the active material and provides continuous pathways for conducting lithium ions. This structure slightly differs for solid electrolytes, which will be discussed in Section 5. The inherent heterogeneity of the structure naturally leads to inhomogeneous distributions of lithium salt concentration, mechanical stresses, and electric potential in the electrode during the charge/discharge cycles. This, in turn, has a fundamental impact on the coupled electrochemical, thermal, and mechanical behavior of the composite electrodes. The discussed electrode models in the current section are formulated at a length-scale of several micrometers, which is sufficient to capture the heterogeneity. In order to evaluate the influence of this heterogeneity on the performance of the battery and to optimize its structural design, a proper composite electrode model is necessary. Spatially resolved models are thus employed in order to represent the different physical fields and their interactions in a heterogeneous structure under specific battery operating conditions.

Nonetheless, the physical processes taking place inside a composite electrode span several length- and time-scales, which renders straightforward modeling of a complete electrode very demanding. This drives the development of homogenization models based on the theory of micromechanics, where the relevant fields are averaged over a representative volume element (RVE). These models allow to bridge the gap in different spatial and temporal scales and can further provide effective quantities for cell-level calculations. Both approaches are discussed in the following sections.

3.1. Spatial field calculation of electrode models

Spatially resolved calculation upon composite electrode models can be considered as a natural extension of the single particle models, where the individual particles are embedded into solid matrices and their surfaces are wetted with electrolyte. These models however exceed the models for single, free-standing particles in that they are able to describe additional electrochemical and mechanical behaviors stemming from the electrode microstructures. Electrode microstructures are reported to be greatly affected by manufacturing processes, such as sintering temperature, compaction pressure, slurry composition, and particle size and shape distributions [254]. By electrochemical simulation upon composite models from actual tomographic or sectioned sample data, these effects can be assessed, aiding the optimization of the corresponding manufacturing processes.

3.1.1. Particle spatial distribution and size polydispersity

Experiments have shown that, through engineering the particle spatial distribution, an electrode's ionic resistance can be decreased concurrently with an improvement of the electronic transport behavior [255]. García et al. [44] carried out calculations based on synthetic two-dimensional microstructures. By varying particle spatial arrangement for a fixed particle volume fraction and for homogeneous particle radii, they evaluated microstructural effects in power density and stress evolution inside the electrode during discharge. Particles in different regions are thereby subjected to different Li intercalation mechanisms: particles close to the anode take on lithium mainly due to the potential drop. For particles far away from anode, on the other hand, the concentration difference is the driving force for intercalation since these particles are electrically shielded from potential gradients. This has an impact on the state of lithiation and on the stress state for different regions within the electrode, resulting in different cycle life expectancies for the constituent particles. Based on this model, Chung et al. [256] assessed the influence of particle size polydispersity and surface roughness on the electro-chemical and mechanical response of an electrode. They showed that, due to a reduced area density, the power density of the battery would be lowered for increasing particle size dispersity, whereas the energy density would be higher in a polydisperse electrode than in a monodisperse electrode. Based on simulations of two-dimensional electrode geometries, Ji et al. [257] showed further that the mechanical stresses in composite electrodes can show a local variation for a given state of charge and that smaller particles experience faster charge/discharge.

The impact of particle size polydispersity on the electrochemical behavior is even more pronounced in phase-separating electrode materials. In order to simulate the inter-particle behavior in a cathode made of phase-separating active material, phase-field models have been employed by Zhao et al. [258], Jesus et al. [259] and Li et al. [260]. Their results showed that phase separation in a particle ensemble can differ greatly from that in stand-alone particles. In particular, it seems to be energetically favorable to establish phase interfaces not only within particles but also across particle-particle contact points, as illustrated in Fig. 6(a and b).

3.1.2. Particle-matrix interaction

In porous electrodes, particles are mechanically connected and supported by binders, which are in general electrochemically stable, well adhesive to particles and current collectors, and sufficiently compliant to compensate particle deformation. Aifantis et al. [262–264] considered cylindrical or spherical particles embedded into a glassy matrix. In their model, the concentration field is not explicitly given but implicitly described through the volumetric expansion. When embedded particles are fully lithiated, the exterior matrix experiences tensile circumferential stresses due to the swelling of the active particles, which can result in radial cracks nucleating at the interface between active particle and matrix. Using a 2D plane stress model, Rahani

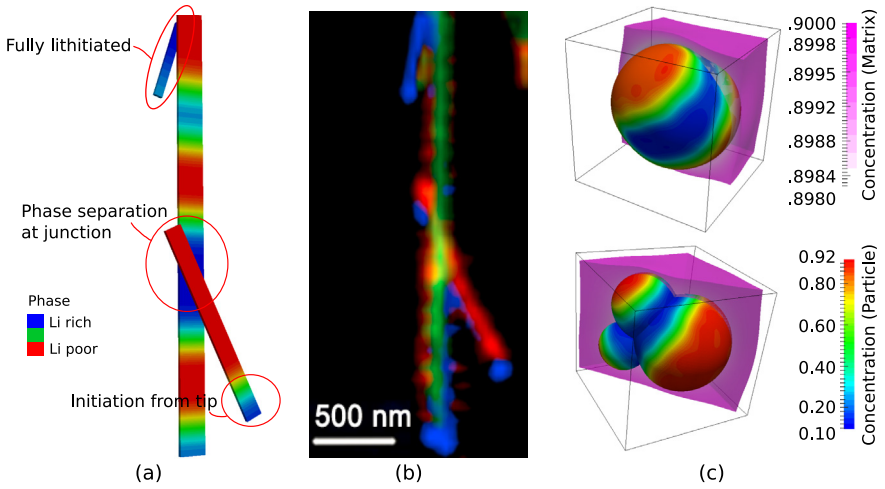

Fig. 6. (a–b) Inter-particle phase separation. (left) simulation results of a connected network of three particles. (right) a reconstructed compositional and phase heterogeneity across the interconnected network based on scanning transmission X-ray microscopy (STXM) maps [259]. (c) Concentration distribution of the deformed composite electrode with spherical and Mickey-mouse-shaped particles embedded in the polymer matrix at one time instance during lithiation [261].

and Shenoy [265] studied the stress distribution inside a graphite-based porous electrode subject to different charge-discharge regimes and graphite diffusivities. In their model, they considered two different microstructures of binder connecting the spherical graphite particles: binder bridges and binder shells. An extension to a 3D model allowed them to derive upper bounds for compressive and tensile stress generated at the binder-particle interface. Xu et al. [266] developed a finite element model simulating the coupled Li diffusion and mechanical stresses for three-dimensional composite electrodes. Based on this model, they simulated $LiNi_xMn_yCo_zO_2$ (NMC) cathodes and SnO anodes and demonstrated that the mechanical confinement through the inactive matrix and the inter-particle contact can give rise to significant capacity losses. Zhao et al. [261] studied a 3D porous cathode comprising an irregular-shaped particle immersed in a polymer matrix with the finite cell method, as shown in Fig. 6 (c). The particles thereby exhibit a phase-separating behavior. A Butler–Volmer-type reaction is imposed at the particle-matrix interface, which governs the flux across the interface through the electro-chemical and mechanical status in both phases. Wang et al. [267] developed a model to study the stress evolution at the contact points and the binder/particle interface of spherical Si particles under cyclic electrochemical condition and thus highlighted the effect of binder mechanical properties, binder fraction, and charge/discharge strategy due to inelastic shape change of Si anodes. Motivated by experimentally observed battery degradation, Kim and Huang [268] studied the stresses on the cathode-electrolyte interface due to the fluid-structure interaction of active material and electrolyte.

3.1.3. Image-based reconstruction of electrode microstructure

In spatially resolved models, microstructures can be either generated artificially, based on porosity and particle size distribution [269,270], or they can be created using image-based methods [271]. Whereas the latter approach is computationally more expensive, in particular for 3D simulations, it preserves the geometric characteristics of the electrodes. This is important insofar as studies have shown that the electrode morphology has a significant influence on the electro-chemo-mechanical behavior of the electrodes. To reconstruct the 3D geometry for calculation, images extracted from micro/nano CT scans or from Focused-Ion Beam (FIB) sectioning are stacked in order to form a 3D voxel structure. This data set is subsequently processed by segmentation, smoothing, filtering, and geometrical reconstruction to yield a model of the geometry. The image-based reconstruction relies heavily upon proper segmentation or identification of different phases such as active particles, binder, or conductive agents and is potentially highly demanding for a better isolation of these intermingled phases. Roberts et al. [272] presented a computational framework that directly resolves the microstructure of many cathode particles and the surrounding electrolyte. They also investigated the particle-to-particle contacts and they found that the largest stresses are located at the particle-to-particle contacts. A similar simulation with a conformal decomposition finite element method was performed by Mendoza et al. [273] on microstructures as illustrated in Fig. 7. In their model, they regarded the mechanical effects of the electrochemically inactive binder and showed that the binder helps to mitigate stress generation between the particles. Kim et al. [274] performed micro-scale simulation on representative volumes generated from actual FIB micrographs. The boundary conditions have thereby been derived from 1D macroscale electrochemical models. With these conditions, they computed both the diffusion-induced stress and the thermal stresses for different macroscale discharge rates and hence, could assess and compare the relative local evolution of DIS and thermal stresses. Wu et al. studied the stress generation inside different regions of reconstructed NMC [275] and $LiCoO_2$ [276] half-cells due to phase transition and Li intercalation. They considered an additional term for phase volume mismatch in the mechanical part which causes high stress state.

3.2. Homogenization of electrode models: effective properties

The electrode models described in the previous section, be they generated artificially or from micrographic images, are subjected to electro-chemo-mechanical modeling under suitable boundary conditions. The heterogeneity of structures is thereby explicitly addressed, and its effect is reflected in the solution fields. In homogenization studies of electrode models, on the other hand, the details of the microstructure are incorporated by RVE models, where effective quantities such as diffusivity, tortuosity, and elastic constants are calculated based on micromechanics theory.

Homogenization of the chemical and electrical properties of composite electrodes have been studied intensively [277–280]. A significant contribution was made by Newman et al. [281–283], who presented one of the first frameworks homogenization of a complete composite electrode. In their model, the porous electrode is assumed to consist of three phases: the electrode phase, the electrolyte phase, and the conductive filler, each characterized through the volume fractions ε_s, ε_e, and ε_f, respectively. For simplified cases, electrodes particles were all assumed spheres with an identical radius R_s that are distributed homogeneously across the electrode. Similarly, the conductive filler is also assumed to be homogeneously distributed, with the electrolyte filling up the remaining space. The effective conductivity k_{eff} and diffusivity D_{eff} inside the electrolyte are then approximated by

$$k_{\text{eff}} = \frac{\varepsilon_e}{\tau} k_e = k_e \varepsilon_e^{1.5}, \quad D_{\text{eff}} = \frac{\varepsilon_e}{\tau} D_e = D_e \varepsilon_e^{1.5}, \tag{16}$$

where k_e and D_e are the respective quantities in a pure electrolyte. τ is

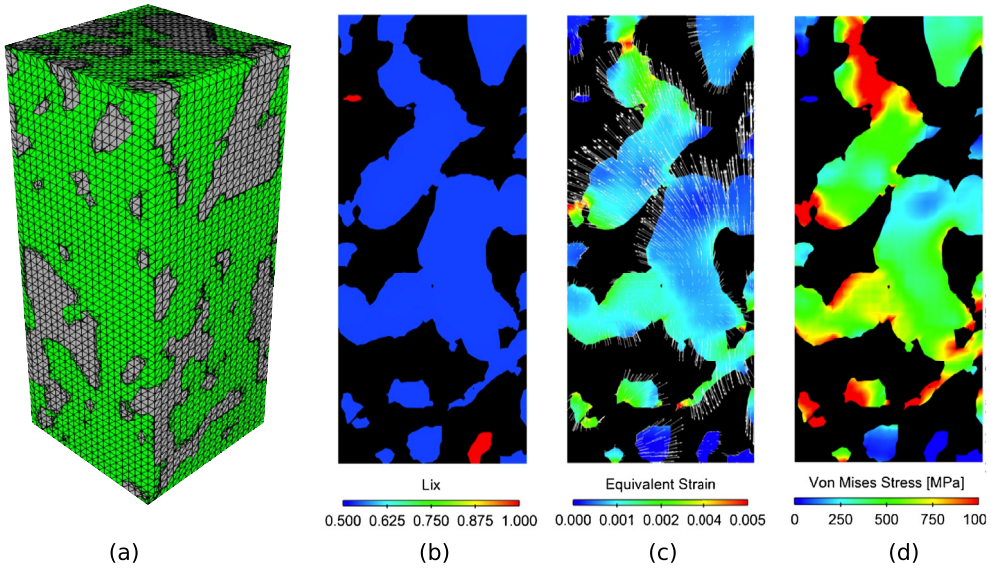

Fig. 7. (a) Numerical mesh for the reconstructed electrode. Distribution of (b) lithium fraction (Lix), (c) equivalent strain and (d) von Mises stress [GPa] at a cross section for baseline case (1C) at a SOC = 1 [273].

the torturosity, taken as $\varepsilon_e^{-0.5}$. Note that the choice of τ is empirical, which accounts for the actual path length of the species in an electrode with spherical particles. There exist other empirical relations that are extensively used in porous electrode models, but they are limited by the assumptions made in their derivation, such as Bruggeman's relation [284,285]. In the early works, the porosity ε_e can also vary with the extent of reaction, without the consideration of expansion and compression of electrode particles (e.g. Eq. (11) in Ref. [281]). The volume change in porous electrodes was considered in the work of Weidner and coworkers [286–289], who based their model on the assumption that solid-phase reaction product during operation contributes to the change of porosity as well as stress-free electrode dimensional change.

Homogenization using reconstructed microstructures have, for instance, been undertaken numerically by Yan et al. [290] and by Wiedemann et al. [291]. Following micromechanics theory, a linear Poisson equation is solved over the solid and electrolyte phases in the reconstructed geometries using certain predefined boundary conditions, enforcing, for instance, an average concentration gradient in the sample. Effective conductivity and diffusivity can then be obtained by dividing the average flux vector by the prescribed average concentration gradient. This approach has been pursued by Hutzenlaub et al. [292], who employed a hybrid segmentation method for a 3D reconstruction for a $LiCoO_2$ composite electrodes consisting of three phases: active material, binder, and pores space. Ebner and Wood [293] used scanning electron microscopy (SEM) micrographs to develop a tortuosity estimation method based on differential effective medium approximation. They validated their methods using different particle shapes with known Bruggeman's estimation. Similarly, Cooper et al. [294] used an image-based modeling method to compare tortuosity factors estimated from Bruggeman's method with geometrical and numerical methods.

For the homogenization of an electrode's mechanical properties, Golmon et al. [295] followed Mori–Tanaka's theory [296], assuming the effective elasticity tensor $\mathbb{C}_{\text{eff}}$ to read

$$\mathbb{C}_{\text{eff}} = \mathbb{C}_m + (1 - \varepsilon_e)(\mathbb{C}_s - \mathbb{C}_m)\mathbb{A}_s, \tag{17}$$

where

$$\mathbb{A}_s = \mathbb{A}_D[\varepsilon_e 1 + (1 - \varepsilon_e)\mathbb{A}_D]^{-1}, \qquad \mathbb{A}_D = [1 + \mathbb{S}\,\mathbb{C}_m^{-1}(\mathbb{C}_s - \mathbb{C}_m)]^{-1}.$$

Here, ε_e is the volume fraction of the electrolyte, $\mathbb{C}_s$ and $\mathbb{C}_m$ denote the stiffness tensors for the active particle and matrix with the electrolyte, respectively, 1 is the identity tensor and $\mathbb{S}$ is the Eshelby tensor. The effect of a macroscopic eigenstrain due to lithium insertion can also be obtained from the micro-scale eigenstrain as shown by Inoue et al. [297].

Apart from analytical expressions, effective coupled chemo-mechanical properties can also be obtained numerically. To that end, Awarke et al. [298] performed two-scale finite element (FE^2) simulations of a composite $LiFePO_4$ cathode and evaluated its displacement field, potential field, and SOC distribution when subjected to external loads and diffusion-induced stress. Its effective elastic modulus and SOC-dependent volumetric expansion were calculated on an RVE, which has a microstructure with monodisperse spheres based on the known material densities, porosity, and particle sizes. The interstitial voids between spheres were assumed to be filled by polymeric binder phase, and periodic boundary conditions were applied for the RVE.

3.3. Concluding remarks

Models for composite electrodes are valuable for evaluating the particle-particle, particle-matrix and particle-electrolyte interactions. In that, they extend the narrow focus made by the particle-level models discussed in the previous section. This allows to identify the effects of (dis-)charge “hot-spots”, inhomogeneous mechanical constraints, chemically inactive binder, and of the heterogeneous chemical reactions taking place throughout the electrode structure and their combined impact on cycle life expectancy of the electrode structure. Current models are however restricted to stress analyses of the considered structures. Thereby, the diffusion is usually considered to be decoupled from mechanical stresses, which excludes a significant driving force from the chemical problem, as was discussed in Section 2. Moreover, due to computational cost, the models currently do not account for mechanical degradation such as fracture of particles or the delamination of the composite structure.

Homogenization techniques are essential for bridging the gap between the electrode scale and the cell scale. The effective quantities calculated from such techniques are the representative characteristics of the composite electrode microstructure and are used in cell models for the prediction of the overall electrochemical and mechanical behavior. However, mechanical effects have so far only found scarce attention, for instance in determining the effect of porosity change under intercalation or due to external stresses. The contributions from mechanical effects have so far not found consideration in the effective transport quantities.

4. Cell level

Cell models have been proposed and studied extensively in order to predict the overall cycling performance of the whole cell. They are, nevertheless, mostly restricted in the study of electrochemical performance while mechanical contributions are disregarded. Reviews of these models are provided by Thomas et al. [299], Santhanagopalan et al. [300], Landstorfer and Jacob [301], and Jokar et al. [302]. However, as will be shown in this section, mechanical stresses in electrodes and separator influence the overall electrochemical performance of the battery cell even with liquid electrolyte. Mechanical effects play an even more significant role in batteries with solid electrolyte, which will be discussed in Section 5.

Modeling the complete functioning of a battery cell involves a set of partial differential equations across the porous electrodes, the electrolyte, and the separator. The computational costs to solve these equations in great detail, be it even for one charge and discharge cycle, are unaffordably high. Thus, simplified cell models with different multi-scale techniques are proposed. In this section, we will review these models, putting our focus on the cell models which consider mechanical contributions to the cell performance. Based on the employed homogenization techniques and the levels of detail that the models can resolve, we organize these models into three categories: pseudo-2D cell models, single-particle cell models, and 2D/3D cell models.

4.1. Pseudo 2D cell models

Pseudo-2D (P2D) models consider two length scales concurrently, namely the cell level and the particle level. These models are denoted as "pseudo-2D" models due to the fact that at both length scales a respective 1D problem is solved. At the cell level, the Li-ion transport and the consequent potential variation are assumed to occur only between the electrodes; at the particle level, a spherical particle with spherical symmetric properties is assumed, which reduces the intercalation process to a 1D problem in radial direction. Understandably, these models are also referred to as "one-plus-one models". The first P2D model, which did not consider mechanical effects, was proposed by Doyle [303] for a Li|PEO_8–$LiCF_3SO_3$ |TiS_2 half cell. Fuller et al. [304] extended this model to consider a full cell in a Li_xC_6 |propylene carbonate–$LiClO_4$ |$LiMn_2O_4$ system. The finite-volume-method-based package Dualfoil [303] was developed for the simulation of the half cell and full cell systems. Despite a wide variety of P2D models considering mechanical stresses, the governing equations at the cell level usually exhibit the same structure, summarized in Eqs. (18) to (20) in Table 1. Note that, in the model presented in Table 1, mechanical stresses at the cell level are disregarded. They are only considered at the particle level, where the stress-assisted diffusion equation in a single spherical particle (e.g. Eq. (7)) is solved at the anode and the cathode. The pore-wall flux $j_{s,k}$ in Eq. (21) is then critical to bridge the two levels, which is based on Butler–Volmer kinetics, involving physical quantities at both cell level and particle level.

This P2D model has been used by Christensen [305] in combination with their earlier work on single particles [19] in order to study the electro-chemo-mechanical response at high currents. Further coupling with thermal effects in the cell level, applied to the description of a lithium-ion polymer battery pouch cell, was performed by Fu et al. [306]. They concluded that the pressure diffusion and the lattice distortion with large deformation have a significant impact on the electrochemical performance of the battery cell. Suthar et al. [307] proposed an optimization framework to estimate optimal charging profiles. Their results show that the local pore wall flux has a significant difference from the average current density, which highlights the importance to apply P2D model to capture the peak radial and tangential stresses. Later, they extended their model to investigate the effect of porosity, thickness, and tortuosity on the degradation of graphite anode [308]. This study shows that a smaller porosity together with a larger tortuosity can lead to a significant reduction in discharge capacity, where the stresses play an important role in capacity fade mechanisms. Dai et al. [309] extended the P2D model to consider an electrode with blended and mixed $LiMn_2O_4$ (LMO) and $LiNi_{0.8}Co_{0.15}Al_{0.05}O_2$ (NCA) particles. They found that stresses generated in the LMO particles are reduced by adding NCA to the cathode, which can improve the cell performance.

Renganathan et al. [310] studied phase transformations within $LiCoO_2$ particles with an extended P2D model, where a two phases system coupled with mechanics has been modeled at the particle level. Their results indicate that particles can be damaged due to the residual strain caused by phase transformation. In order to consider the influence of phase separation and particle morphology, Bai et al. [311] considered a cell with spheroidal particles that experience phase separation, as shown in Fig. 8. They concluded that stresses can play a major role in modifying the capacity, and that phase separation inside an active particle can lead to a long potential plateau during discharge.

In order to account for external loading at the cell level, Golmon et al. [295] extended the P2D model by adding a RVE for the mechanical bridging between the cell and particle level. The effective elastic tensor was calculated based on Mori-Tanaka's theory, as

Table 1
The governing equations for the P2D model at the cell level and for bridging between the particle and the cell levels. The models for the particle level can be found in detail in Section 2. In the equations, subscripts n, p, and s represent the negative electrode, positive electrode and separator regions, respectively. In each region, there are two phases: a solid particle phase (with subscript s) and a liquid electrolyte phase (with subscript e). At the cell level, one solves for the liquid concentration c_e and the electrostatic potentials ϕ_s and ϕ_e in all three regions. c_k is the lithium concentration inside the particle with the subscript representing the electrodes. Its surface concentration is denoted by a superscript surf and the maximum concentration by the suffix max. D_{eff} and k_{eff} are the effective diffusivity and conductivity in the electrolyte defined in Section 3, and σ_{eff} is the effective conductivity of solid phase. $j_{s,k}$ denotes a scalar flux between a particle and the surrounding electrolyte, governed by a Butler–Volmer equation depending on the overpotential η. Comparing the expression of Eq. (21) and Eq. (12) in Section 2.1, $K_k\sqrt{(c_k^{\max}-c_k^{\text{surf}})c_k^{\text{surf}}c_{e,k}}$ equals to an exchange current i_0. K represents the reaction rate for (de-)lithiation. Note that in the separator region, $j_s = 0$, thus leading to a vanishing source term in Eqs. (18) to (20).

Region	Governing equations	
Cell level (k=n, p,s)	$\varepsilon_k\frac{\partial c_{e,k}}{\partial t} = \nabla\cdot(D_{\text{eff},k}\nabla c_{e,k}) + a_k(1-t_+)j_{s,k}$	(18)
	$\nabla(\sigma_{\text{eff},k}\nabla\phi_{s,k}) - a_k F j_{s,k} = 0$	(19)
	$\nabla\left(k_{\text{eff},k}\left[\nabla\phi_{e,k} - \frac{RT}{F}(1-t_+^0)\nabla\ln c_{e,k}\right]\right) + a_k F j_{s,k} = 0$	(20)
Level bridging (k=n,p)	$j_{s,k} = K_k\sqrt{(c_k^{\max}-c_k^{\text{surf}})c_k^{\text{surf}}c_{e,k}}\left[\exp\left(\frac{F\eta_k}{2RT}\right) - \exp\left(-\frac{F\eta_k}{2RT}\right)\right]$	(21)
	$\eta_k = \phi_{s,k} - \phi_{e,k} - U_k(c_k^{\text{surf}})$	(22)

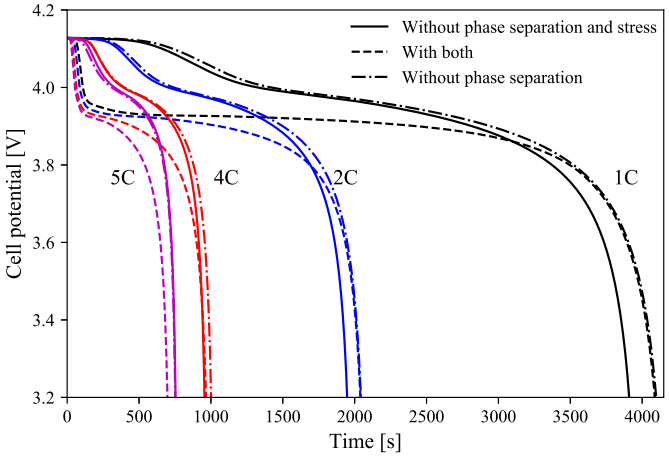

Fig. 8. Evolution of a Li|PEO-$LiCF_3SO_3$|$LiMn_2O_4$ cell potential during discharge with models considering different coupling cases in cathode particles at different discharge rate: one model considering both stress-assisted diffusion and phase separation, one considering only stresses and the last one disregarding both. For the modeling, Eqs. (18) to (22) and the mechanically coupled Cahn–Hilliard diffusion model described in Section 2.2.2 are employed. It is shown that stresses in general improve cell capacity, especially at low discharge rates. Phase separation promotes a stable discharge potential for a long time.

discussed in Eq. (17). They applied their work to the study of a Li-foil|$LiMn_2O_4$ half-cell and the results show good agreements with previous published work as well as the experimental observations. Based on Golmon's work, Xiao et al. [312] studied the stress distribution in polymeric separators in a LiC_6 |$LiPF_6$ |$Li_yMn_2O_4$ battery. In their model, instead of an analytical expression, they build a numerical RVE (submodel) to obtain the stress-strain relation, where different stacks of particles are investigated. They concluded that the local strain at the indented areas was much higher than the nominal strain of the separator, which is dependent upon the particle size and particle packing. Xie and Yuan [313] further incorporated SEI formation in the model and simulated the capacity fading process. Behrou and Maute [314] introduced a damage variable to the active particles to investigate the capacity fade of LIBs due to accumulated damage of the active particles. They have also discussed the influence of particle size polydispersity on the battery performance and they concluded that cathodes with uniform particle size will lead to more significant capacity fade than with non-uniform particles.

4.2. Single-particle cell models

Single-particle cell models (SP models) can be considered as a simplified version of P2D models, where the spatial variation over both electrodes at the cell level is neglected, such that all the active particles share the same distribution of current density on the surface during cycling. Thus, the pore-wall flux $j_{s,k}$ will be computed only once for each electrode, with either the expressions such as Eq. (21), or an analytic expression based on averaged pore-wall area. Please note that, in this review, a “single-particle” model refers to a cell model described in this section, whereas a “single particle” refers to the models discussed in Section 2.1.

Using the volume fraction ($\varepsilon_{s,k}$) and the radius of active particles ($R_{s,k}$), the total surface area $A_{s,k}$ and the pore wall flux density $j_{s,k}$ of active particles per unit volume of composite electrode can be expressed as

$$A_{s,k} = \frac{3\varepsilon_{s,k}}{R_{s,k}}, \qquad j_{s,k} = \frac{J_{app}R_{s,k}}{3\varepsilon_{s,k}}, \tag{23}$$

where J_{app} is the applied flux. With the simplified $j_{s,k}$, Eqs. (18) to (20) can be solved independently, thus improving the computational efficiency. Moreover, since the simulations for single particles occur only once per electrode, all the complex physics identified in Section 2 can be considered for different electrode materials, such as plastification, phase separation, and fracture. This facilitates the investigation of the influence of particle behavior on cell performance.

Purkayastha and McMeeking [315] derived a simplified SP model with two assumptions: firstly, Li^+ is the only mobile charge carrier in the electrolyte; secondly, the electrodes always operate close to equilibrium. The first assumption yields a linear relationship between the electric field and the current density inside the electrolyte. The second assumption leads to a linear relationship between the current density on the surface of active particles and the overpotential through linearized Butler–Volmer kinetics. The stresses inside the active particles in both electrodes are thereby described similar to the basic model described in Section 2.1, where the stress generation can be mapped in terms of battery performance and design parameters. Their results show that the gradient of stress plays a significant role in lithium diffusion. A low-order SP cell model considering stress-enhanced diffusion was derived by Li et al. [316]. In this model, the concentration of electrolyte is represented by an approximated analytical expression to improve computational efficiency. The mechanical coupled model shows that for medium to high C-rate charge/discharge processes stresses plays an important role. In particular, the stresses can increase diffusivity, resulting in a considerable change in surface concentration and hence in an increased cell performance. Based on this model, Li et al. [317] developed a degradation model which considers SEI formation and crack propagation due to the stresses generated by the volume expansion of the active particle. They concluded that the crack propagation accelerated the SEI layer formation, leading to a significant capacity fade.

4.3. 2D/3D cell models

The last class of battery cell models explicitly models two or three spatial dimensions at the cell level. The first work in this regard has been undertaken by García et al. [44] with an application in a Li_xC|$Li_yMn_2O_4$ battery cell, where the distributions of the electrochemical and mechanical fields were calculated for porous electrode microstructure. In this model, unlike the P2D and SP models, the porous electrolyte microstructure was explicitly modeled, circumventing the need to employ effective coefficient for Li transport. Their work provided a framework for modeling effects of electrode microstructures that cannot be treated in mean-field models. However, as pointed out already in Section 2.1, their model disregarded mechanical contribution to the overall electrochemical performance of battery cell.

A similar model was proposed by Purkayastha and McMeeking [318], who integrated a 2D two-way coupled spherical particle model into a 2D cell model. In their model, they analyzed the influence among active particles and their influence on the cell performance. They performed a parameter analysis, developing non-dimensional parameters based on particle morphology and material properties. Their results showed that particle distribution as well as electrode material properties play big role in predicting the stress generation within the particle and the cell performance. Nevertheless, these models are still considering spherical particles for electrode active materials. In order to gain the understanding of stress distribution of the real battery cell, Wu et al. [319] developed a microstructurally resolved model of a Li_xC_6 |PP|$Li_yMn_2O_4$ cell. In their model, a conductive binder covering the active particle was also explicitly modeled and their results suggest that a softer binder can provide better interfacial adhesion between the binder and particles.

Ferrese and Newman [320] proposed an alternative model that uses porous-electrode theory with a smeared-out microstructure (model in Table 1) and a second spatial dimension at the cell level. Using this model, they studied the mechanical effect of a stiff separator to a lithium-metal anode and found that a stiff polymer separator can make

the lithium to deform both elastically and plastically which, as a consequence, can flatten the electrode surface considerably.

A fully coupled electro-chemo-mechanical model that considered the interactions at both the particle and the cell level was developed by Wu and Lu [321] in a multiscale setting. The model in Table 1 was thereby employed for the cell level, and Eq. (21) was modified such that $j_{s,k}$ included also stress effects. This model was employed to the study of the impact of small inactive regions within an electrode, demonstrating the importance of electrode homogeneity in order to avert electrode degradation. This degradation also a significant problem for large-format batteries where it was found that the loss of $LiMn_2O_4$ active material in a LMO|carbon cell is more serious at the electrode edge than in the bulk of the electrode. Dai et al. [322] found that this edge effect is due to the misalignment of the cathode and anode. At a larger scale, Rieger et al. [323] placed 21 P2D cells between two 2D current collector foils in order to explore the electro-chemo-mechanical behavior in a large-format pouch cell. Their results indicate that high stresses in the positive electrode arise over a wide range of discharge processes and are strongly correlated to the current density distribution.

Full 3D models consider the physical behavior variation in three spatial directions, allowing an in-depth investigation of the influence of spatial inhomogeneity on the electrochemical performance of battery cells. In 3D models, electrode microstructures play very important roles in electrochemical and mechanical performance of batteries. The earlier works mainly focused on the electrochemical behavior of the battery [324] and studies have been performed to compare the models with a fully resolved microstructure to P2D models [325]. Stress analyses in LCO and NMC cathodes reconstructed from FIB-SEM scans or from X-ray tomography have been performed by Wu et al. [275,276] and highlight the influence of complex microstructures in the resulting stress levels.

4.4. Concluding remarks

Cell models are very important since their outcomes can be directly compared with experimental measures, which offers optimization criteria for the electrodes and the electrolyte. Current research focuses mainly on the electrochemical behavior, with only a few studies employing mechanically coupled models. This choice is motivated by the fact that liquid electrolyte can well accommodate active electrode particle swelling and shrinkage. Despite accumulated evidence on the importance of mechanical effects on cell performance, even for liquid electrolytes, mechanical effects are still considered to be a secondary factor.

5. All-solid-state batteries

All-solid-state lithium batteries (SSBs) emerged as a promising alternative to currently used LIBs, which feature flammable organic liquid electrolytes [326,327]. Apart from safety gains, solid electrolytes (SE) also enable the use of lithium metal as anode, which significantly increases the volumetric and gravimetric energy density of a cell [327]. Solid electrolytes span wide classes of materials, ranging from organic polymers to inorganic ceramics. Although, in general, they show lower ionic conductivity ($\sim 10^{-4} Scm^{-1}$) than their liquid counterparts ($\sim 10^{-2}\ Scm^{-1}$), some polymers and inorganic ceramic solids, including garnet oxides and sulfides, exhibit an ionic conductivity comparable to liquid electrolytes [328,329]. The ionic conductivity inside the electrolyte is therefore not the bottleneck that prevents successful applications of SEs in LIBs. The challenge is rather to integrate SEs into high-performance batteries. Apart from electrochemical stability [330], mechanical compatibility with electrodes plays also a big role. In batteries with liquid electrolytes, as already shown in previous sections, mechanical stresses mainly arise in active particles during cyclic charge and discharge, and the overall cell performance is thus affected through mechanically modified pore-wall flux. Liquid electrolytes in general show good compliance to the active particles' deformation and they do not degradate directly due to mechanical stresses. However, when solid electrolytes—ceramic electrolytes in particular—are employed, electrolytes alone can cause mechanical issues. Firstly, the rigid nature of SEs makes their contact area with electrode particles very limited, which results in a large resistance [331]. This contact area can be further reduced due to large swelling and shrinkage of particles, as shown in Fig. 2(f). Surface coating is thus crucial in order to maintain a good contact between electrolyte and electrodes [396]; a proper external pressure is also necessary for mechanical integrity. However, this external pressure should not be too large because ceramic electrolytes are brittle and vulnerable to fracture. Composite-structured electrolytes combining a ceramic scaffold with polymer infill are thus proposed to offer a good ionic conductivity and fracture resistivity at the same time [332]. Theoretical model for deriving optimized designs are nonetheless lacking in the literature.

From the modeling point of view, most mechanically coupled models summarized from previous sections can be directly adapted for SSBs. At the particle level, bulk governing equations depend only on the electrode active materials, thus remaining unchanged. The boundary conditions, especially mechanical constraints, should be modified since solid electrolytes provide stronger mechanical confinements. Homogenization methods at the composite electrode level also remain valid, with liquid electrolyte being replaced by SE with the same volume fraction. However, the modeling of SE is slightly different because mechanical stresses are critical in SEs, which are mostly absent in liquid electrolytes. In this section, we will first introduce models for SEs, and the emphasis will be mainly on the difference from the model for liquid electrolytes. We will then focus on varied proposed models that try to describe the mechanisms of lithium dendritic growth in the electrolyte.

5.1. Mechanistic and degradation modeling of solid electrolyte

Solid electrolytes can, in general, be divided into two groups: organic polymers and inorganic ceramics. Most solid polymeric electrolytes are using high-molecular-weight polymers, such as poly (ethylene oxide) (PEO) and/or poly (propylene oxide) (PPO), as solvents for different Li^+ salts [333]. Ionic conductivity mechanism in polymeric electrolytes involves both Li^+ diffusion and polymer segmental motion [334]. Li^+ transport in ceramic electrolytes, on the other hand, is associated with ionic hopping between the interstitials and vacancies in crystalline structure [335], and anions are usually considered as non-mobile. Bucci et al. [336] started from a model describing species diffusion in a lattice material with large deformation (as shown in active materials) and extended it in order to consider multiple species and electric field. A similar formulation was also employed by Grazioli et al. [337]. Goyal and Monroe [338], on the other hand, started from Newman's concentrated-solution theory for liquid electrolyte and modified the mechanical part of Gibb's free energy from

$$\mathrm{d}G_{\mathrm{mech}}^{\mathrm{liquid}} = V\,\mathrm{d}p \tag{24}$$

to

$$\mathrm{d}G_{\mathrm{mech}}^{\mathrm{solid}} = V\,\mathrm{d}p - \frac{1}{3}\mathrm{dev}\boldsymbol{\varepsilon}\colon \mathrm{d}(\mathrm{dev}\boldsymbol{\sigma}) \tag{25}$$

in order to consider both the volumetric and deviatoric part of stresses in the solid electrolyte. In Eq. (25), dev$\boldsymbol{\varepsilon}$ and dev$\boldsymbol{\sigma}$ are the deviatoric part of strain and stress of the electrolyte, respectively. Note that the sign difference of Eq. (25) with Eq. (4) in the original paper [338] is due to the fact that in that paper $\boldsymbol{\sigma}$ is defined as compressive (negative) stress. It should also be pointed out that a more general expression of Gibb's free energy is expressed in terms of a thermodynamic tension $\boldsymbol{\tau}$ and its conjugate $\boldsymbol{\nu}$, leading to

$$\mathrm{d}G_{\mathrm{mech}} = -\boldsymbol{\nu}\cdot\mathrm{d}\boldsymbol{\tau} = -\boldsymbol{\varepsilon}\colon \mathrm{d}\boldsymbol{\sigma} \tag{26}$$

in a small deformation regime. It is worth noting that, although it is

highly popular to employ the Poisson–Nernst–Planck (PNP) equation to govern ion transport in electrolyte (e.g. Refs. [339,340]), Dreyer et al. [341] pointed out the deficiencies PNP model and derived a thermodynamically consistent formulation for non-compressible liquid electrolyte. Earlier than that, Landstorfer et al. [342] also developed a modified PNP model for ion diffusion in solid electrolyte without considering mechanical stresses. The mechanically coupled model in solid electrolyte beyond PNP equation was then proposed by Braun et al. [343], where the deviatoric contribution of electrolyte is disregarded. This model can naturally account for the space-charge layer, without involving the Gouy–Chapman theory.

Due to the stiff nature of many electrolytes and lithium intercalation-induced large deformation of electrode particles, the composite structures of electrolytes and electrode particles are likely to crack within each phase and delaminate from each other [344,345]. The fracture of the particles has been already discussed in Section 2. As for the SE, it is natural to predict that an SE is less likely to fracture if its compliance is improved. However, Bucci et al. [346] found that compliant sulfide electrolytes are more prone to micro-cracking than brittle ceramic ones. They attributed this to the fact that more compliant SEs allow for larger deformation, and thus result in higher stress concentrations. Using a random walk analysis, they further calculated how the effective conductivity is affected by micro-cracking [347]. In their work, they predicted a linear relationship between the average diffusivity and the mechanical degradation. They also observed an increased heterogeneity with progressive damage, which, in turn, increases stress concentrations. Delamination between the active particles with SEs and current collectors is another big issue that contributes to the mechanical failure [348,349]. Guo et al. [350] studied the delamination between current collector and electrode due to wrinkling of electrode in a layer-structured battery. They found that single-blister buckling is more likely to occur in a battery with liquid electrolyte, and multi-blistering buckling has higher chances to take place in SSBs. At the cell level, Behrou and Maute [351] employed a P2D model, using a modification of the flux in Eq. (18) with a stress-drifting term, and analyzed the damage evolution of the battery due to degradation in the electrode active particles. The model demonstrated that particles with large aspect ratio will operate better in terms of damage-induced capacity fade inside solid state battery.

5.2. Modeling of lithium deposition

Lithium plating usually occurs when lithium metal is used as anode, and unstable lithium deposition—such as formation of lithium dendrites and filaments—can penetrate the separator, giving rise to a short circuit. However, the use of pure Li metal anodes should not be disregarded, as it allows for a significantly increased energy density over traditional LIBs with porous electrodes [327].

One major driving force for the application of SEs is the widely shared belief that the mechanical stresses arising within SEs can suppress dendrite growth. However, accumulated evidences show that lithium dendrites grow regardless of electrolyte materials [352–355]. Even SEs with high elastic moduli—predicted from theoretical modeling—cannot effectively suppress lithium dendrites [17]. A corresponding theory has yet to be proposed. Due to the aforementioned reasons, SSBs well deserve the investigation from mechanical aspects.

The mechanism of lithium dendritic growth is not completely clear. Some models established based on Na systems with β-alumina as the electrolyte can offer insights into instable metal deposition in ceramics [356,357]. The first model on lithium deposition in a polymer electrolyte was proposed by Monroe and Newman, who considered the contribution of bulk and surface stresses to the electrochemical reaction of lithium deposition [20,358,359]. They concluded that surface stress and bulk pressure contributed deposition stability, and that their contribution increased with an enhanced electrolyte shear modulus. Their theory was confirmed by Stone et al. for a battery system with very stiff polymer electrolytes and good adhesion [360]. Tikekar et al. [361] modified Monroe and Newman's theory to consider a polymer with non-mobile anions. They concluded that, by using a polymer with immobilized anions, stable electrodeposition can be achieved even with moderate shear modulus.

In ceramic electrolytes, however, the Monroe–Newman-based models appear to be not applicable. Ceramic electrolytes in general have very large elastic moduli and in them, Li^+ is the only mobile ion. They are supposed to have better performance against lithium dendritic growth. Nonetheless, Cheng et al. [362] showed that lithium dendrites formation can occur even for an electrolyte whose shear modulus is far above the critical value estimated in the Monroe–Newman model. Further, Porz et al. [17] performed Li-deposition experiments on surfaces of amorphous, single-crystalline, and polycrystalline electrolytes. Based on these experiments, they proposed that lithium plated preferably inside pre-existing flaws, leading, for instance, to the propagation of cracks. A flawless surface, on the other hand, will not be penetrated even at high current density. They proposed a model based on the concept that reduced lithium wedges and cracks open a pre-existing flaw despite of the low shear modulus and yield strength of lithium. The critical overpotential is thus expressed as a function of the fracture toughness of SE. Raj and Wolfenstine [363] proposed a model that considers lithium nucleation in the ceramic electrolyte at the grain boundary. The coupling of mechanical stresses and the electrical potential was shown by the electro-chemo-mechanical potential. The excess potential served as the nucleation barrier for dendrite formation. They concluded that the critical current above which lithium nucleates within the electrolyte depends on the ionic conductivity and fracture strength of the electrolyte. It was further proposed by Natsiavas et al. [21] that the electrolyte morphology plays a major role for lithium dendrite formation. To that end, they developed a 3D model to discuss the instability of lithium-electrolyte interface due to lithium bulk and surface transport, lithium deposition, and elastic stresses. They concluded that interfacial roughness played a crucial role in triggering the lithium dendrite growth, and that a pre-stretch will always substantially reduce the roughening of the lithium surface during cycling. Despite all these efforts, it is still debatable which model, if it exists at all, can fully cover the mechanism of lithium dendrite growth.

5.3. Concluding remarks

Mechanical stress is the one of the most important factors in designing solid-state batteries. There are a handful of models that incorporate electro-chemo-mechanical behavior of solid electrolytes. Their applications in describing functioning and failure of these SEs are still deficient. Simulations are needed in order to provide an optimal design of these SEs in terms of volume fraction, structural design, as well as mechanical constraint in order to provide a solid yet fracture-free contact between the electrode and electrolyte. Moreover, the understanding of lithium dendritic growth is still in its infancy. To the authors' knowledge, there is not yet a single theory that can explain the lithium dendritic growth in an SE satisfactorily. To achieve this, a joint work from electrochemical and mechanical aspects is essential.

6. Conclusions

The role of mechanical effects on the deterioration of lithium-ion batteries has in the last two decades experienced considerable attention by the scientific community and the industry alike. Lithium-ion batteries provide a rich field of mechanical phenomena at the microscale alone, comprising, to name only a few, large deformations coupled with nonlinear elasticity, plastification, fracture, anisotropic material behavior, structural instability, and phase separation phenomena. This has motivated a vast amount of experimental and theoretical studies that investigate and try to predict this behavior. The initial simple model assumptions have thereby been successively replaced by more realistic

model parameters. Nonetheless, there remain several open issues regarding the mechanically coupled modeling of Li-ion batteries, in addition to those mentioned for each scale at the end of corresponding sections.

Tremendous progress has been made on modeling the performance of lithium-ion batteries at the different scales involved, be it in the form of the strongly predictive battery cell models such as P2D or SPM, the composite-level modeling of diffusion and stresses, or the description of plasticity and failure of free-standing electrode particles. What is currently lacking is the integration of these disconnected modeling efforts into a true multiscale model, where microscale mechanical effects inform and affect the material and the battery cell performance at the higher scales.

A major factor limiting the veracity of the discussed models lies in the employed material parameters. To an increasing degree, factors such as crystal anisotropy are regarded in the computational studies. The computation of appropriate parameters and their transfer from the atomistic level to a continuum view is, in our view, still undertaken too seldom.

Overcoming these roadblocks to further efficiency increases for lithium-ion batteries requires, to a growing extent, the collaboration of researchers from both electrochemistry and the mechanical community. In order to aid this endeavour, a shared language and understanding is vital. With this review we try to present, to expert and newcomer alike, a comprehensive overview of the modeling efforts that have been made in the last years to describe and understand mechanical phenomena at three different scales of a lithium-ion battery. We envision that the insights on modeling and material/cell behavior gained in these reports are not restricted to lithium-ion batteries but are transferable to other battery chemistries such as Na-ion or Mg-ion batteries and other energy technologies featuring a strong coupling between ionic/electric transport and mechanics, for instance fuel cells or supercapacitors.

Acknowledgment

B.-X. Xu would particularly like to thank the Adolf Messer Foundation for awarding her the Adolf Messer Prize and for the financial support.

References

[1] J.-M. Tarascon, M. Armand, Issues and challenges facing rechargeable lithium batteries, Nature 414 (2001) 359–367.
[2] G.-A. Nazri, G. Pistoia (Eds.), Lithium Batteries: Science and Technology, Springer US, 2003.
[3] D. Abraham, D.W. Dees, J. Knuth, E. Reynolds, R. Gerald, Y.-E. Hyung, I. Belharouak, M. Stoll, E. Sammann, S. MacLaren, R. Haasch, R. Twesten, M. Sardela, V. Battaglia, E. Cairns, J. Kerr, M. Kerlau, R. Kostecki, J. Lei, L. Norin, Diagnostic Examination of Generation 2 Lithium-ion Cells and Assessment Ofperformance Degradation Mechanisms, Technical Report ANL-05/21 Argonne National Lab, 2005.
[4] A. Mukhopadhyay, B.W. Sheldon, Deformation and stress in electrode materials for Li-ion batteries, Prog. Mater. Sci. 63 (2014) 58–116.
[5] M.E. Stournara, P.R. Guduru, V.B. Shenoy, Elastic behavior of crystalline Li-Sn phases with increasing Li concentration, J. Power Sources 208 (2012) 165–169.
[6] Y. Qi, H. Guo, J. Hector, G. Louis, A. Timmons, Threefold increase in the Young's modulus of graphite negative electrode during lithium intercalation, J. Electrochem. Soc. 157 (2010) A558–A566.
[7] C.K. Chan, H. Peng, G. Liu, K. Mcllwrath, X.F. Zhang, R.A. Huggins, Y. Cui, High-performance lithium battery anodes using silicon nanowires, Nat. Nanotechnol. 3 (2008) 31–35.
[8] M. Ebner, F. Marone, M. Stampanoni, V. Wood, Visualization and quantification of electrochemical and mechanical degradation in Li ion batteries, Science 342 (2013) 716–720.
[9] L.Y. Beaulieu, K.W. Eberman, R.L. Turner, L.J. Krause, J.R. Dahn, Colossal reversible volume changes in lithium alloys, Electrochem. Solid State Lett. 4 (2001) A137–A140.
[10] S.W. Lee, M.T. McDowell, L.A. Berla, W.D. Nix, Y. Cui, Fracture of crystalline silicon nanopillars during electrochemical lithium insertion, Proc. Natl. Acad. Sci. U.S.A. 109 (2012) 4080–4085.
[11] J.Y. Huang, L. Zhong, C.M. Wang, J.P. Sullivan, W. Xu, L.Q. Zhang, S.X. Mao, N.S. Hudak, X.H. Liu, A. Subramanian, H. Fan, L. Qi, A. Kushima, J. Li, In situ observation of the electrochemical lithiation of a single SnO_2 nanowire electrode, Science 330 (2010) 1515.
[12] L. Bagetto, D. Danilov, P.H.L. Notten, Honeycomb-structured silicon: remarkable morphological changes induced by electrochemical (de)lithiation, Adv. Mater. 23 (2011) 1563–1566.
[13] M.K. Jangid, F.J. Sonia, R. Kali, B. Ananthoju, A. Mukhopadhyay, Insights into the effects of multi-layered graphene as buffer/interlayer for a-Si during lithiation/delithiation, Carbon 111 (2017) 602–616.
[14] R. Koerver, I. Aygün, T. Leichtweiß, C. Dietrich, W. Zhang, J.O. Binder, P. Hartmann, W.G. Zeier, J. Janek, Capacity fade in solid-state batteries: interphase formation and chemomechanical processes in nickel-rich layered oxide cathodes and lithium thiophosphate solid electrolytes, Chem. Mater. 29 (2017) 5574–5582.
[15] H. Wu, G. Chan, J.W. Choi, I. Ryu, Y. Yao, M.T. McDowell, S.W. Lee, A. Jackson, Y. Yang, L. Hu, Y. Cui, Stable cycling of double-walled silicon nanotube battery anodes through solid-electrolyte interphase control, Nat. Nanotechnol. 7 (2012) 310–315.
[16] I. Laresgoiti, S. Käbitz, M. Ecker, D.U. Sauer, Modeling mechanical degradation in lithium ion batteries during cycling: solid electrolyte interphase fracture, J. Power Sources 300 (2015) 112–122.
[17] L. Porz, T. Swamy, B.W. Sheldon, D. Rettenwander, T. Frömling, H.L. Thaman, S. Berendts, R. Uecker, W.C. Carter, Y.-M. Chiang, Mechanism of lithium metal penetration through inorganic solid electrolytes, Adv. Energy Mater. 7 (2017) 1701003.
[18] G. Kermani, E. Sahraei, Review: characterization and modeling of the mechanical properties of lithium-ion batteries, Energies 10 (2017) 1730.
[19] J. Christensen, J. Newman, Stress generation and fracture in lithium insertion materials, J. Solid State Electrochem. 10 (2006) 293–319.
[20] C. Monroe, J. Newman, The effect of interfacial deformation on electrodeposition kinetics, J. Electrochem. Soc. 151 (2004) A880–A886.
[21] P.P. Natsiavas, K. Weinberg, D. Rosato, M. Ortiz, Effect of prestress on the stability of electrode-electrolyte interfaces during charging in lithium batteries, J. Mech. Phys. Solid. 95 (2016) 92–111.
[22] X. Cheng, M. Pecht, In situ stress measurement techniques on li-ion battery electrodes: a review, Energies 10 (2017) 951.
[23] A.A. Franco, Multiscale modelling and numerical simulation of rechargeable lithium ion batteries: concepts, methods and challenges, RSC Adv. 3 (2013) 13027–13058.
[24] D. Grazioli, M. Magri, A. Salvadori, Computational modeling of Li-ion batteries, Comput. Mech. 58 (2016) 889–909.
[25] Y.F. Gao, M. Cho, M. Zhou, Mechanical reliability of alloy-based electrode materials for rechargeable Li-ion batteries, J. Mech. Sci. Technol. 27 (2013) 1205–1224.
[26] R. Xu, K. Zhao, Electrochemomechanics of electrodes in Li-ion batteries: a review, J. Electrochem. En. Conv. Stor. 13 (2016) 030803.
[27] J. Swallow, W. Woodford, Y. Chen, Q. Lu, J. Kim, D. Chen, Y.-M. Chiang, W. Carter, B. Yildiz, H. Tuller, et al., Chemomechanics of ionically conductive ceramics for electrical energy conversion and storage, J. Electroceram. 32 (2014) 3–27.
[28] M.T. McDowell, S. Xia, T. Zhu, The mechanics of large-volume-change transformations in high-capacity battery materials, Extreme Mech. Lett. 9 (2016) 480–494.
[29] S. Zhang, Chemomechanical modeling of lithiation-induced failure in high-volume-change electrode materials for lithium ion batteries, npj Comput. Mater. 3 (2017) 7.
[30] S. Zhang, K. Zhao, T. Zhu, J. Li, Electrochemomechanical degradation of high-capacity battery electrode materials, Prog. Mater. Sci. 89 (2017) 479–521.
[31] J. Newman, K. Thomas-Alyea, Electrochemical Systems, Electrochemical Society Series, John Wiley & Sons, 2004.
[32] S. Prussin, Generation and distribution of dislocations by solute diffusion, J. Appl. Phys. 32 (1961) 1876–1881.
[33] J.C.-M. Li, Physical chemistry of some microstructural phenomena, Metall. Trans. A 9 (1978) 1353–1380.
[34] F. Larché, J.W. Cahn, A linear theory of thermochemical equilibrium of solids under stress, Acta Metall. 21 (1973) 1051–1063.
[35] F. Larché, J.W. Cahn, A nonlinear theory of thermochemical equilibrium of solids under stress, Acta Metall. 26 (1978) 53–60.
[36] F.C. Larché, The interactions of composition and stress in crystalline solids, J. Res. Natl. Bur. Stand. 89 (1984) 467–500.
[37] I.V. Belova, G.E. Murch, Thermal and diffusion-induced stresses in crystalline solids, J. Appl. Phys. 77 (1995) 127–134.
[38] E.C. Aifantis, On the problem of diffusion in solids, Acta Mech. 37 (1980) 265–396.
[39] I.R.K. Wilson, E.C. Aifantis, On the theory of stress-assisted diffusion, i, Acta Mech. 45 (1982) 273–296.
[40] D.J. Unger, E.C. Aifantis, On the theory of stress-assisted diffusion, ii, Acta Mech. 47 (1983) 117–151.
[41] P.A. Taylor, E.C. Aifantis, On the theory of diffusion in linear viscoelastic media, Acta Mech. 44 (1982) 259–298.
[42] G.B. Stephenson, Deformation during interdiffusion, Acta Metall. 36 (1988) 2663–2683.
[43] S.P. Girrens, F.W. Smith, Constituent diffusion in a deformable thermoelastic solid, J. Appl. Mech. 54 (1987) 441–446.
[44] R.E. García, Y.-M. Chiang, W.C. Carter, P. Limthongkul, C.M. Bishop, Microstructural modeling and design of rechargeable lithium-ion batteries, J. Electrochem. Soc. 152 (2005) A255–A263.
[45] S.-B. Son, S.C. Kim, C.S. Kang, T.A. Yersak, Y.-C. Kim, C.-G. Lee, S.-H. Moon,

J.S. Cho, J.-T. Moon, K.H. Oh, S.-H. Lee, A highly reversible nano-Si anode enabled by mechanical confinement in an electrochemically activated $Li_xTi_4Ni_4Si_7$ matrix, Adv. Energy Mater. 2 (2012) 1226–1231.
[46] F. Hao, D. Fang, Diffusion-induced stresses of spherical core-shell electrodes in lithium-ion batteries: the effects of the shell and surface/interface stress, J. Electrochem. Soc. 160 (2013) A595–A600.
[47] F. Hao, D. Fang, Tailoring diffusion-induced stresses of core-shell nanotube electrodes in lithium-ion batteries, J. Appl. Phys. 113 (2013) 013507.
[48] D. Molina Piper, T.A. Yersak, S.-H. Lee, Effect of compressive stress on electrochemical performance of silicon anodes, J. Electrochem. Soc. 160 (2013) A77–A81.
[49] B.W. Sheldon, S.K. Soni, X. Xiao, Y. Qi, Stress contributions to solution thermodynamics in Li-Si alloys, Electrochem. Solid State Lett. 15 (2012) A9–A11.
[50] M.T. McDowell, S.W. Lee, I. Ryu, H. Wu, W.D. Nix, J.W. Choi, Y. Cui, Novel size and surface oxide effects in silicon nanowires as lithium battery anodes, Nano Lett. 11 (2011) 4018–4025.
[51] T. Ichitsubo, K. Tokuda, S. Yagi, M. Kawamori, T. Kawaguchi, T. Doi, M. Oishi, E. Matsubara, Elastically constrained phase-separation dynamics competing with the charge process in the $LiFePO_4/FePO_4$ system, J. Mater. Chem. 1 (2013) 2567–2577.
[52] F. Ning, S. Li, B. Xu, C. Ouyang, Strain tuned Li diffusion in $LiCoO_2$ material for Li ion batteries: a first principles study, Solid State Ionics 263 (2014) 46–48.
[53] A. Moradabadi, P. Kaghazchi, J. Rohrer, K. Albe, Influence of elastic strain on the thermodynamics and kinetics of lithium vacancy in bulk-$LiCoO_2$, Phys. Rev. Materials 2 (2018) 015402.
[54] N. Muralidharan, C.N. Brock, A.P. Cohn, D. Schauben, R.E. Carter, L. Oakes, D.G. Walker, C.L. Pint, Tunable mechanochemistry of lithium battery electrodes, ACS Nano 11 (2017) 6243–6251.
[55] S. Natarajan, Hirshikesh, N. Swaminathan, R.K. Annabattula, Effects of stress-diffusion interactions in an isotropic elastic medium in the presence of geometric discontinuities, J. Coupled Syst. Multiscale Dyn. 4 (2016) 230–240.
[56] X. Zhang, W. Shyy, A.M. Sastry, Numerical simulation of intercalation-induced stress in Li-ion battery electrode particles, J. Electrochem. Soc. 154 (2007) A910–A916.
[57] H.-Y. Amanieu, H.N.M. Thai, S.Y. Luchkin, D. Rosato, D.C. Lupascu, M.-A. Keip, J. Schröder, A.L. Kholkin, Electrochemical strain microscopy time spectroscopy: model and experiment on $LiMn_2O_4$, J. Appl. Phys. 118 (2015) 055101.
[58] M.W. Verbrugge, B.J. Koch, Modeling lithium intercalation of single-fiber carbon microelectrodes, J. Electrochem. Soc. 143 (1996) 600–608.
[59] G.G. Botte, R.E. White, Modeling lithium intercalation in a porous carbon electrode, J. Electrochem. Soc. 148 (2001) A54–A66.
[60] M. Papakyriakou, X. Wang, S. Xia, Characterization of stress-diffusion coupling in lithiated germanium by nanoindentation, Exp. Mech. 58 (2018) 613–625.
[61] Y. Li, K. Zhang, B. Zheng, F. Yang, Effect of local velocity on diffusion-induced stress in large-deformation electrodes of lithium-ion batteries, J. Power Sources 319 (2016) 168–177.
[62] I. Ryu, J.W. Choi, Y. Cui, W.D. Nix, Size-dependent fracture of Si nanowire battery anodes, J. Mech. Phys. Solid. 59 (2011) 1717–1730.
[63] P. Stein, B. Xu, 3d Isogeometric Analysis of intercalation-induced stresses in Li-ion battery electrode particles, Comput, Methods Appl. Mech. Engrg. 268 (2014) 225–244.
[64] C. Miehe, S. Mauthe, H. Ulmer, Formulation and numerical exploitation of mixed variational principles for coupled problems of Cahn-Hilliard-type and standard diffusion in elastic solids, Int. J. Numer. Methods Eng. 99 (2014) 737–762.
[65] C.V. Di Leo, E. Rejovitzky, L. Anand, Diffusion–deformation theory for amorphous silicon anodes: the role of plastic deformation on electrochemical performance, Int. J. Solid Struct. 67–68 (2015) 283–296.
[66] A. Krischok, C. Linder, On the enhancement of low-order mixed finite element methods for the large deformation analysis of diffusion in solids, Int. J. Numer. Methods Eng. 106 (2016) 278–297.
[67] A. Bard, L. Faulkner, Electrochemical Methods: Fundamentals and Applications, Wiley, 2000.
[68] Y.T. Cheng, M.W. Verbrugge, Evolution of stress within a spherical insertion electrode particle under potentiostatic and galvanostatic operation, J. Power Sources 190 (2009) 453–460.
[69] B.C. Han, A. Van der Ven, D. Morgan, G. Ceder, Electrochemical modeling of intercalation processes with phase field models, Electrochim. Acta 49 (2004) 4691–4699.
[70] D. Zhang, B.N. Popov, R.E. White, Modeling lithium intercalation of a single spinel particle under potentiodynamic control, J. Electrochem. Soc. 147 (2000) 831.
[71] S. Golmon, K. Maute, S.H. Lee, M.L. Dunn, Stress generation in silicon particles during lithium insertion, Appl. Phys. Lett. 97 (2010) 2008–2011.
[72] E. Bohn, T. Eckl, M. Kamlah, R. McMeeking, A model for lithium diffusion and stress generation in an intercalation storage particle with phase change, J. Electrochem. Soc. 160 (2013) A1638–A1652.
[73] H. Dal, C. Miehe, Computational electro-chemo-mechanics of lithium-ion battery electrodes at finite strains, Comput. Mech. 55 (2014) 303–325.
[74] V. Sethuraman, M. Chon, M. Shimshak, N. Van Winkle, P. Guduru, In situ measurement of biaxial modulus of Si anode for Li-ion batteries, Electrochem. Commun. 12 (2010) 1614–1617.
[75] V.A. Sethuraman, V. Srinivasan, A.F. Bower, P.R. Guduru, In situ measurements of stress-potential coupling in lithiated silicon, J. Electrochem. Soc. 157 (2010) A1253–A1261.
[76] V.A. Sethuraman, M.J. Chon, M. Shimshak, V. Srinivasan, P.R. Guduru, In situ measurements of stress evolution in silicon thin films during electrochemical lithiation and delithiation, J. Power Sources 195 (2010) 5062–5066.
[77] V.A. Sethuraman, A. Nguyen, M.J. Chon, S.P.V. Nadimpalli, H. Wang, D.P. Abraham, A.F. Bower, V.B. Shenoy, P.R. Guduru, Stress evolution in composite silicon electrodes during lithiation/delithiation, J. Electrochem. Soc. 160 (2013) A739–A746.
[78] K. Zhao, W.L. Wang, J. Gregoire, M. Pharr, Z. Suo, J.J. Vlassak, E. Kaxiras, Lithium-assisted plastic deformation of silicon electrodes in lithium-ion batteries: a first-principles theoretical study, Nano Lett. 11 (2011) 2962–2967.
[79] A. Bower, P. Guduru, V. Sethuraman, A finite strain model of stress, diffusion, plastic flow, and electrochemical reactions in a lithium-ion half-cell, J. Mech. Phys. Solid. 59 (2011) 804–828.
[80] A.F. Bower, E. Chason, P.R. Guduru, B.W. Sheldon, A continuum model of deformation, transport and irreversible changes in atomic structure in amorphous lithium–silicon electrodes, Acta Mater. 98 (2015) 229–241.
[81] F.C. Larche, J.W. Cahn, Thermochemical equilibrium of multiphase solids under stress, Acta Metall. 26 (1978) 1579–1589.
[82] Y. Gao, M. Cho, M. Zhou, Stress relaxation through interdiffusion in amorphous lithium alloy electrodes, J. Mech. Phys. Solid. 61 (2013) 579–596.
[83] D.R. Baker, M.W. Verbrugge, A.F. Bower, Thermodynamics, stress, and stefan-maxwell diffusion in solids: application to small-strain materials used in commercial lithium-ion batteries, J. Solid State Electrochem. 20 (2016) 163–181.
[84] A. Salvadori, R. McMeeking, D. Grazioli, M. Magri, A coupled model of transport-reaction-mechanics with trapping. part i – small strain analysis, J. Mech. Phys. Solid. 114 (2018) 1–30.
[85] G. Singh, T.K. Bhandakkar, Analytical investigation of binder's role on the diffusion induced stresses in lithium ion battery through a representative system of spherical isolated electrode particle enclosed by binder, J. Electrochem. Soc. 164 (2017) A608–A621.
[86] L. Anand, A Cahn–Hilliard-type theory for species diffusion coupled with large elastic–plastic deformations, J. Mech. Phys. Solid. 60 (2012) 1983–2002.
[87] K. Zhao, M. Pharr, S. Cai, J.J. Vlassak, Z. Suo, Large plastic deformation in high-capacity lithium-ion batteries caused by charge and discharge, J. Am. Ceram. Soc. 94 (2011) s226–s235.
[88] Z. Cui, F. Gao, J. Qu, A finite deformation stress-dependent chemical potential and its applications to lithium ion batteries, J. Mech. Phys. Solid. 60 (2012) 1280–1295.
[89] G. Bucci, S.P.V. Nadimpalli, V.A. Sethuraman, A.F. Bower, P.R. Guduru, Measurement and modeling of the mechanical and electrochemical response of amorphous Si thin film electrodes during cyclic lithiation, J. Mech. Phys. Solid. 62 (2014) 276–294.
[90] Z. Jia, W.K. Liu, Rate-dependent stress evolution in nanostructured Si anodes upon lithiation, Appl. Phys. Lett. 109 (2016) 163903.
[91] K. Zhao, G.A. Tritsaris, M. Pharr, W.L. Wang, O. Okeke, Z. Suo, J.J. Vlassak, E. Kaxiras, Reactive flow in silicon electrodes assisted by the insertion of lithium, Nano Lett. 12 (2012) 4397–4403.
[92] L. Brassart, Z. Suo, Reactive flow in large-deformation electrodes of lithium-ion batteries, Int. J. Appl. Mech. 04 (2012) 1250023.
[93] L. Brassart, K. Zhao, Z. Suo, Cyclic plasticity and shakedown in high-capacity electrodes of lithium-ion batteries, Int. J. Solid Struct. 50 (2013) 1120–1129.
[94] M. Pharr, Z. Suo, J.J. Vlassak, Variation of stress with charging rate due to strain-rate sensitivity of silicon electrodes of Li-ion batteries, J. Power Sources 270 (2014) 569–575.
[95] S.M. Khosrownejad, W.A. Curtin, Model for charge/discharge-rate-dependent plastic flow in amorphous battery materials, J. Mech. Phys. Solid. 94 (2016) 167–180.
[96] H. Gabrisch, R. Yazami, B. Fultz, A transmission electron microscopy study of cycled $LiCoO_2$, J. Power Sources 119–121 (2003) 674–679.
[97] H. Wang, Y.-I. Jang, B. Huang, D.R. Sadoway, Y.-M. Chiang, Electron microscopic characterization of electrochemically cycled $LiCoO_2$ and $Li(Al,Co)O_2$ battery cathodes, J. Power Sources 81–82 (1999) 594–598.
[98] A. Ulvestad, A. Singer, J. Clark, H. Cho, J. Kim, J. Maser, Y. Meng, O. Shpyrko, Topological defect dynamics in operando battery nanoparticles, Science 348 (2015) 1344–1347.
[99] M. Legros, G. Dehm, E. Arzt, T.J. Balk, Observation of giant diffusivity along dislocation cores, Science 319 (2008) 1646–1649.
[100] L. Zhong, X.H. Liu, G.F. Wang, S.X. Mao, J.Y. Huang, Multiple-stripe lithiation mechanism of individual SnO_2 nanowires in a flooding geometry, Phys. Rev. Lett. 106 (2011) 248302.
[101] M. Mao, A. Nie, J. Liu, H. Wang, S.X. Mao, Q. Wang, K. Li, X. Zhang, Atomic resolution observation of conversion-type anode RuO_2 during the first electrochemical lithiation, Nanotechnology 26 (2015) 125404.
[102] A. Nie, L.-Y. Gan, Y. Cheng, H. Asayesh-Ardakani, Q. Li, C. Dong, R. Tao, F. Mashayek, H.-T. Wang, U. Schwingenschlögl, R.F. Klie, R.S. Yassar, Atomic-scale observation of lithiation reaction front in nanoscale sno_2 materials, ACS Nano 7 (2013) 6203–6211.
[103] P. Wei, J. Zhou, X. Pang, H. Liu, K. Deng, G. Wang, Y. Wu, B. Chen, Effects of dislocation mechanics on diffusion-induced stresses within a spherical insertion particle electrode, J. Mater. Chem. 2 (2013) 1128–1136.
[104] Y. Estrin, Dislocation theory based constitutive modelling: foundations and applications, J. Mater. Process. Technol. 80–81 (1998) 33–39.
[105] F. Yang, Comments on Effects of dislocation mechanics on diffusion-induced stresses within a spherical insertion particle electrode, J. Mater. Chem. 2 (2014) 17183–17184.
[106] F. Yang, A simple model for diffusion-induced dislocations during the lithiation of crystalline materials, Theor. Appl. Mech. Lett. 4 (2014) 051001.
[107] B. Chen, J. Zhou, J. Zhu, Z. Liu, Diffusion induced stress and the distribution of dislocations in a nanostructured thin film electrode during lithiation, RSC Adv. 4

(2014) 64216–64224.
[108] J. Zhu, J. Zhou, B. Chen, Z. Liu, T. Liu, Dislocation effect on diffusion-induced stress for lithiation in hollow spherical electrode, J. Solid State Electrochem. 20 (2016) 37–46.
[109] J. Li, Q. Fang, F. Liu, Y. Liu, Analytical modeling of dislocation effect on diffusion induced stress in a cylindrical lithium ion battery electrode, J. Power Sources 272 (2014) 121–127.
[110] B. Chen, J. Zhou, J. Zhu, T. Liu, Z. Liu, Effect of misfit dislocation on Li diffusion and stress in a phase transforming spherical electrode, J. Electrochem. Soc. 162 (2015) H493–H500.
[111] B. Chen, J. Zhou, R. Cai, Analytical model for crack propagation in spherical nano electrodes of lithium-ion batteries, Electrochim. Acta 210 (2016) 7–14.
[112] Z. Liu, J. Zhou, B. Chen, J. Zhu, Interaction between dislocation mechanics on diffusion induced stress and electrochemical reaction in a spherical lithium ion battery electrode, RSC Adv. 5 (2015) 74835–74843.
[113] Y.-T. Cheng, M.W. Verbrugge, The influence of surface mechanics on diffusion induced stresses within spherical nanoparticles, J. Appl. Phys. 10 (2008) 083521.
[114] R. Deshpande, Y.-T. Cheng, M.W. Verbrugge, Modeling diffusion-induced stress in nanowire electrode structures, J. Power Sources 195 (2010) 5081–5088.
[115] J. Li, D. Lu, Q. Fang, Y. Liu, P. Wen, Cooperative surface effect and dislocation effect in lithium ion battery electrode, Solid State Ionics 274 (2015) 46–54.
[116] X. Li, Q. Fang, J. Li, H. Wu, Y. Liu, P. Wen, Diffusion-induced stress and strain energy affected by dislocation mechanisms in a cylindrical nanoanode, Solid State Ionics 281 (2015) 21–28.
[117] Z. Ma, H. Wu, Y. Wang, Y. Pan, C. Lu, An electrochemical-irradiated plasticity model for metallic electrodes in lithium-ion batteries, Int. J. Plast. 88 (2017) 188–203.
[118] Y. Wang, Z. Ma, W. Lei, Y. Zou, C. Lu, Double effect of electrochemical reaction and substrate on hardness in electrodes of lithium-ion batteries, Acta Mech. 227 (2016) 2505–2510.
[119] Z. Ma, Z. Xie, C. Wang, YanAND. Lu, Softening by electrochemical reaction-induced dislocations in lithium-ion batteries, Scripta Mater. 127 (2017) 33–36.
[120] H.-Y.S. Huang, Y.-X. Wang, Dislocation based stress developments in lithium-ion batteries, J. Electrochem. Soc. 159 (2012) A815–A821.
[121] X. Li, Q. Fang, H. Wu, J. Li, Y. Liu, P. Wen, Misfit dislocations induced by lithium-ion diffusion in a thin film anode, J. Solid State Electrochem. 21 (2017) 419–427.
[122] C.J. Wen, R.A. Huggins, Chemical diffusion in intermediate phases in the lithium-silicon system, J. Solid State Chem. 37 (1981) 271–278.
[123] M.J. Chon, V.A. Sethuraman, A. McCormick, V. Srinivasan, P.R. Guduru, Real-time measurement of stress and damage evolution during initial lithiation of crystalline silicon, Phys. Rev. Lett. 107 (2011) 045503.
[124] X.H. Liu, J.Y. Huang, In situ TEM electrochemistry of anode materials in lithium ion batteries, Energy Environ. Sci. 4 (2011) 3844–3860.
[125] X.H. Liu, J.W. Wang, S. Huang, F. Fan, X. Huang, Y. Liu, S. Krylyuk, J. Yoo, S.A. Dayeh, A.V. Davydov, S.X. Mao, S.T. Picraux, S. Zhang, J. Li, T. Zhu, J.Y. Huang, In situ atomic-scale imaging of electrochemical lithiation in silicon, Nat. Nanotechnol. 7 (2012) 749–756.
[126] J. Rohrer, K. Albe, Insights into degradation of Si anodes from first-principle calculations, J. Phys. Chem. C 117 (2013) 18796–18803.
[127] X.H. Liu, F. Fan, H. Yang, S. Zhang, J.Y. Huang, T. Zhu, Self-limiting lithiation in silicon nanowires, ACS Nano 7 (2013) 1495–1503.
[128] J.W. Wang, Y. He, F. Fan, X.H. Liu, S. Xia, Y. Liu, C.T. Harris, H. Li, J.Y. Huang, S.X. Mao, T. Zhu, Two-phase electrochemical lithiation in amorphous silicon, Nano Lett. 13 (2013) 709–715.
[129] M.T. McDowell, S.W. Lee, J.T. Harris, B.A. Korgel, C. Wang, W.D. Nix, Y. Cui, In situ TEM of two-phase lithiation of amorphous silicon nanospheres, Nano Lett. 13 (2013) 758–764.
[130] C. Delmas, M. Maccario, L. Croguennec, F. Le Cras, F. Weill, Lithium deintercalation in $LiFePO_4$ nanoparticles via a domino-cascade model, Nat. Mater. 7 (2008) 665–671.
[131] A. Van der Ven, J. Bhattacharya, A.A. Belak, Understanding Li diffusion in Li-intercalation compounds, Acc. Chem. Res. 46 (2013) 1216–1225.
[132] S. Huang, F. Fan, J. Li, S. Zhang, T. Zhu, Stress generation during lithiation of high-capacity electrode particles in lithium ion batteries, Acta Mater. 61 (2013) 4354–4364.
[133] H. Yang, W. Liang, X. Guo, C.-M. Wang, S. Zhang, Strong kinetics-stress coupling in lithiation of Si and Ge anodes, Extreme Mech. Lett. 2 (2015) 1–6.
[134] Y. Hu, X. Zhao, Z. Suo, Averting cracks caused by insertion reaction in lithium-ion batteries, J. Mater. Res. 25 (2010) 1007–1010.
[135] Y. Liu, P. Lv, J. Ma, R. Bai, H.L. Duan, Stress fields in hollow core-shell spherical electrodes of lithium ion batteries, Proc. R. Soc. A 470 (2014) 20140299.
[136] X.H. Liu, L. Zhong, S. Huang, S.X. Mao, T. Zhu, J.Y. Huang, Size-dependent fracture of silicon nanoparticles during lithiation, ACS Nano 6 (2012) 1522–1531.
[137] R. Deshpande, Y.-T. Cheng, M.W. Verbrugge, A. Timmons, Diffusion induced stresses and strain energy in a phase-transforming spherical electrode particle, J. Electrochem. Soc. 158 (2011) A718–A724.
[138] M.T. McDowell, I. Ryu, S.W. Lee, C. Wang, W.D. Nix, Y. Cui, Studying the kinetics of crystalline silicon nanoparticle lithiation with in situ transmission electron microscopy, Adv. Mater. 24 (2012) 6034–6041.
[139] A. Vemulapally, R. Kali, A. Bhandakkar, Tanmay K. ANDMukhopadhyay, Transformation plasticity provides insights into concurrent phase transformation and stress relaxation observed during electrochemical Li alloying of Sn thin film, J. Phys. Chem. C 122 (2018) 16561–16573.
[140] A.F. Bower, P.R. Guduru, E. Chason, Analytical solutions for composition and stress in spherical elastic–plastic lithium-ion electrode particles containing a propagating phase boundary, Int. J. Solid Struct. 69–70 (2015) 328–342.
[141] X. Zhang, S.W. Lee, H.-W. Lee, Y. Cui, C. Linder, A reaction-controlled diffusion model for the lithiation of silicon in lithium-ion batteries, Extreme Mech. Lett. 4 (2015) 61–75.
[142] Z. Jia, T. Li, Intrinsic stress mitigation via elastic softening during two-step electrochemical lithiation of amorphous silicon, J. Mech. Phys. Solid. 91 (2016) 278–290.
[143] R. Xu, K. Zhao, Mechanical interactions regulated kinetics and morphology of composite electrodes in Li-ion batteries, Extreme Mech. Lett. 8 (2016) 13–21.
[144] Y. Zhao, P. Stein, B.-X. Xu, Isogeometric analysis of mechanically coupled Cahn–Hilliard phase segregation in hyperelastic electrodes of Li-ion batteries, Comput. Methods Appl. Mech. Eng. 297 (2015) 325–347.
[145] M. Huttin, M. Kamlah, Phase-field modeling of stress generation in electrode particles of lithium ion batteries, Appl. Phys. Lett. 101 (2012) 133902.
[146] E.A. Guggenheim, Mixtures: the Theory of the Equlibrium Properties of Some Simple Classes of Mixtures Solutions and Alloys, Clarendon Press, 1952.
[147] C.V. Di Leo, E. Rejovitzky, L. Anand, A Cahn–Hilliard-type phase-field theory for species diffusion coupled with large elastic deformations: application to phase-separating Li-ion electrode materials, J. Mech. Phys. Solid. 70 (2014) 1–29.
[148] L. Chen, F. Fan, L. Hong, J. Chen, Y.Z. Ji, S.L. Zhang, T. Zhu, L.Q. Chen, A phase-field model coupled with large elasto-plastic deformation: application to lithiated silicon electrodes, J. Electrochem. Soc. 161 (2014) F3164–F3172.
[149] Y. Zhao, B.-X. Xu, P. Stein, D. Gross, Phase-field study of electrochemical reactions at exterior and interior interfaces in Li-ion battery electrode particles, Comput. Methods Appl. Mech. Eng. 312 (2016) 428–446.
[150] D.A. Cogswell, M.Z. Bazant, Coherency strain and the kinetics of phase separation in $LiFePO_4$ nanoparticles, ACS Nano 6 (2012) 2215–2225.
[151] N. Nadkarni, E. Rejovitsky, D. Fraggedakis, C.V. Di Leo, R.B. Smith, P. Bai, M.Z. Bazant, Interplay of phase boundary anisotropy and electro-autocatalytic surface reactions on the lithium intercalation dynamics in Li_xFePO_4 platelet-like nanoparticles, Phys. Rev. Materials 2 (2018) 085406.
[152] M. Tang, J.F. Belak, M.R. Dorr, Anisotropic phase boundary morphology in nanoscale olivine electrode particles, J. Phys. Chem. C 115 (2011) 4922–4926.
[153] M. Tang, H.-Y. Huang, N. Meethong, Y.-H. Kao, W.C. Carter, Y.-M. Chiang, Model for the particle size, overpotential, and strain dependence of phase transition pathways in storage electrodes: application to nanoscale olivines, Chem. Mater. 21 (2009) 1557–1571.
[154] M. Tang, W.C. Carter, J.F. Belak, Y.-M. Chiang, Modeling the competing phase transition pathways in nanoscale olivine electrodes, Electrochim. Acta 56 (2010) 969–976.
[155] Y.-H. Kao, M. Tang, N. Meethong, J. Bai, W.C. Carter, Y.-M. Chiang, Overpotential-dependent phase transformation pathways in lithium iron phosphate battery electrodes, Chem. Mater. 22 (2010) 5845–5855.
[156] V.B. Shenoy, P. Johari, Y. Qi, Elastic softening of amorphous and crystalline Li-Si phases with increasing Li concentration: a first-principles study, J. Power Sources 195 (2010) 6825–6830.
[157] J.B. Ratchford, B.A. Crawford, J. Wolfenstine, J.L. Allen, C.A. Lundgren, Young's modulus of polycrystalline Li12si7 using nanoindentation testing, J. Power Sources 211 (2012) 1–3.
[158] S. Lee, J. Park, A.M. Sastry, W. Lu, Molecular dynamics simulations of SOC-dependent elasticity of $Li_xMn_2O_4$ spinels in Li-ion batteries, J. Electrochem. Soc. 160 (2013) A968–A972.
[159] Y. Qi, L.G. Hector, C. James, K.J. Kim, Lithium concentration dependent elastic properties of battery electrode materials from first principles calculations, J. Electrochem. Soc. 161 (2014) F3010–F3018.
[160] R. Deshpande, Y. Qi, Y.-T. Cheng, Effects of concentration-dependent elastic modulus on diffusion-induced stresses for battery applications, J. Electrochem. Soc. 157 (2010) A967.
[161] B. Yang, Y.P. He, J. Irsa, C.A. Lundgren, J.B. Ratchford, Y.P. Zhao, Effects of composition-dependent modulus, finite concentration and boundary constraint on Li-ion diffusion and stresses in a bilayer Cu-coated Si nano-anode, J. Power Sources 204 (2012) 168–176.
[162] Z. Guo, T. Zhang, H. Hu, Y. Song, J. Zhang, Effects of hydrostatic stress and concentration-dependent elastic modulus on diffusion-induced stresses in cylindrical Li-ion batteries, J. Appl. Mech. 81 (2013) 031013.
[163] X.H. Liu, H. Zheng, L. Zhong, S. Huang, K. Karki, L.Q. Zhang, Y. Liu, A. Kushima, W.T. Liang, J.W. Wang, J.-H. Cho, E. Epstein, S.A. Dayeh, S.T. Picraux, T. Zhu, J. Li, J.P. Sullivan, J. Cumings, C. Wang, S.X. Mao, Z.Z. Ye, S. Zhang, J.Y. Huang, Anisotropic swelling and fracture of silicon nanowires during lithiation, Nano Lett. 11 (2011) 3312–3318.
[164] M. Pharr, K. Zhao, X. Wang, Z. Suo, J.J. Vlassak, Kinetics of initial lithiation of crystalline silicon electrodes of lithium-ion batteries, Nano Lett. 12 (2012) 5039–5047.
[165] Q. Zhang, Y. Cui, E. Wang, Anisotropic lithium insertion behavior in silicon nanowires: binding energy, diffusion barrier, and strain effect, J. Phys. Chem. C 115 (2011) 9376–9381.
[166] W. Hong, A kinetic model for anisotropic reactions in amorphous solids, Extreme Mech. Lett. 2 (2015) 46–51.
[167] V.I. Levitas, H. Attariani, Anisotropic compositional expansion in elastoplastic materials and corresponding chemical potential: large-strain formulation and application to amorphous lithiated silicon, J. Mech. Phys. Solid. 69 (2014) 84–111.
[168] H. Yang, S. Huang, X. Huang, F. Fan, W. Liang, X.H. Liu, L.-Q. Chen, J.Y. Huang, J. Li, T. Zhu, S. Zhang, Orientation-dependent interfacial mobility governs the anisotropic swelling in lithiated silicon nanowires, Nano Lett. 12 (2012) 1953–1958.
[169] H. Yang, F. Fan, W. Liang, X. Guo, T. Zhu, S. Zhang, A chemo-mechanical model of lithiation in silicon, J. Mech. Phys. Solid. 70 (2014) 349–361.

[170] Y. An, B.C. Wood, J. Ye, Y.-M. Chiang, Y.M. Wang, M. Tang, H. Jiang, Mitigating mechanical failure of crystalline silicon electrodes for lithium batteries by morphological design, Phys. Chem. Chem. Phys. 17 (2015) 17718–17728.
[171] S. Hu, Y. Li, K.M. Rosso, M.L. Sushko, Mesoscale phase-field modeling of charge transport in nanocomposite electrodes for lithium-ion batteries, J. Phys. Chem. C 117 (2013) 28–40.
[172] S. Han, J. Park, W. Lu, A.M. Sastry, Numerical study of grain boundary effect on li + effective diffusivity and intercalation-induced stresses in li-ion battery active materials, J. Power Sources 240 (2013) 155–167.
[173] S.K. Vanimisetti, N. Ramakrishnan, Effect of the electrode particle shape in Li-ion battery on the mechanical degradation during charge-discharge cycling, Proc. IMechE Part C: J. Mech. Eng. Sci. 226 (2012) 2192–2213.
[174] P. Stein, Y. Zhao, B.-X. Xu, Effects of surface tension and electrochemical reactions in Li-ion battery electrode nanoparticles, J. Power Sources 332 (2016) 154–169.
[175] S.J. Harris, R.D. Deshpande, Y. Qi, I. Dutta, Y.-T. Cheng, Mesopores inside electrode particles can change the Li-ion transport mechanism and diffusion-induced stress, J. Mater. Res. 25 (2010) 1433–1440.
[176] Z. Jia, T. Li, Stress-modulated driving force for lithiation reaction in hollow nano-anodes, J. Power Sources 275 (2015) 866–876.
[177] R. Purkayastha, R. McMeeking, Stress due to the intercalation of lithium in cubic-shaped particles: a parameter study, Meccanica 51 (2016) 3081–3096.
[178] B. Suthar, V.R. Subramanian, Lithium intercalation in core-shell materials – theoretical analysis, J. Electrochem. Soc. 161 (2014) A682–A692.
[179] N. Swaminathan, S. Balakrishnan, K. George, Elasticity and size effects on the electrochemical response of a graphite, Li-ion battery electrode particle, J. Electrochem. Soc. 163 (2016) A488–A498.
[180] C. Lim, B. Yan, L. Yin, L. Zhu, Simulation of diffusion-induced stress using reconstructed electrodes particle structures generated by micro/nano-CT, Electrochim. Acta 75 (2012) 279–287.
[181] M. Chung, J. Seo, X. Zhang, A. Sastry, Implementing realistic geometry and measured diffusion coefficients into single particle electrode modeling based on experiments with single $LiMn_2O_4$ spinel particles, J. Electrochem. Soc. 158 (2011) A371–A378.
[182] V. Malavé, J. Berger, H. Zhu, R.J. Kee, A computational model of the mechanical behavior within reconstructed Li_xCoO_2 Li-ion battery cathode particles, Electrochim. Acta 130 (2014) 707–717.
[183] J. Hun, M. Chung, M. Park, S. Woo, X. Zhang, A. Marie, Generation of realistic particle structures and simulations of internal stress: a numerical/AFM study of $LiMn_2O_4$ particles, J. Electrochem. Soc. 158 (2011) A434–A442.
[184] Y. Lu, Y. Ni, Effects of particle shape and concurrent plasticity on stress generation during lithiation in particulate Li-ion battery electrodes, Mech. Mater. 91 (2015) 372–381.
[185] M. Okubo, E. Hosono, J. Kim, M. Enomoto, N. Kojima, T. Kudo, H. Zhou, I. Honma, Nanosize effect on high-rate Li-ion intercalation in $LiCoO_2$ electrode, J. Am. Chem. Soc. 129 (2007) 7444–7452.
[186] P. Poizot, S. Laruelle, S. Grugeon, L. Dupont, J.-M. Tarascon, Nano-sized transition-metal oxides as negative-electrode materials for lithium-ion batteries, Nature 407 (2000) 496–499.
[187] H. Sclar, D. Kovacheva, E. Zhecheva, R. Stoyanova, R. Lavi, G. Kimmel, J. Grinblat, O. Girshevitz, F. Amalraj, O. Haik, E. Zinigrad, B. Markovsky, D. Aurbach, On the performance of $LiNi_{1/3}Mn_{1/3}Co_{1/3}O_2$ nanoparticles as a cathode material for lithium-ion batteries, J. Electrochem. Soc. 156 (2009) A938–A948.
[188] Y.J. Wei, K. Nikolowski, S.Y. Zhan, H. Ehrenberg, S. Oswald, G. Chen, C.Z. Wang, H. Chen, Electrochemical kinetics and cycling performance of nano Li $[Li_{0.23}Co_{0.3}Mn_{0.47}]O_2$ cathode material for lithium ion batteries, Electrochem. Commun. 11 (2009) 2008–2011.
[189] A. Van der Ven, M. Wagemaker, Effect of surface energies and nano-particle size distribution on open circuit voltage of Li-electrodes, Electrochem. Commun. 11 (2009) 881–884.
[190] W. Qi, J.G. Shapter, Q. Wu, T. Yin, G. Gao, D. Cui, Nanostructured anode materials for lithium-ion batteries: principle, recent progress and future perspectives, J. Mater. Chem. 5 (2017) 19521.
[191] N. Zhao, L. Fu, L. Yang, T. Zhang, G. Wang, Y. Wu, T. van Ree, Nanostructured anode materials for Li-ion batteries, Pure Appl. Chem. 80 (2008) 2283–2295.
[192] G.A. Horrocks, M.F. Likely, J.M. Velazquez, S. Banerjee, Finite size effects on the structural progression induced by lithiation of V_2O_5 : a combined diffraction and Raman spectroscopy study, J. Mater. Chem. 1 (2013) 15265–15277.
[193] J. Wan, A.F. Kaplan, J. Zheng, X. Han, Y. Chen, N.J. Weadock, N. Faenza, S. Lacey, T. Li, J. Guo, L. Hu, Two dimensional silicon nanowalls for lithium ion batteries, J. Mater. Chem. 2 (2014) 6051–6057.
[194] J.-H. Jeong, K.-H. Kim, D.-W. Jung, K. Kim, S.-M. Lee, E.-S. Oh, High-performance characteristics of silicon inverse opal synthesized by the simple magnesium reduction as anodes for lithium-ion batteries, J. Power Sources 300 (2015) 182–189.
[195] C.J. Chalker, H. An, J. Zavala, A. Parija, S. Banerjee, J.L. Lutkenhaus, J.D. Batteas, Fabrication and electrochemical performance of structured mesoscale open shell V_2O_5 networks, Langmuir 33 (2017) 5975–5981.
[196] Q. Xiao, M. Gu, H. Yang, B. Li, C. Zhang, Y. Liu, F. Liu, F. Dai, L. Yang, Z. Liu, X. Xiao, G. Liu, P. Zhao, S. Zhang, C. Wang, Y. Lu, M. Cai, Inward lithium-ion breathing of hierarchically porous silicon anodes, Nat. Commun. 6 (2015) 8844.
[197] J. Ye, A.C. Baumgaertel, Y.M. Wang, J. Biener, M.M. Biener, Structural optimization of 3D porous electrodes for high-rate performance lithium ion batteries, ACS Nano 9 (2015) 2194–2202.
[198] X. Xia, C.V. Di Leo, X.W. Gu, J.R. Greer, In situ lithiation-delithiation of mechanically robust Cu-Si core-shell nanolattices in a scanning electron microscope, ACS Energy Lett 1 (2016) 492–499.
[199] J. Wang, H.L. Duan, Z.P. Huang, B.L. Karihaloo, A scaling law for properties of nano-structured materials, Proc. R. Soc. A 462 (2006) 1355–1363.
[200] J. Wang, Z. Huang, H. Duan, S. Yu, X. Feng, G. Wang, W. Zahng, T. Wang, Surface stress effect in mechanics of nanostructured materials, Acta Mech. Solida Sin. 24 (2011) 52–82.
[201] D. Davydov, A. Javili, P. Steinmann, On molecular statics and surface-enhanced continuum modeling of nano-structures, Comput. Mater. Sci. 69 (2013) 510–519.
[202] D. Gross, R. Müller, M. Müller, B.-X. Xu, K. Albe, On the origin of inhomogeneous stress and strain distributions in single-crystalline metallic nanoparticles, Int. J. Mater. Res. 102 (2011) 743–747.
[203] J.W. Gibbs, The Scientific Papers of J. Willard Gibbs vol. 1, Longmans Green and Co, 1906.
[204] R. Shuttleworth, The surface tension of solids, Proc. Phys. Soc. 63 (1950) 444–457.
[205] C. Herring, Surface tension as a motivation for sintering, in: J.M. Ball, D. Kinderlehrer, P. Podio-Guidugli, M. Slemrod (Eds.), Fundamental Contributions to the Continuum Theory of Evolving Phase Interfaces in Solids, Springer, Berlin, Heidelberg, 1999, pp. 33–69, , https://doi.org/10.1007/978-3-642-59938-5.
[206] M.E. Gurtin, A.I. Murdoch, A continuum theory of elastic material surfaces, Arch. Ration. Mech. Anal. 57 (1975) 291–323.
[207] A.T. McBride, A. Javili, P. Steinmann, S. Bargmann, Geometrically nonlinear continuum thermomechanics with surface energies coupled to diffusion, J. Mech. Phys. Solid. 59 (2011) 2116–2133.
[208] J. Weissmüller, J.W. Cahn, Mean stresses in microstructures due to interface stresses: a generalization of a capillary equation for solids, Acta Mater. 45 (1997) 1899–1906.
[209] F. Hao, X. Gao, D. Fang, Diffusion-induced stresses of electrode nanomaterials in lithium-ion battery: the effects of surface stress, J. Appl. Phys. 112 (2012) 103507.
[210] C.M. DeLuca, K. Maute, M.L. Dunn, Effects of electrode particle morphology on stress generation in silicon during lithium insertion, J. Power Sources 196 (2011) 9672–9681.
[211] J.-L. Zang, Y.-P. Zhao, A diffusion and curvature dependent surface elastic model with application to stress analysis of anode in lithium ion battery, Int. J. Eng. Sci. 61 (2012) 156–170.
[212] Y. Lu, P. Zhang, F. Wang, K. Zhang, X. Zhao, Reaction-diffusion-stress coupling model for li-ion batteries: the role of surface effects on electrochemical performance, Electrochim. Acta 274 (2018) 359–369.
[213] P. Stein, A. Moradabadi, M. Diehm, B.-X. Xu, K. Albe, The influence of anisotropic surface stresses and bulk stresses on defect thermodynamics in $LiCoO_2$ nanoparticles, Acta Mater. 159 (2018) 225–240.
[214] T.K. Bhandakkar, H.T. Johnson, Diffusion induced stresses in buckling battery electrodes, J. Mech. Phys. Solid. 60 (2012) 1103–1121.
[215] J. Chakraborty, C.P. Please, A. Goriely, S.J. Chapman, Combining mechanical and chemical effects in the deformation and failure of a cylindrical electrode particle in a Li-ion battery, Int. J. Solid Struct. 54 (2015) 66–81.
[216] K. Zhang, Y. Li, B. Zheng, G. Wu, J. Wu, F. Yang, Large deformation analysis of diffusion-induced buckling of nanowires in lithium-ion batteries, Int. J. Solid Struct. 108 (2017) 230–243.
[217] K. Zhang, Y. Li, J. Wu, B. Zheng, F. Yang, Lithiation-induced buckling of wire-based electrodes in lithium-ion batteries: a phase-field model coupled with large deformation, Int. J. Solid Struct. (2018).
[218] C. Yu, X. Li, T. Ma, J. Rong, R. Zhang, J. Shaffer, Y. An, Q. Liu, B. Wei, H. Jiang, Silicon thin films as anodes for high-performance lithium-ion batteries with effective stress relaxation, Adv. Energy Mater. 2 (2011) 68–73.
[219] X. Wang, W. Zeng, L. Hong, W. Xu, H. Yang, F. Wang, H. Duan, M. Tang, H. Jiang, Stress-driven lithium dendrite growth mechanism and dendrite mitigation by electroplating on soft substrates, Nature Energy 3 (2018) 227–235.
[220] Z. Jia, T. Li, Failure mechanics of a wrinkling thin film anode on a substrate under cyclic charging and discharging, Extreme Mech. Lett. 8 (2016) 273–282.
[221] M.E. Stournara, X. Xiao, Y. Qi, P. Johari, P. Lu, B.W. Sheldon, H. Gao, V.B. Shenoy, Li segregation induces structure and strength changes at the amorphous Si/Cu interface, Nano Lett. 13 (2013) 4759–4768.
[222] G.R. Hardin, Y. Zhang, C.D. Fincher, M. Pharr, Interfacial fracture of nanowire electrodes of lithium-ion batteries, JOM 69 (2017) 1519–1523.
[223] R. Xu, L.S. de Vasconcelos, J. Shi, J. Li, K. Zhao, Disintegration of meatball electrodes for $LiNi_xMn_yCo_zO_2$ cathode materials, Exp. Mech. 58 (2018) 549–559.
[224] R. Xu, K. Zhao, Corrosive fracture of electrodes in Li-ion batteries, J. Mech. Phys. Solid. 121 (2018) 258–280.
[225] Y. Itou, Y. Ukyo, Performance of $LiNiCoO_2$ materials for advanced lithium-ion batteries, J. Power Sources 146 (2005) 39–44.
[226] D. Wang, X. Wu, Z. Wang, L. Chen, Cracking causing cyclic instability of $LiFePO_4$ cathode material, J. Power Sources 140 (2005) 125–128.
[227] P. Yan, J. Zheng, M. Gu, J. Xiao, J.-G. Zhang, C.-M. Wang, Intragranular cracking as a critical barrier for high-voltage usage of layer-structured cathode for lithium-ion batteries, Nat. Commun. 8 (2017) 14101.
[228] J. Christensen, J. Newman, A mathematical model of stress generation and fracture in lithium manganese oxide, J. Electrochem. Soc. 153 (2006) A1019.
[229] M. Qu, W.H. Woodford, J.M. Maloney, W.C. Carter, Y.-M. Chiang, K.J. Van Vliet, Nanomechanical quantification of elastic, plastic, and fracture properties of $LiCoO_2$, Adv. Energy Mater. 2 (2012) 940–944.
[230] J.G. Swallow, W.H. Woodford, F.P. McGrogan, N. Ferralis, Y.-M. Chiang, K.J.V. Vliet, Effect of electrochemical charging on elastoplastic properties and fracture toughness of Li_xCoO_2, J. Electrochem. Soc. 161 (2014) F3084–F3090.
[231] R. Xu, H. Sun, L. S. d. Vasconcelos, K. Zhao, Mechanical and structural degradation of $LiNi_xMn_yCo_zO_2$ cathode in Li-ion batteries: an experimental study, J. Electrochem. Soc. 164 (2017) A3333–A3341.
[232] R. Grantab, V.B. Shenoy, Pressure-gradient dependent diffusion and crack propagation in lithiated silicon nanowires, J. Electrochem. Soc. 159 (2012)

A584–A591.
[233] T.K. Bhandakkar, H. Gao, Cohesive modeling of crack nucleation under diffusion induced stresses in a thin strip: implications on the critical size for flaw tolerant battery electrodes, Int. J. Solid Struct. 47 (2010) 1424–1434.
[234] I. Ryu, S.W. Lee, H. Gao, Y. Cui, W.D. Nix, Microscopic model for fracture of crystalline Si nanopillars during lithiation, J. Power Sources 255 (2014) 274–282.
[235] R. Grantab, V.B. Shenoy, Location- and orientation-dependent progressive crack propagation in cylindrical graphite electrode particles, J. Electrochem. Soc. 158 (2011) A948–A954.
[236] S.K. Soni, B.W. Sheldon, X. Xiao, M.W. Verbrugge, A. Dongjoon, H. H, G. Huajian, Stress mitigation during the lithiation of patterned amorphous Si Islands, J. Electrochem. Soc. 159 (2011) A38–A43.
[237] H. Haftbaradaran, S.K. Soni, B.W. Sheldon, X. Xiao, H. Gao, Modified stoney equation for patterned thin film electrodes on substrates in the presence of interfacial sliding, J. Appl. Mech. 79 (2012) 031018.
[238] B. Lu, Y. Song, J. Zhang, Time to delamination onset and critical size of patterned thin film electrodes of lithium ion batteries, J. Power Sources 289 (2015) 168–183.
[239] C. Miehe, H. Dal, A. Raina, A phase field model for chemo-mechanical induced fracture in lithium-ion battery electrode particles, Int. J. Numer. Methods Eng. 106 (2015) 683–711.
[240] B.-X. Xu, Y. Zhao, P. Stein, Phase field modeling of electrochemically induced fracture in Li-ion battery with large deformation and phase segregation, GAMM-Mitt. 39 (2016) 92–109.
[241] M. Klinsmann, D. Rosato, M. Kamlah, R.M. McMeeking, Modeling crack growth during Li insertion in storage particles using a fracture phase field approach, J. Mech. Phys. Solid. 92 (2016) 313–344.
[242] M. Klinsmann, D. Rosato, M. Kamlah, R.M. McMeeking, Modeling crack growth during Li extraction in storage particles using a fracture phase field approach, J. Electrochem. Soc. 163 (2016) A102–A118.
[243] P. Barai, P.P. Mukherjee, Stochastic analysis of diffusion induced damage in lithium-ion battery electrodes, J. Electrochem. Soc. 160 (2013) A955–A967.
[244] P. Barai, P.P. Mukherjee, Mechano-electrochemical stochastics in high-capacity electrodes for energy storage, J. Electrochem. Soc. 163 (2016) A1120–A1137.
[245] W.H. Woodford, W. Craig Carter, Y.-M. Chiang, Design criteria for electrochemical shock resistant battery electrodes, Energy Environ. Sci. 5 (2012) 8014–8024.
[246] B. Wu, W. Lu, Mechanical-electrochemical modeling of agglomerate particles in lithium-ion battery electrodes, J. Electrochem. Soc. 163 (2016) A3131–A3139.
[247] W.H. Woodford, Y.-M. Chiang, W.C. Carter, Electrochemical shock of intercalation electrodes: a fracture mechanics analysis, J. Electrochem. Soc. 157 (2010) A1052–A1059.
[248] G. Sun, T. Sui, B. Song, H. Zheng, L. Lu, A.M. Korsunsky, On the fragmentation of active material secondary particles in lithium ion battery cathodes induced by charge cycling, Extreme Mech. Lett. 9 (2016) 449–458.
[249] M. Gauthier, T.J. Carney, A. Grimaud, L. Giordano, N. Pour, H.-H. Chang, D.P. Fenning, S.F. Lux, O. Paschos, C. Bauer, F. Maglia, S. Lupart, P. Lamp, Y. Shao-Horn, Electrode-electrolyte interface in Li-ion batteries: current understanding and new insights, J. Phys. Chem. Lett. 6 (2015) 4653–4672.
[250] A. Wang, S. Kadam, H. Li, S. Shi, Y. Qi, Review on modeling of the anode solid electrolyte interphase (SEI) for lithium-ion batteries, npj Comput. Mater. 4 (2018) 15.
[251] E. Rejovitzky, C.V. Di Leo, L. Anand, A theory and a simulation capability for the growth of a solid electrolyte interphase layer at an anode particle in a Li-ion battery, J. Mech. Phys. Solid. 78 (2015) 210–230.
[252] P. Guan, L. Liu, X. Lin, Simulation and experiment on solid electrolyte interphase (SEI) morphology evolution and lithium-ion diffusion, J. Electrochem. Soc. 162 (2015) A1798–A1808.
[253] D.A. Freedman, D. Roundy, T.A. Arias, Elastic effects of vacancies in strontium titanate: short and long-range strain fields, elastic dipole tensors, and chemical strain, Phys. Rev. B 80 (2009) 064108.
[254] V. Wenzel, H. Nirschl, D. Nötzel, Challenges in lithium-ion-battery slurry preparation and potential of modifying electrode structures by different mixing processes, Energy Technol. 3 (2015) 692–698.
[255] Z. Liu, T.W. Verhallen, D.P. Singh, H. Wang, M. Wagemaker, S. Barnett, Relating the 3D electrode morphology to Li-ion battery performance; a case for lifepo4, J. Power Sources 324 (2016) 358–367.
[256] D.-W. Chung, P.R. Shearing, N.P. Brandon, S.J. Harris, R.E. García, Particle size polydispersity in li-ion batteries, J. Electrochem. Soc. 161 (2014) A422–A430.
[257] L. Ji, Z. Guo, Y. Wu, Computational and experimental observation of Li-ion concentration distribution and diffusion-induced stress in porous battery electrodes, Energy Technol. 5 (2017) 1702–1711.
[258] Y. Zhao, L.R. De Jesus, P. Stein, G.A. Horrocks, S. Banerjee, B.-X. Xu, Modeling of phase separation across interconnected electrode particles in lithium-ion batteries, RSC Adv. 7 (2017) 41254–41264.
[259] L.R.D. Jesus, Y. Zhao, G.A. Horrocks, J.L. Andrews, P. Stein, B.-X. Xu, S. Banerjee, Lithiation across interconnected V_2O_5 nanoparticle networks, J. Mater. Chem. 5 (2017) 20141–20152.
[260] Y. Li, F. El Gabaly, T.R. Ferguson, R.B. Smith, N.C. Bartelt, J.D. Sugar, K.R. Fenton, D.A. Cogswell, A.L.D. Kilcoyne, T. Tyliszczak, M.Z. Bazant, W.C. Chueh, Current-induced transition from particle-by-particle to concurrent intercalation in phase-separating battery electrodes, Nat. Mater. 13 (2014) 1149–1156.
[261] Y. Zhao, D. Schillinger, B.-X. Xu, Variational boundary conditions based on the Nitsche method for fitted and unfitted isogeometric discretizations of the mechanically coupled Cahn–Hilliard equation, J. Comp. Physiol. 340 (2017) 177–199.
[262] K.E. Aifantis, J.P. Dempsey, Stable crack growth in nanostructured Li-batteries, J. Power Sources 143 (2005) 203–211.
[263] K.E. Aifantis, S.A. Hackney, J.P. Dempsey, Design criteria for nanostructured Li-ion batteries, J. Power Sources 165 (2007) 874–879.
[264] B.J. Dimitrijevic, K.E. Aifantis, K. Hackl, The influence of particle size and spacing on the fragmentation of nanocomposite anodes for Li batteries, J. Power Sources 206 (2012) 343–348.
[265] E.K. Rahani, V.B. Shenoy, Role of plastic deformation of binder on stress evolution during charging and discharging in lithium-ion battery negative electrodes, J. Electrochem. Soc. 160 (2013) A1153–A1162.
[266] R. Xu, L. S. d. Vasconcelos, K. Zhao, Computational analysis of chemomechanical behaviors of composite electrodes in Li-ion batteries, J. Mater. Res. 31 (2016) 2715–2727.
[267] H. Wang, S.P. Nadimpalli, V.B. Shenoy, Inelastic shape changes of silicon particles and stress evolution at binder/particle interface in a composite electrode during lithiation/delithiation cycling, Extreme Mech. Lett. 9 (2016) 430–438.
[268] S. Kim, H.-Y.S. Huang, Mechanical stresses at the cathode-electrolyte interface in lithium-ion batteries, J. Mater. Res. 31 (2016) 3506–3512.
[269] B. Vijayaraghavan, D.R. Ely, Y.-M. Chiang, R. García-García, R.E. García, An analytical method to determine tortuosity in rechargeable battery electrodes, J. Electrochem. Soc. 159 (2012) A548–A552.
[270] D. Westhoff, J. Feinauer, K. Kuchler, T. Mitsch, I. Manke, S. Hein, A. Latz, V. Schmidt, Parametric stochastic 3D model for the microstructure of anodes in lithium-ion power cells, Comput. Mater. Sci. 126 (2017) 453–467.
[271] M. Ebner, D.-W. Chung, R.E. García, V. Wood, Tortuosity anisotropy in lithium-ion battery electrodes, Adv. Energy Mater. 4 (2014) 1301278.
[272] S.A. Roberts, V.E. Brunini, K.N. Long, A.M. Grillet, A framework for three-dimensional mesoscale modeling of anisotropic swelling and mechanical deformation in lithium-ion electrodes, J. Electrochem. Soc. 161 (2014) F3052–F3059.
[273] H. Mendoza, S.A. Roberts, V.E. Brunini, A.M. Grillet, Mechanical and electrochemical response of a $LiCoO_2$ cathode using reconstructed microstructures, Electrochim. Acta 190 (2016) 1–15.
[274] S. Kim, J. Wee, K. Peters, H.-Y.S. Huang, Multiphysics coupling in lithium-ion batteries with reconstructed porous microstructures, J. Phys. Chem. C 122 (2018) 5280–5290.
[275] L. Wu, X. Xiao, Y. Wen, J. Zhang, Three-dimensional finite element study on stress generation in synchrotron X-ray tomography reconstructed nickel-manganese-cobalt based half cell, J. Power Sources 336 (2016) 8–18.
[276] L. Wu, Y. Wen, J. Zhang, Three-dimensional finite element study on Li diffusion induced stress in FIB-SEM reconstructed $LiCoO_2$ half cell, Electrochim. Acta 222 (2016) 814–820.
[277] G.-A. Nazri, G. Pistoia, Lithium Batteries: Science and Technology, Springer Science & Business Media, 2008.
[278] D. Andre, M. Meiler, K. Steiner, C. Wimmer, T. Soczka-Guth, D. Sauer, Characterization of high-power lithium-ion batteries by electrochemical impedance spectroscopy. i. experimental investigation, J. Power Sources 196 (2011) 5334–5341.
[279] C. Chen, J. Liu, K. Amine, Symmetric cell approach and impedance spectroscopy of high power lithium-ion batteries, J. Power Sources 96 (2001) 321–328.
[280] J. Park, W. Lu, A.M. Sastry, Numerical simulation of stress evolution in lithium manganese dioxide particles due to coupled phase transition and intercalation, J. Electrochem. Soc. 158 (2011) A201.
[281] J. Newman, W. Tiedemann, Porous-electrode theory with battery applications, AIChE J. 21 (1975) 25–41.
[282] M. Doyle, T.F. Fuller, J. Newman, Modeling of galvanostatic charge and discharge of the lithium/polymer/insertion cell, J. Electrochem. Soc. 140 (1993) 1526–1533.
[283] M. Doyle, J. Newman, A.S. Gozdz, C.N. Schmutz, J.-M. Tarascon, Comparison of modeling predictions with experimental data from plastic lithium ion cells, J. Electrochem. Soc. 143 (1996) 1890–1903.
[284] D. a. G. Bruggeman, Berechnung verschiedener physikalischer Konstanten von heterogenen Substanzen. I. Dielektrizitätskonstanten und Leitfähigkeiten der Mischkörper aus isotropen Substanzen, Ann. Phys. 416 (1935) 636–664.
[285] B. Tjaden, S.J. Cooper, D.J. Brett, D. Kramer, P.R. Shearing, On the origin and application of the Bruggeman correlation for analysing transport phenomena in electrochemical systems, Curr. Opin. Chem. Eng. 12 (2016) 44–51.
[286] P.M. Gomadam, J.W. Weidner, Modeling volume changes in porous electrodes, J. Electrochem. Soc. 153 (2006) A179–A186.
[287] T.R. Garrick, K. Kanneganti, X. Huang, J.W. Weidner, Modeling volume change due to intercalation into porous electrodes, J. Electrochem. Soc. 161 (2014) E3297–E3301.
[288] T.R. Garrick, X. Huang, V. Srinivasan, J.W. Weidner, Modeling volume change in dual insertion electrodes, J. Electrochem. Soc. 164 (2017) E3552–E3558.
[289] T.R. Garrick, K. Higa, S.-L. Wu, Y. Dai, X. Huang, V. Srinivasan, J.W. Weidner, Modeling battery performance due to intercalation driven volume change in porous electrodes, J. Electrochem. Soc. 164 (2017) E3592–E3597.
[290] B. Yan, C. Lim, L. Yin, L. Zhu, Three dimensional simulation of galvanostatic discharge of $LiCoO_2$ cathode based on X-ray nano-CT images, J. Electrochem. Soc. 159 (2012) A1604–A1614.
[291] A.H. Wiedemann, G.M. Goldin, S.A. Barnett, H. Zhu, R.J. Kee, Effects of three-dimensional cathode microstructure on the performance of lithium-ion battery cathodes, Electrochim. Acta 88 (2013) 580–588.
[292] T. Hutzenlaub, S. Thiele, R. Zengerle, C. Ziegler, Three-dimensional reconstruction of a $LiCoO_2$ li-ion battery cathode, Electrochem. Solid State Lett. 15 (2011) A33–A36.
[293] M. Ebner, V. Wood, Tool for tortuosity estimation in lithium ion battery porous electrodes, J. Electrochem. Soc. 162 (2015) A3064–A3070.

[294] S. Cooper, A. Bertei, P. Shearing, J. Kilner, N. Brandon, Taufactor, An open-source application for calculating tortuosity factors from tomographic data, SoftwareX 5 (2016) 203–210.
[295] S. Golmon, K. Maute, M.L. Dunn, Numerical modeling of electro-chemical–mechanical interactions in lithium polymer batteries, Comput. Struct. 87 (2009) 1567–1579.
[296] T. Mori, K. Tanaka, Average stress in matrix and average elastic energy of materials with misfitting inclusions, Acta Metall. 21 (1973) 571–574.
[297] G. Inoue, K. Ikeshita, M. Iwabu, Y. Sagae, M. Kawase, Simulation of lithium-ion battery with effect of volume expansion of active materials, ECS Trans 80 (2017) 275–282.
[298] A. Awarke, S. Lauer, M. Wittler, S. Pischinger, Quantifying the effects of strains on the conductivity and porosity of $LiFePO_4$ based Li-ion composite cathodes using a multi-scale approach, Comput. Mater. Sci. 50 (2011) 871–879.
[299] K.E. Thomas, R.M. Darling, J. Newman, Mathematical modeling of lithium batteries, in: W. van Schalkwijk, B. Scrosati (Eds.), Advances in Lithium-ion Batteries, Kluwer Academic/Plenum, 2002, pp. 345–392.
[300] S. Santhanagopalan, Q. Guo, P. Ramadass, R.E. White, Review of models for predicting the cycling performance of lithium ion batteries, J. Power Sources 156 (2006) 620–628.
[301] M. Landstorfer, T. Jacob, Mathematical modeling of intercalation batteries at the cell level and beyond, Chem. Soc. Rev. 42 (2013) 3234–3252.
[302] A. Jokar, B. Rajabloo, M. Désilets, M. Lacroix, Review of simplified pseudo-two-dimensional models of lithium-ion batteries, J. Power Sources 327 (2016) 44–55.
[303] M. Doyle, Modeling of galvanostatic charge and discharge of the lithium/polymer/insertion cell, J. Electrochem. Soc. 140 (1993) 1526.
[304] T.F. Fuller, M. Doyle, J. Newman, Simulation and optimization of the dual lithium ion insertion cell, J. Electrochem. Soc. 141 (1994) 1–10.
[305] J. Christensen, Modeling diffusion-induced stress in Li-ion cells with porous electrodes, J. Electrochem. Soc. 157 (2010) A366–A380.
[306] R. Fu, M. Xiao, S.Y. Choe, Modeling, validation and analysis of mechanical stress generation and dimension changes of a pouch type high power Li-ion battery, J. Power Sources 224 (2013) 211–224.
[307] B. Suthar, P.W.C. Northrop, R.D. Braatz, V.R. Subramanian, Optimal charging profiles with minimal intercalation-induced stresses for lithium-ion batteries using reformulated pseudo 2-dimensional models, J. Electrochem. Soc. 161 (2014) F3144–F3155.
[308] B. Suthar, P.W.C. Northrop, D. Rife, V.R. Subramanian, Effect of porosity, thickness and tortuosity on capacity fade of anode, J. Electrochem. Soc. 162 (2015) A1708–A1717.
[309] Y. Dai, L. Cai, R.E. White, Simulation and analysis of stress in a li-ion battery with a blended $LiMn_2O_4$ and $LiNi_{0.8}Co_{0.15}Al_{0.05}O_2$ cathode, J. Power Sources 247 (2014) 365–376.
[310] S. Renganathan, G. Sikha, S. Santhanagopalan, R.E. White, Theoretical analysis of stresses in a lithium ion cell, J. Electrochem. Soc. 157 (2010) A155–A163.
[311] Y. Bai, Y. Zhao, W. Liu, B.-X. Xu, Two-level Modeling of Lithium-ion Batteries, (2019) (submitted for publication).
[312] X. Xiao, W. Wu, X. Huang, A multi-scale approach for the stress analysis of polymeric separators in a lithium-ion battery, J. Power Sources 195 (2010) 7649–7660.
[313] Y. Xie, C. Yuan, An integrated anode stress model for commercial Li_xC_6-$Li_yMn_2O_4$ battery during the cycling operation, J. Power Sources 274 (2015) 101–113.
[314] R. Behrou, K. Maute, Multiscale modeling of non-local damage evolution in lithium-ion batteries, ECS Trans 77 (2017) 1163–1177.
[315] R. Purkayastha, R.M. McMeeking, A linearized model for lithium ion batteries and maps for their performance and failure, J. Appl. Mech. 79 (2012) 031021–031021.
[316] J. Li, N. Lotfi, R.G. Landers, J. Park, A single particle model for lithium-ion batteries with electrolyte and stress-enhanced diffusion physics, J. Electrochem. Soc. 164 (2017) A874–A883.
[317] J. Li, K. Adewuyi, N. Lotfi, R. Landers, J. Park, A single particle model with chemical/mechanical degradation physics for lithium ion battery state of health (soh) estimation, Appl. Energy 212 (2018) 1178–1190.
[318] R.T. Purkayastha, R.M. McMeeking, An integrated 2-D model of a lithium ion battery: the effect of material parameters and morphology on storage particle stress, Comput. Mech. 50 (2012) 209–227.
[319] W. Wu, X. Xiao, M. Wang, X. Huang, A microstructural resolved model for the stress analysis of lithium-ion batteries, J. Electrochem. Soc. 161 (2014) A803–A813.
[320] A. Ferrese, J. Newman, Mechanical deformation of a lithium-metal anode due to a very stiff separator, J. Electrochem. Soc. 161 (2014) A1350–A1359.
[321] B. Wu, W. Lu, A battery model that fully couples mechanics and electrochemistry at both particle and electrode levels by incorporation of particle interaction, J. Power Sources 360 (2017) 360–372.
[322] Y. Dai, L. Cai, R.E. White, Simulation and analysis of inhomogeneous degradation in large format $LiMn_2O_4$/carbon cells, J. Electrochem. Soc. 161 (2014) E3348–E3356.
[323] B. Rieger, S.V. Erhard, S. Kosch, M. Venator, A. Rheinfeld, A. Jossen, Multi-dimensional modeling of the influence of cell design on temperature, displacement and stress inhomogeneity in large-format lithium-ion cells, J. Electrochem. Soc. 163 (2016) A3099–A3110.
[324] C.-W. Wang, A.M. Sastry, Mesoscale modeling of a Li-ion polymer cell, J. Electrochem. Soc. 154 (2007) A1035–A1047.
[325] S. Lee, A.M. Sastry, J. Park, Study on microstructures of electrodes in lithium-ion batteries using variational multi-scale enrichment, J. Power Sources 315 (2016) 96–110.
[326] J.F. Oudenhoven, L. Baggetto, P.H. Notten, All-solid-state lithium-ion microbatteries: a review of various three-dimensional concepts, Adv. Energy Mater. 1 (2011) 10–33.
[327] J. Janek, W.G. Zeier, A solid future for battery development, Energy 500 (2016) 300.
[328] R. Agrawal, G. Pandey, Solid polymer electrolytes: materials designing and all-solid-state battery applications: an overview, J. Phys. D 41 (2008) 223001.
[329] J.W. Fergus, Ceramic and polymeric solid electrolytes for lithium-ion batteries, J. Power Sources 195 (2010) 4554–4569.
[330] W.D. Richards, L.J. Miara, Y. Wang, J.C. Kim, G. Ceder, Interface Stability Solid-State Batteries 28 (2016) 266–273.
[331] Y.-S. Hu, Batteries: Getting Solid 1 (????) 16042.
[332] S. Zekoll, C. Marriner-Edwards, A.K.O. Hekselman, J. Kasemchainan, C. Kuss, D.E.J. Armstrong, D. Cai, R.J. Wallace, F.H. Richter, J.H.J. Thijssen, P.G. Bruce, Hybrid electrolytes with 3d bicontinuous ordered ceramic and polymer microchannels for all-solid-state, Batteries 11 (2018) 185–201.
[333] Y.V. Baskakova, O.V. Yarmolenko, O.N. Efimov, Polymer gel electrolytes for lithium batteries, Russ. Chem. Rev. 81 (2012) 367.
[334] M. Park, X. Zhang, M. Chung, G.B. Less, A.M. Sastry, A review of conduction phenomena in Li-ion batteries, J. Power Sources 195 (2010) 7904–7929.
[335] J.C. Bachman, S. Muy, A. Grimaud, H.-H. Chang, N. Pour, S.F. Lux, O. Paschos, F. Maglia, S. Lupart, P. Lamp, et al., Inorganic solid-state electrolytes for lithium batteries: mechanisms and properties governing ion conduction, Chem. Rev. 116 (2015) 140–162.
[336] G. Bucci, Y.-M. Chiang, W.C. Carter, Formulation of the coupled electro-chemical–mechanical boundary-value problem, with applications to transport of multiple charged species, Acta Mater. 104 (2016) 33–51.
[337] D. Grazioli, O. Verners, V. Zadin, D. Brandell, A. Simone, Electrochemical-mechanical modeling of solid polymer electrolytes: impact of mechanical stresses on Li-ion battery performance, Electrochim. Acta (2018) in press.
[338] P. Goyal, C.W. Monroe, New foundations of Newman's theory for solid electrolytes: thermodynamics and transient balances, J. Electrochem. Soc. 164 (2017) E3647–E3660.
[339] K. Becker-Steinberger, S. Funken, M. Landstorfer, K. Urban, A mathematical model for all solid-state lithium-ion batteries, ECS Transactions 25 (2010) 285–296.
[340] D. Danilov, R. a. H. Niessen, P.H.L. Notten, Modeling all-solid-state Li-ion batteries, J. Electrochem. Soc. 158 (2011) A215–A222.
[341] W. Dreyer, C. Guhlke, R. Müller, Overcoming the shortcomings of the Nernst–Planck model, Phys. Chem. Chem. Phys. 15 (2013) 7075–7086.
[342] M. Landstorfer, S. Funken, T. Jacob, An advanced model framework for solid electrolyte intercalation batteries, Phys. Chem. Chem. Phys. 13 (2011) 12817–12825.
[343] S. Braun, C. Yada, A. Latz, Thermodynamically consistent model for space-charge-layer formation in a solid electrolyte, J. Phys. Chem. C 119 (2015) 22281–22288.
[344] X. Su, T. Zhang, X. Liang, H. Gao, B.W. Sheldon, Employing nanoscale surface morphologies to improve interfacial adhesion between solid electrolytes and Li ion battery cathodes, Acta Mater. 98 (2015) 175–181.
[345] X. Su, K. Guo, T. Ma, P.A. Tamirisa, H. Ye, H. Gao, B.W. Sheldon, Deformation and chemomechanical degradation at solid electrolyte–electrode interfaces, ACS Energy Lett. 2 (2017) 1729–1733.
[346] G. Bucci, T. Swamy, Y.-M. Chiang, W.C. Carter, Modeling of internal mechanical failure of all-solid-state batteries during electrochemical cycling, and implications for battery design, J. Mater. Chem. 5 (2017) 19422–19430.
[347] G. Bucci, T. Swamy, Y.-M. Chiang, W.C. Carter, Random walk analysis of the effect of mechanical degradation on all-solid-state battery power, J. Electrochem. Soc. 164 (2017) A2660–A2664.
[348] G. Bucci, T. Swamy, S. Bishop, B.W. Sheldon, Y.-M. Chiang, W.C. Carter, The effect of stress on battery-electrode capacity, J. Electrochem. Soc. 164 (2017) A645–A654.
[349] G. Bucci, B. Talamini, A. Renuka Balakrishna, Y.-M. Chiang, W.C. Carter, Mechanical instability of electrode-electrolyte interfaces in solid-state batteries, Phys. Rev. Mater. 2 (2018) 105407.
[350] K. Guo, P.A. Tamirisa, B.W. Sheldon, X. Xiao, H. Gao, Pop-up delamination of electrodes in solid-state batteries, J. Electrochem. Soc. 165 (2018) A618–A625.
[351] R. Behrou, K. Maute, Numerical modeling of damage evolution phenomenon in solid-state lithium-ion batteries, J. Electrochem. Soc. 164 (2017) A2573–A2589.
[352] C. Brissot, M. Rosso, J.N. Chazalviel, S. Lascaud, Dendritic growth mechanisms in lithium/polymer cells, J. Power Sources 81–82 (1999) 925–929.
[353] C. Brissot, M. Rosso, J.N. Chazalviel, S. Lascaud, Concentration measurements in lithium/polymer–electrolyte/lithium cells during cycling, J. Power Sources 94 (2001) 212–218.
[354] R.D. Schmidt, J. Sakamoto, In-situ, non-destructive acoustic characterization of solid state electrolyte cells, J. Power Sources 324 (2016) 126–133.
[355] J.-G. Zhang, W. Xu, W.A. Henderson, Characterization and modeling of lithium dendrite growth, Lithium Metal Anodes and Rechargeable Lithium Metal Batteries, Springer Series in Materials Science, Springer, Cham, 2017, pp. 5–43, , https://doi.org/10.1007/978-3-319-44054-5_2.
[356] R.D. Armstrong, T. Dickinson, J. Turner, The breakdown of β-alumina ceramic electrolyte, Electrochim. Acta 19 (1974) 187–192.
[357] L.A. Feldman, L.C. De Jonghe, Initiation of mode I degradation in sodium-beta alumina electrolytes, J. Mater. Sci. 17 (1982) 517–524.
[358] C. Monroe, J. Newman, Dendrite growth in lithium/polymer systems: a propagation model for liquid electrolytes under galvanostatic conditions, J. Electrochem. Soc. 150 (2003) A1377–A1384.
[359] C. Monroe, J. Newman, The impact of elastic deformation on deposition kinetics at lithium/polymer interfaces, J. Electrochem. Soc. 152 (2005) A396–A404.
[360] G.M. Stone, S.A. Mullin, A.A. Teran, D.T. Hallinan, A.M. Minor, A. Hexemer,

N.P. Balsara, Resolution of the modulus versus adhesion dilemma in solid polymer electrolytes for rechargeable lithium metal batteries, J. Electrochem. Soc. 159 (2012) A222–A227.
[361] M.D. Tikekar, L.A. Archer, D.L. Koch, Stabilizing electrodeposition in elastic solid electrolytes containing immobilized anions, Sci. Adv. 2 (2016) e1600320.
[362] E.J. Cheng, A. Sharafi, J. Sakamoto, Intergranular Li metal propagation through polycrystalline $Li_{6.25}Al_{0.25}La_3Zr_2O_{12}$ ceramic electrolyte, Electrochim, Acta 223 (2017) 85–91.
[363] R. Raj, J. Wolfenstine, Current limit diagrams for dendrite formation in solid-state electrolytes for Li-ion batteries, J. Power Sources 343 (2017) 119–126.
[364] Islam, Fisher, Lithium and sodium battery cathode materials: computational insights into voltage, diffusion and nanostructural properties, Chem. Soc. Rev. 43 (2014) 185, https://doi.org/10.1039/c3cs60199d.
[365] Haftbaradaran, et al., A surface locking instability for atomic intercalation into a solid electrode, Appl. Phys. Lett. 96 (2010) 091909, , https://doi.org/10.1063/1.3330940.
[366] Tealdi, et al., Feeling the strain: enhancing ionic transport in olivine phosphate cathodes for Li- and Na-ion batteries through strain effects, J. Mater. Chem. A 4 (2018) 6998, https://doi.org/10.1039/c5ta09418f.
[367] Sarkar, Aquino, Changes in electrodic reaction rates due to elastic stress and stress-induced surface patterns, Electrochim. Acta 111 (2013) 814, https://doi.org/10.1016/j.electacta.2013.08.085.
[368] Ma, et al., Eigenstress model for electrochemistry of solid surfaces, Scientific reports 6 (2016) 26897, https://doi.org/10.1038/srep26897 AND.
[369] Yang, Generalized > Butler-Volmer relation on a curved electrode surface under the action of stress, Sci. China-Phys. Mech. Astron. 59 (11) (2016) 114611, https://doi.org/10.1007/s11433-016-0198-6.
[370] Haftbaradaran, et al., Continuum and atomistic models of strongly coupled diffusion, stress, and solute concentration, J. Power Sources 196 (2011) 361, https://doi.org/10.1016/j.jpowsour.2010.06.080.
[371] Li, et al., Effect of local deformation on the coupling between diffusion and stress in lithium-ion battery, Int. J. Solids Struct. 87 (2016) 81, https://doi.org/10.1016/j.ijsolstr.2016.02.029.
[372] Wang, et al., Effect of chemical stress on diffusion in a hollow cylinder, J. Appl. Phys. 91 (12) (2002) 9584, https://doi.org/10.1063/1.1477624.
[373] Soni, et al., Diffusion Mediated Lithiation Stresses in Si Thin Film Electrodes, J. Electrochem. Soc. 159 (9) (2012) A1520, https://doi.org/10.1149/2.009209jes.
[374] Gao, Zhou, Strong dependency of lithium diffusion on mechanical constraints in high-capacity Li-ion battery electrodes, Acta Mech. Sinica 28 (4) (2012) 1068, https://doi.org/10.1007/s10409-012-0141-4.
[375] An, Jiang, A finite element simulation on transient large deformation and mass diffusion in electrodes for lithium ion batteries, Modelling Simul. Mater. Sci.. Eng. 21 (2013) 074007, , https://doi.org/10.1088/0965-0393/21/7/074007.
[376] Zhao, et al., Inelastic hosts as electrodes for high-capacity lithium-ion batteries, J. Appl. Phys. 109 (2011) 016110, , https://doi.org/10.1063/1.3525990.
[377] Walk, et al., Comparison of a phase-field model for intercalation induced stresses in electrode particles of lithium ion batteries for small and finite deformation theory, Eur. J. Mech. A-Solid 48 (2014) 74, https://doi.org/10.1016/j.euromechsol.2014.02.020.
[378] Cui et al., "Interface-reaction controlled diffusion in binary solids with applications to lithiation of silicon in lithium-ion batteries", J. Mech. Phys. Solids 61:293, 10.1016/j.jmps.2012.11.001 AND.
[379] Weinberg, et al., A Chemo-Mechanical Model of Diffusion in Reactive Systems, Entropy 20 (2018) 140, https://doi.org/10.3390/e20020140.
[380] Li, et al., Fluid-enhanced surface diffusion controls intraparticle phase transformations, Nat. Mater. 17 (2018) 915, https://doi.org/10.1038/s41563-018-0168-4.
[381] Nowack, et al., Design and fabrication of microspheres with hierarchical internal structure for tuning battery performance, Adv. Sci. 2 (2015) 1500078, https://doi.org/10.1002/advs.201500078.
[382] Cho, et al., Numerical and experimental investigation of (de)lithiation-induced strains in bicontinuous silicon-coated nickel inverse opal anodes, Acta Mater 107 (2016) 289, https://doi.org/10.1016/j.actamat.2016.01.064.
[383] Cho, et al., Modeling of stresses and strains during (de)lithiation of Ni3Sn2-coated nickel inverse-opal anodes, ACS Appl. Mater. Interfaces 9 (18) (2017) 15433, https://doi.org/10.1021/acsami.7b01640.
[384] Malik, et al., Particle size dependence of the ionic diffusivity, Nano Lett 10 (2010) 4123, https://doi.org/10.1021/nl1023595.
[385] Gao, Zhou, Strong stress-enhanced diffusion in amorphous lithium alloy nanowire electrodes, J. Appl. Phys. 109 (2011) 014310, , https://doi.org/10.1063/1.3530738.
[386] Gao, et al., A chemo-mechanics framework for elastic solids with surface stress, Proc. R. Soc. A 471 (2015) 20150366, https://doi.org/10.1098/rspa.2015.0366.
[387] Bower, Guduru, A simple finite element model of diffusion, finite deformation, plasticity and fracture in lithium ion insertion electrode materials, Modelling Simul. Mater. Sci.. Eng. 20 (2012) 045004, , https://doi.org/10.1088/0965-0393/20/4/045004.
[388] Chen, et al., Diffusion Induced Damage and Impedance Response in Lithium-Ion Battery Electrodes, J. Electrochem. Soc. 161 (14) (2014) A2138, https://doi.org/10.1149/2.0651414jes.
[389] Chen, et al., Scaling Relations for Intercalation Induced Damage in Electrodes, Electrochim. Acta 204 (2016) 31, https://doi.org/10.1016/j.electacta.2016.03.106.
[390] Haftbaradaran, et al., Method to deduce the critical size for interfacial delamination of patterned electrode structures and application to lithiation of thin-film silicon islands, J. Power Sources 206 (2012) 357, https://doi.org/10.1016/j.jpowsour.2012.01.097.
[391] Zaho, et al., Fracture of electrodes in lithium-ion batteries caused by fast charging, J. Appl. Phys. 108 (2010) 073517, , https://doi.org/10.1063/1.3492617.
[392] Zhao, et al., Inelastic hosts as electrodes for high-capacity lithium-ion batteries, J. Appl. Phys. 109 (2011) 016110, , https://doi.org/10.1063/1.3525990.
[393] Zhao, et al., Fracture and debonding in lithium-ion batteries with electrodes of hollow core-shell nanostructures, J. Power Sources 218 (6) (2012), https://doi.org/10.1016/j.jpowsour.2012.06.074.
[394] Gao, Zhou, Coupled mechano-diffusional driving forces for fracture in electrode materials, J. Power Sources 230 (2013) 176, https://doi.org/10.1016/j.jpowsour.2012.12.034.
[395] Zhang, et al., Constitutive behavior and progressive mechanical failure of electrodes in lithium-ion batteries, J. Power Sources 357 (2017) 126, https://doi.org/10.1016/j.jpowsour.2017.04.103.
[396] Hüter, et al., Electrode–electrolyte interface stability in solid state electrolyte systems: influence of coating thickness under varying residual stresses, AIMS Mater. Sci. 4 (4) (2017) 867, https://doi.org/10.3934/matersci.2017.4.867.
[397] Purkayastha, McMeeking, A parameter study of intercalation of lithium into storage particlesin a lithium-ion battery, Comp. Mater. Sci. 80 (2) (2013), https://doi.org/10.1016/j.commatsci.2012.11.050.
[398] Zhang, Kamlah, Phase-field modeling of the particle size and average concentration dependent miscibility gap in nanoparticles of $Li_xMn_2O_4$, Li_xFePO_4, and Na_xFePO_4 during insertion, Electrochim. Acta 298 (2019) 31, https://doi.org/10.1016/j.electacta.2018.12.007.